Activating a High-Spin Iron(II) Complex to Thermal Spin-Crossover with an Inert Non-Isomorphous Molecular Dopant

Malcolm A. Halcrow[a,*], Hari Babu Vasili[b], Christopher M. Pask[a], Alexander N. Kulak[a] and Oscar Cespedes[b]

[a]*School of Chemistry, University of Leeds, Woodhouse Lane, Leeds LS2 9JT, United Kingdom.*
E-mail: m.a.halcrow@leeds.ac.uk

[b]*School of Physics and Astronomy, University of Leeds, WH Bragg Building, Leeds LS2 9JT, United Kingdom.*

Supporting Information

Table S1 Stoichiometries and analytical data for the $[Fe_xNi_{1-x}(bpp)_2][ClO_4]_2$ solid solutions. The metal composition x in each sample is the average of the three Fe:Ni ratios in the Table, and has an estimated error of ±0.03.[a]

					Fe:Ni ratio calculated from:[a]		
	x[a]	C found (calcd)	H found (calcd)	N found (calcd)	Synthesis stoichiometry	$\chi_M T$ (300 K)[b]	EDX
1a[c]	0.53	38.9 (38.9)	2.55 (2.67)	20.4 (20.6)	0.53:0.47	0.51:0.49	0.56:0.44
2a[c]	0.74	38.9 (39.0)	2.50 (2.68)	20.3 (20.7)	0.73:0.27	0.73:0.27	0.75:0.25
3a	0.87	38.9 (39.0)	2.67 (2.68)	20.5 (20.7)	0.88:0.12	0.87:0.13	0.87:0.13
4a	0.94	39.0 (39.0)	2.58 (2.68)	20.5 (20.7)	0.94:0.06	0.95:0.05	0.92:0.08
1b	0.52	39.1 (38.9)	2.51 (2.67)	20.6 (20.6)	0.51:0.49	0.49:0.51	0.56:0.44
2b	0.74	38.8 (39.0)	2.45 (2.68)	20.5 (20.7)	0.73:0.27	0.73:0.27	0.75:0.25
3b	0.88	39.0 (39.0)	2.37 (2.68)	20.2 (20.7)	0.88:0.12	0.86:0.14	0.88:0.12
4b	0.93	38.6 (39.0)	2.70 (2.68)	20.5 (20.7)	0.94:0.06	0.93:0.07	0.91:0.09

[a]Estimated errors on the metal ratios are ±0.01 based on the synthesis stoichiometry; ±0.02 from the magnetic measurements; and ±0.02 from the EDX element maps (Figure S1). [b]The measured $\chi_M T$ data and the reference $\chi_M T$ values used in these calculations are given in Table 1. [c]Single crystal X-ray analyses of these compounds gave refined values of x = 0.50(2) for **1a**, and x = 0.76(3) for **2a**.

Polycrystalline **1a**

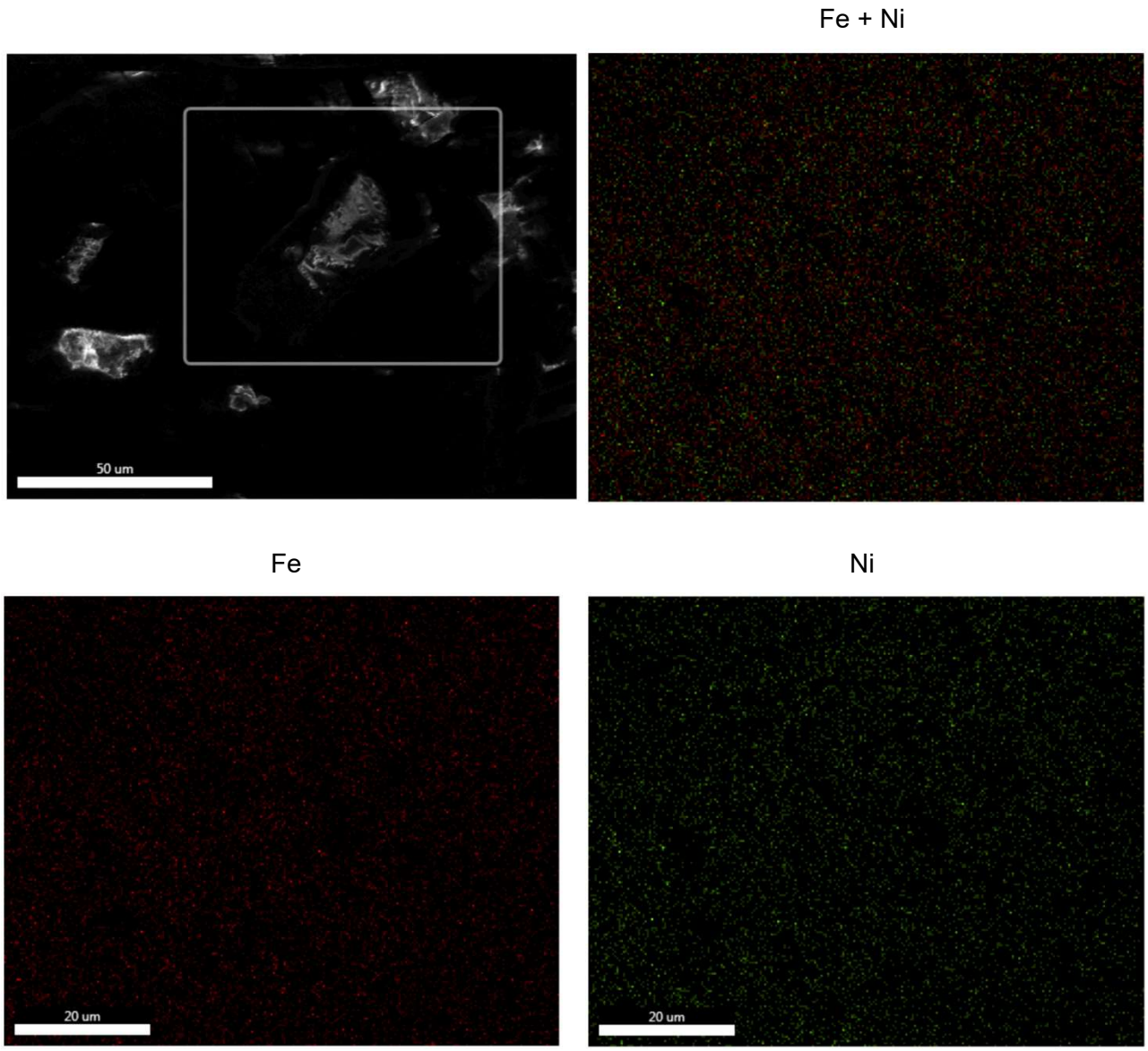

Figure S1 Iron and nickel EDX element maps for the solid solutions in this work (Table S1).

Polycrystalline **2a**

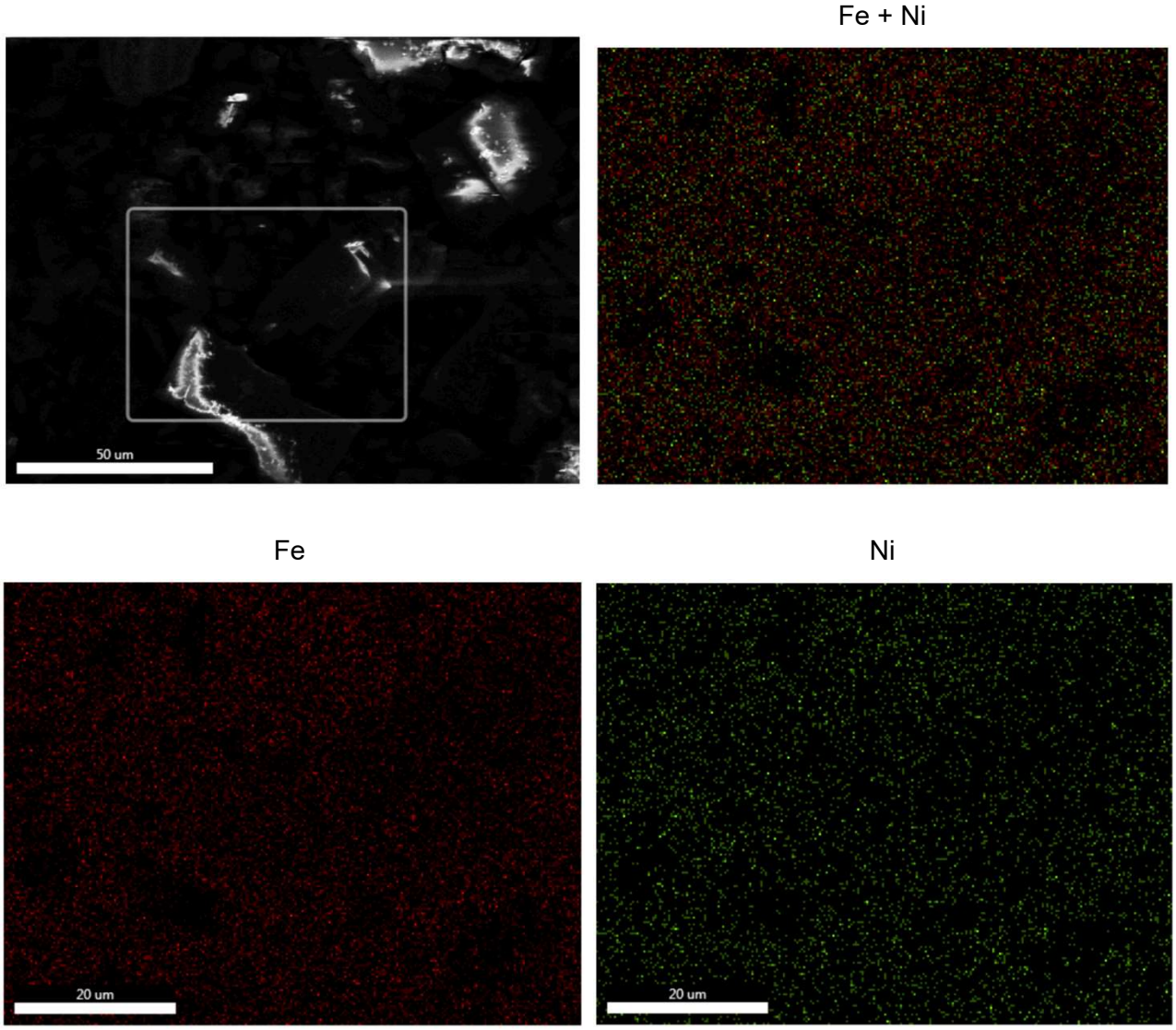

Figure S1 continued.

Polycrystalline **3a**

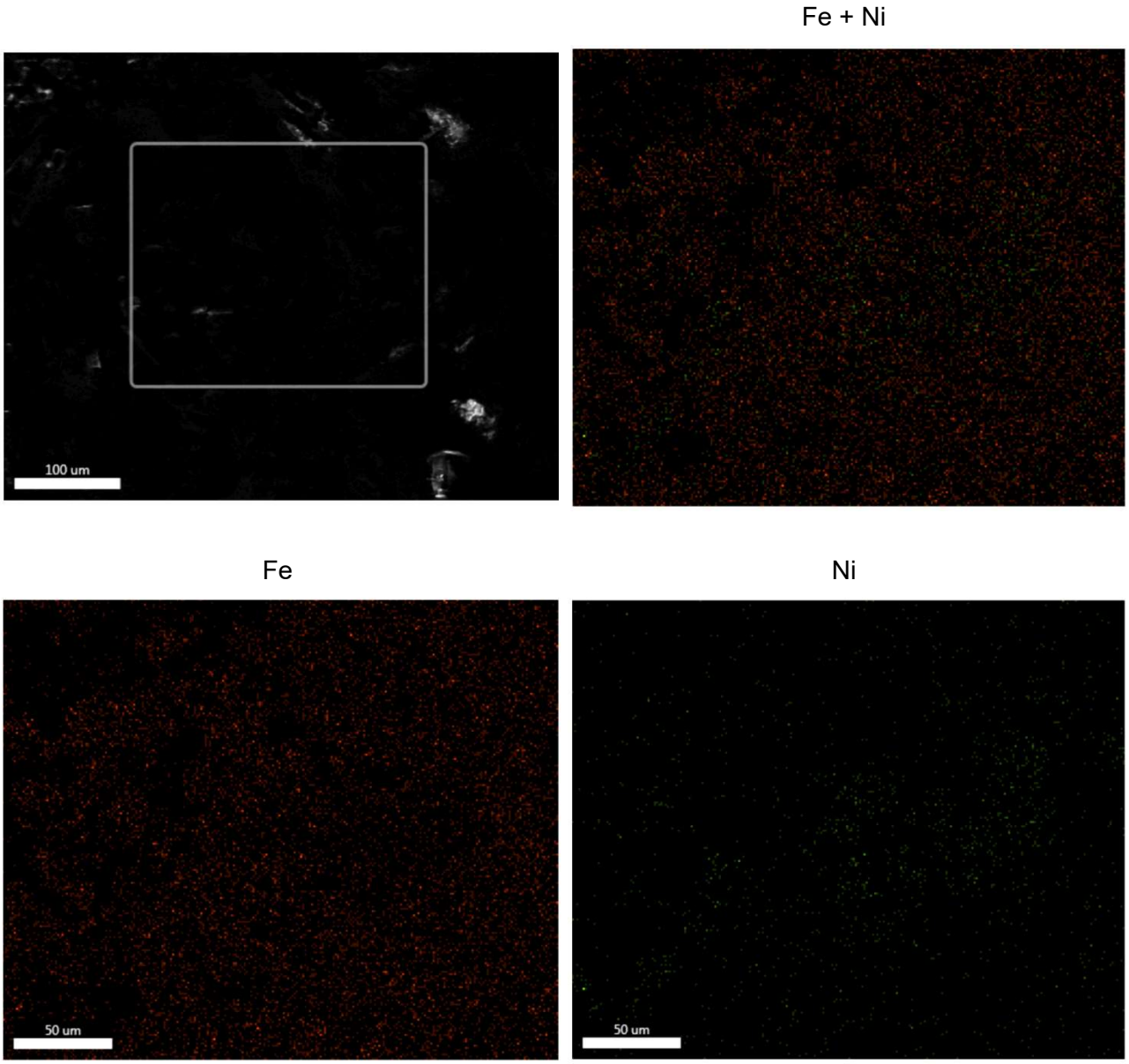

Figure S1 continued.

Polycrystalline **4a**

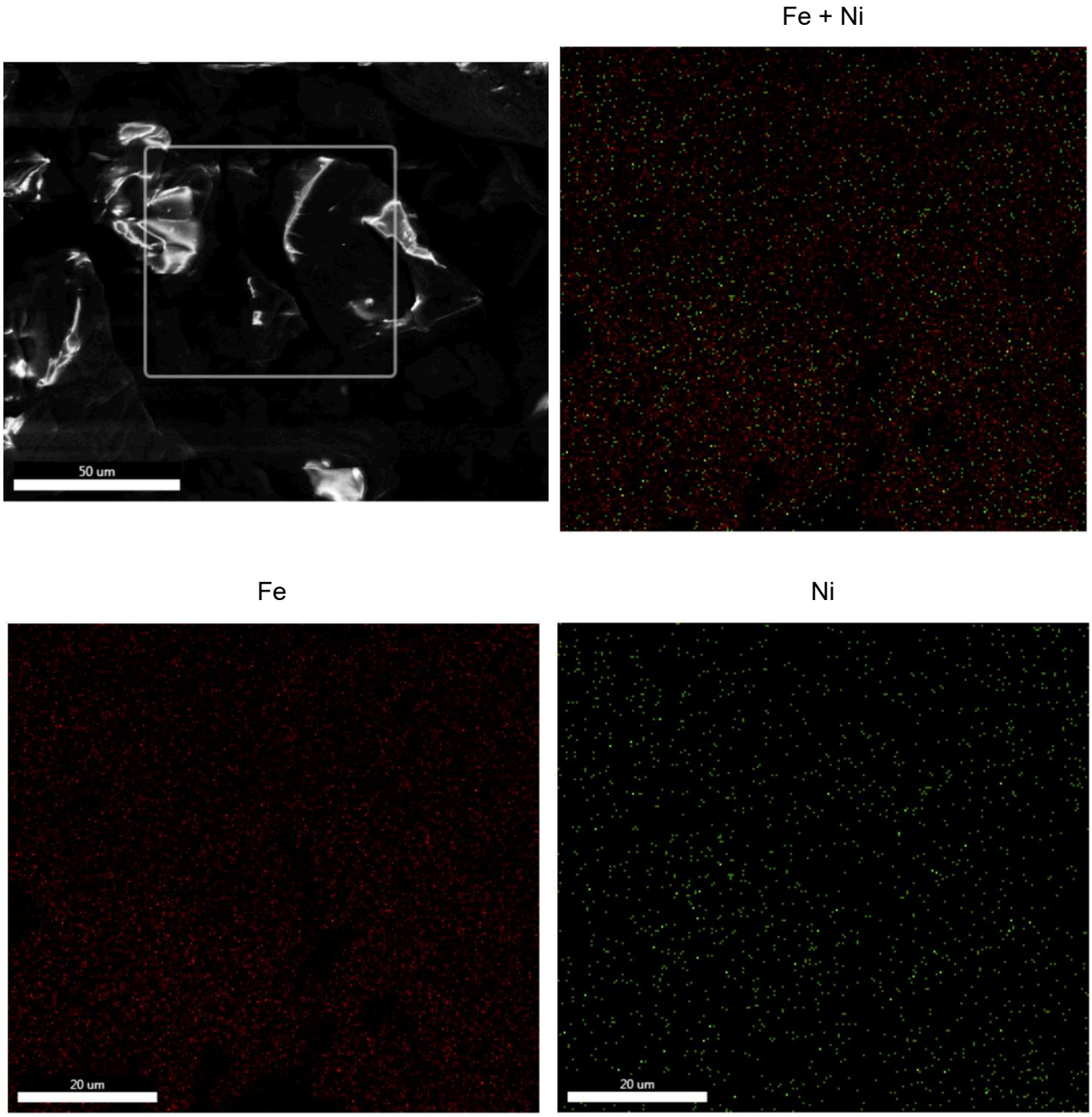

Figure S1 continued.

Rapidly precipitated **1b**

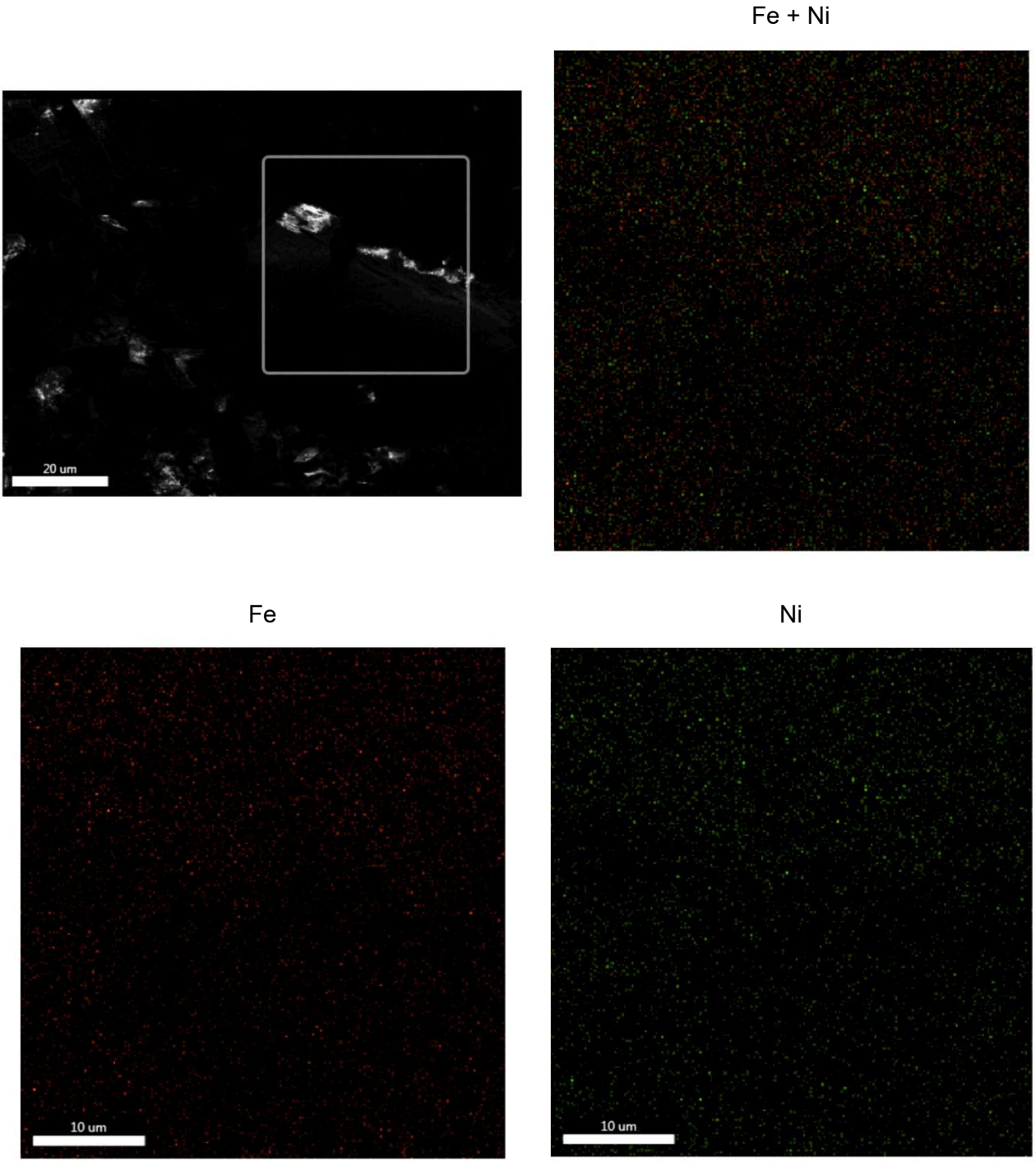

Figure S1 continued.

Rapidly precipitated **2b**

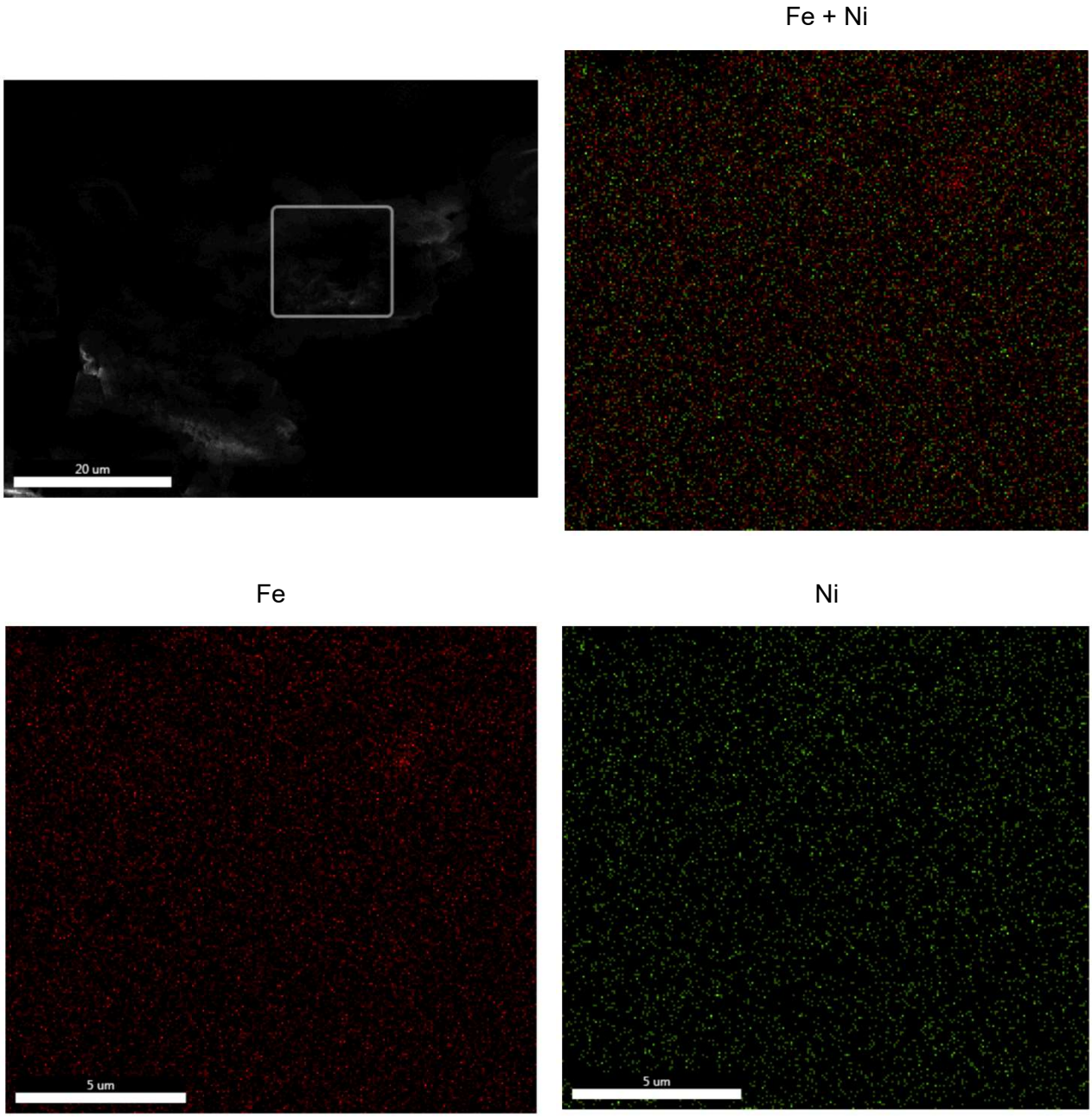

Figure S1 continued.

Rapidly precipitated **3b**

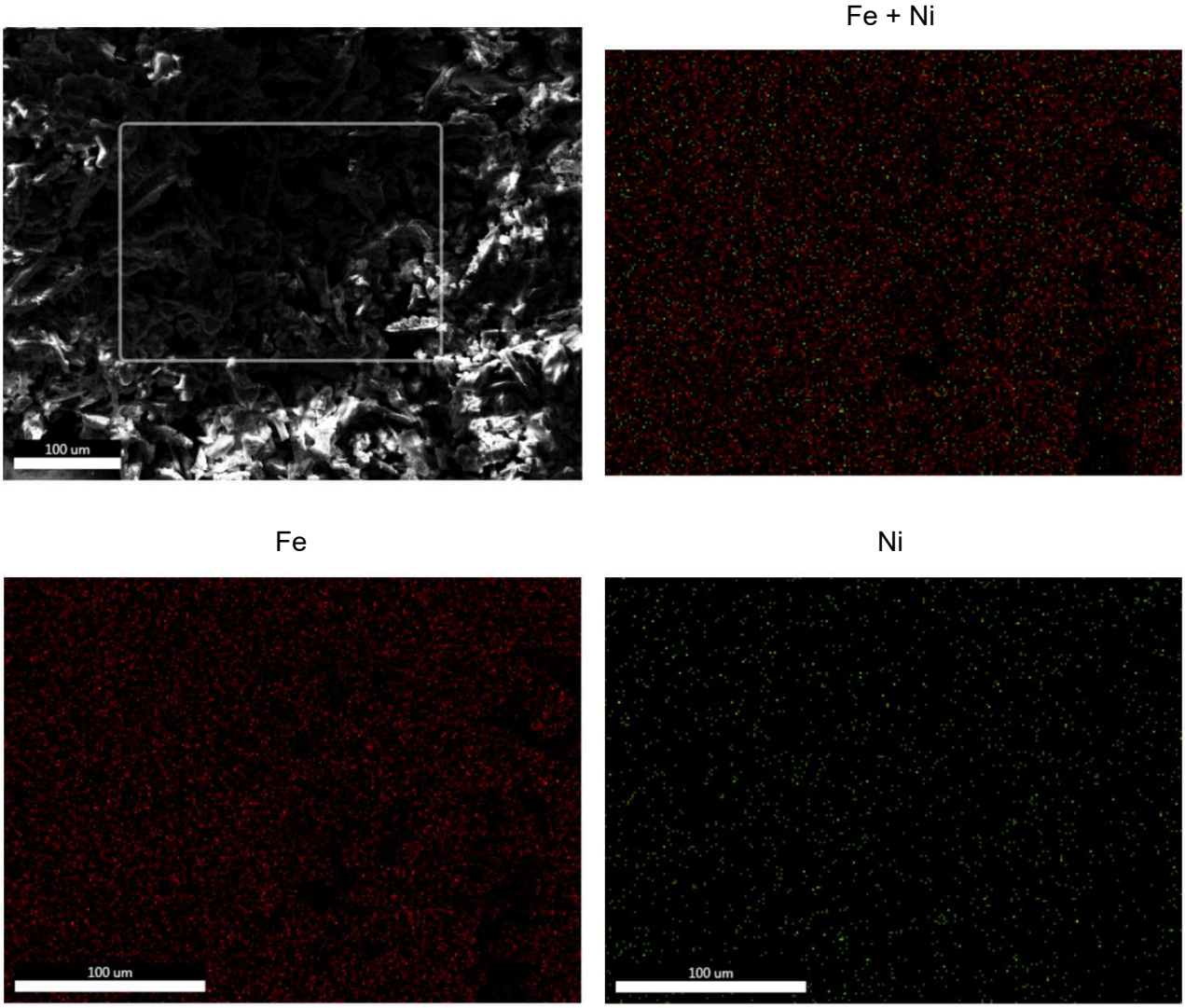

Figure S1 continued.

Rapidly precipitated **4b**

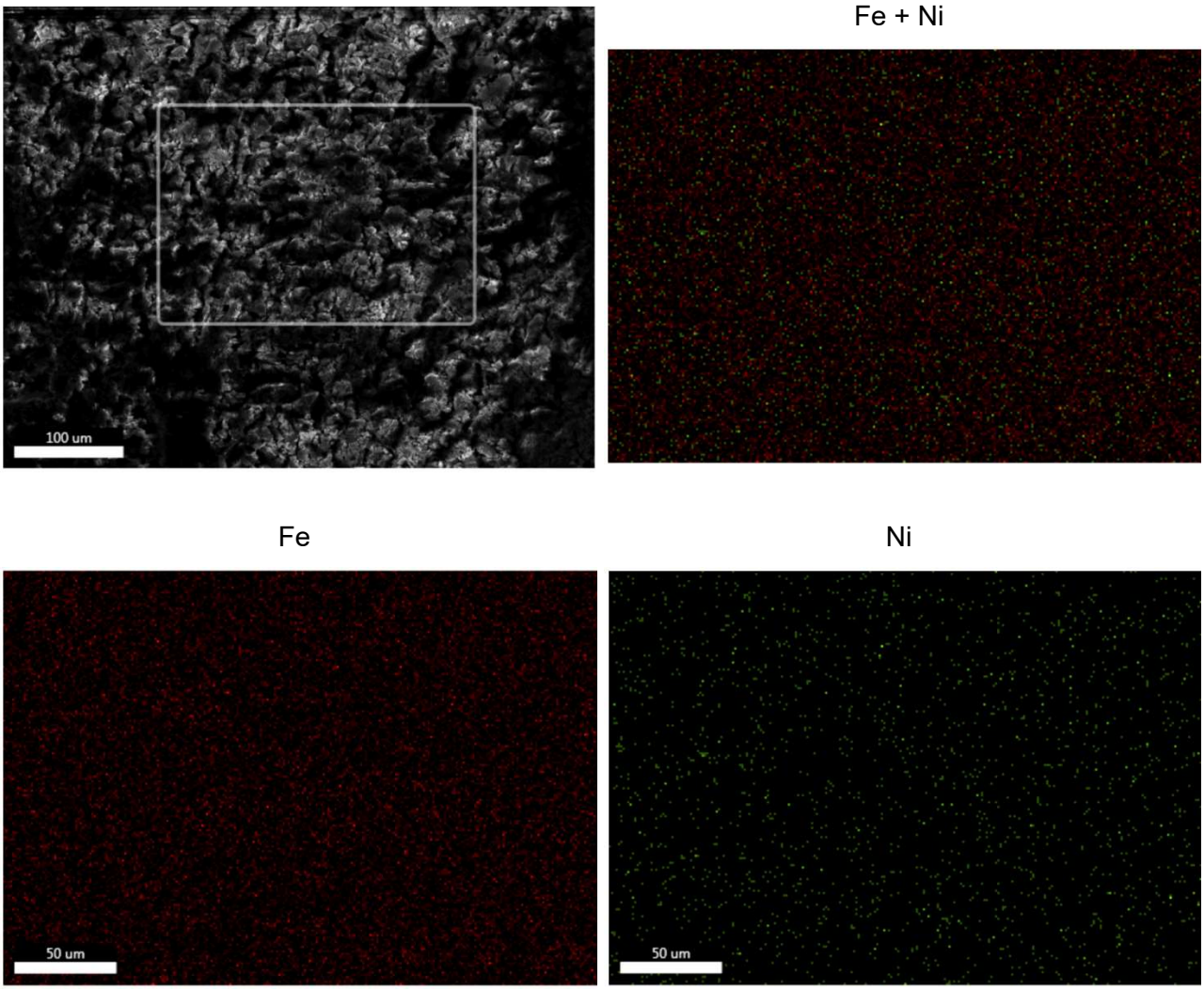

Figure S1 continued.

Single Crystal Structure Analyses

Diffraction data were measured with an Agilent Supernova or a Nonius Kappa-CCD diffractometer, which were fitted with an Oxford Cryostream low-temperature device. Monochromated Cu-K_α (λ = 1.5418 Å) or Mo-K_α (λ = 0.7107 Å) radiation was used for different measurements. Experimental details of the structure determinations are given in Table S2. All the structures were solved by direct methods *(SHELXTL*[2]), and developed by full least-squares refinement on F^2 (*SHELXL-2018*[3]). Crystallographic figures and powder pattern simulations were prepared using *XSEED*,[4] and publication materials were prepared using *Olex2*.[5]

Unless otherwise stated, all non-H atoms in these structures were refined anisotropically, while H atoms were placed in calculated positions and refined using a riding model.

Structure refinement of $[Ni(bpp)_2][ClO_4]_2$. One ClO_4^- ion is disordered over two orientations, with a refined occupancy ratio of 0.71:0.29. This was treated using the refined distance restraints Cl–O = 1.44(2) and O···O = 2.36(2) Å. All non-H atoms except the minor anion disorder site were refined anisotropically, and H atoms were placed in calculated positions and refined using a riding model.

Structure refinements of $[Fe(bpp)_2][ClO_4]_2$ and $[Fe(bpp)_2][PF_6]_2$. The structures of these isomorphous compounds have been previously published at 120 or 150 K.[2,3] However, simulations of room temperature powder diffraction data based on those published structures deviated significantly from experiment at higher angle. Hence, the structures were remeasured at room temperature, for use in the powder pattern simulations.

Their asymmetric units contain half a complex cation with Fe(1) spanning the C_2 axis $-x$, y, $0.5-z$; and, one unique anion on a general crystallographic site. The anion in both structures is disordered over two half-occupied orientations. The ClO_4^- ion was fully disordered, and modelled using the refined distance restraints Cl–O = 1.42(2) and O···O = 2.32(2) Å. *SHELXL* ISOR constraints were also applied to the partial O atoms. In the PF_6 salt, the F atoms were disordered about an ordered, wholly occupied P atom. These were treated with refined restraints P–F = 1.58(2) Å, and no thermal ellipsoid constraints were required.

Structure refinements of $[Fe_xNi_{1-x}(bpp)_2][ClO_4]_2$ (x = 0.50, 1a; x = 0.76, 2a). The variable temperature unit cell measurements and the full data collections were performed using the same crystal of each sample.

Full datasets of both compounds were collected at 100 K, when the crystals are low-spin. The metal atom occupancy was refined by allowing the coordinates of Fe(1) and Ni(1) to refine separately, with U_{iso} fixed at the value obtained when the metal site was allowed to freely refine. That yielded x = 0.50(2) for **1a** and 0.76(3) for **2a**, which are consistent with the expected compositions of those samples (Table 2, main article). In the final least squares cycles, the metal atoms were treated as a single Fe_x/Ni_{1-x} mixed-metal site containing partial iron and nickel atoms with the same atomic coordinates and displacement parameters. The refined metal compositions are confirmed by the bond lengths and angles about Fe(1)/Ni(1), which agree well with weighted average values calculated from the pure Fe and Ni complexes based on those compositions (Table S6). No anion disorder is present in either model.

A full refinement of **1a** in its high-spin state at 300 K was also achieved. Both ClO_4^- ions are disordered over three orientations at this temperature, some of which share a common Cl atom. These were treated with the refined distance restraints Cl–O = 1.44(2) and O···O = 2.36(2) Å; an antibumping restraint between an N atom and a partial O atom was also applied to avoid an unrealistic intermolecular contact. The anisotropic displacement parameters of Fe(1) and Ni(1) were also constrained to be the same, as above. All crystallographically ordered non-H atoms plus the partial metal sites and Cl atoms were refined anisotropically at this temperature.

The anisotropic displacement parameters of Fe(1) and Ni(1) were constrained to be the same for all three of these refinements, which was required for them to converge successfully.

Table S2 Experimental data for the crystal structures in this work.

	Precursor compounds			Solid solutions		
	$[Ni(bpp)_2][ClO_4]_2$	$[Fe(bpp)_2][ClO_4]_2$	$[Fe(bpp)_2][PF_6]_2$	**1a**		**2a**
molecular formula	$C_{22}H_{18}Cl_2N_{10}NiO_8$	$C_{22}H_{18}Cl_2FeN_{10}O_8$	$C_{22}H_{18}F_{12}FeN_{10}P_2$	$C_{22}H_{18}Cl_2Fe_{0.50}N_{10}Ni_{0.50}O_8$		$C_{22}H_{18}Cl_2Fe_{0.76}N_{10}Ni_{0.24}O_8$
M_r	680.07	677.21	768.25	678.64		677.90
crystal class	monoclinic	monoclinic	monoclinic	monoclinic		monoclinic
space group	$P2_1$	$C2/c$	$C2/c$	$P2_1$		$P2_1$
a / Å	8.5069(3)	14.5206(2)	14.6500(5)	8.5567(7)	8.4913(4)	8.4873(5)
b / Å	8.5670(2)	9.3323(1)	9.4890(4)	8.6233(6)	8.5507(4)	8.5486(5)
c / Å	18.8513(7)	20.1872(2)	20.6037(5)	19.2053(15)	18.7250(8)	18.6946(10)
α / °	90	90	90	90	90	90
β / °	97.645(3)	99.014(1)	98.792(2)	96.371(7)	98.181(4)	98.424(5)
γ / °	90	90	90	90	90	90
V / Å^3	1361.64(8)	2701.80(5)	2830.54(17)	1408.35(19)	1345.72(11)	1341.74(13)
Z	2	4	4	2	2	2
T / K	100(2)	300(2)	300(2)	300(2)	100(2)	100(2)
μ / mm^{-1}	0.976[c]	6.904[d]	0.761[c]	0.867[c]	0.908[c]	0.868[c]
D_c / g cm^{-3}	1.659	1.665	1.803	1.600	1.675	1.678
measured reflections	15835	12271	10906	11743	11197	10773
independent reflections	6658	2656	3234	6235	5975	5799
R_{int}	0.034	0.049	0.043	0.031	0.032	0.035
parameters	409	242	269	422	388	388
restraints	21	64	12	62	1	1
R_1 [$F_0 > 4\sigma(F_0)$][a]	0.035	0.043	0.036	0.053	0.038	0.049
wR_2, all data[b]	0.069	0.124	0.100	0.121	0.074	0.093
goodness of fit	1.050	1.123	1.023	1.106	1.033	1.111
$\Delta\rho_{min/max}$ / eÅ^{-3}	–0.52/0.28	–0.30/0.62	–0.35/0.26	–0.30/0.31	–0.53/0.63	–0.51/0.49
Flack parameter	0.003(6)	–	–	–0.019(10)	–0.017(9)	0.018(10)
CCDC	2332656	2332657	2332658	2332659	2332660	2332661

[a] $R = \Sigma[|F_o| - |F_c|] / \Sigma|F_o|$ [b] $wR = [\Sigma w(F_o^2 - F_c^2) \ / \ \Sigma wF_o^4]^{1/2}$ [c] Collected with Mo-K_α radiation. [d] Collected with Cu-K_α radiation.

Definitions of the structural parameters in Tables S3-S6 and Tables S11-S17.

Θ is defined as follows:

$$\Theta = \sum_{i=1}^{24} 60 - \beta_i$$

where β_i are the 24 unique N–Fe–N angles measured on the projection of two triangular faces of the octahedron along their common pseudo-threefold axis (Scheme S1). Θ indicates the distortion of a formally octahedral metal ion towards a trigonal prismatic structure. A perfectly octahedral complex gives $\Theta = 0$.[7,8]

Because the high-spin state of a complex has a much more plastic structure than the low-spin, this is reflected in Θ which is usually much larger in the high-spin state. The absolute values of these parameters depend on the metal/ligand combination in the compound under investigation, however.[9]

The change in Θ during SCO is an important contributor to $T_{½}$, in materials that are isomorphous or adopt similar modes of crystal packing.[10,11] We recently showed that correlation operates for $[Fe(bpp)_2]^{2+}$ complex salts, with the terpyridine embrace lattice type.[11] That is discussed in the main article.

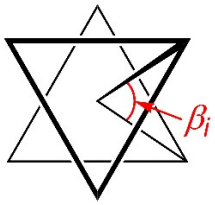

Scheme S1 Angles used in the definition of the coordination distortion parameter Θ.

The parameters in Scheme S2 define the magnitude of an angular Jahn-Teller distortion, that is often observed in high-spin $[Fe(bpp)_2]^{2+}$ derivatives ($\theta \leq 90°$, $\phi \leq 180°$).[12,13] They are also a useful indicator of the molecular geometry, in defining the disposition of the two ligands around the metal ion. Spin-crossover can be inhibited if θ and ϕ deviate too strongly from their ideal values,[13,14] because the associated rearrangement to a more regular low-spin coordination geometry ($\theta \approx 90°$, $\phi \approx 180°$) cannot be accommodated by a rigid solid lattice.[15] In less distorted examples, significant changes in θ and ϕ between the spin states can be associated with enhanced SCO cooperativity.[16]

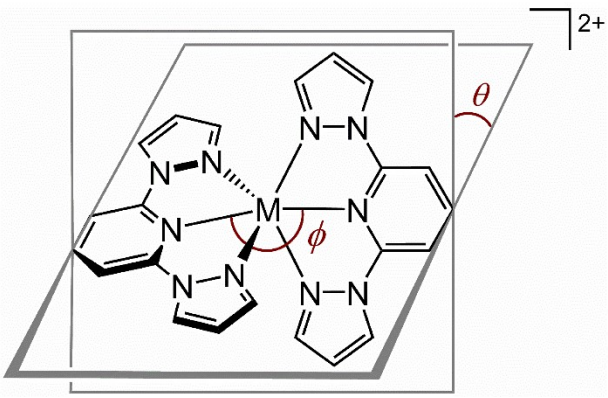

Scheme S2 θ and ϕ, used to discuss the coordination geometries of $[M(bpp)_2]^{2+}$ derivatives ($M^{2+} = Fe^{2+}$, Mn^{2+}, Co^{2+}, Ni^{2+}, Cu^{2+}, Zn^{2+} or Ru^{2+}).

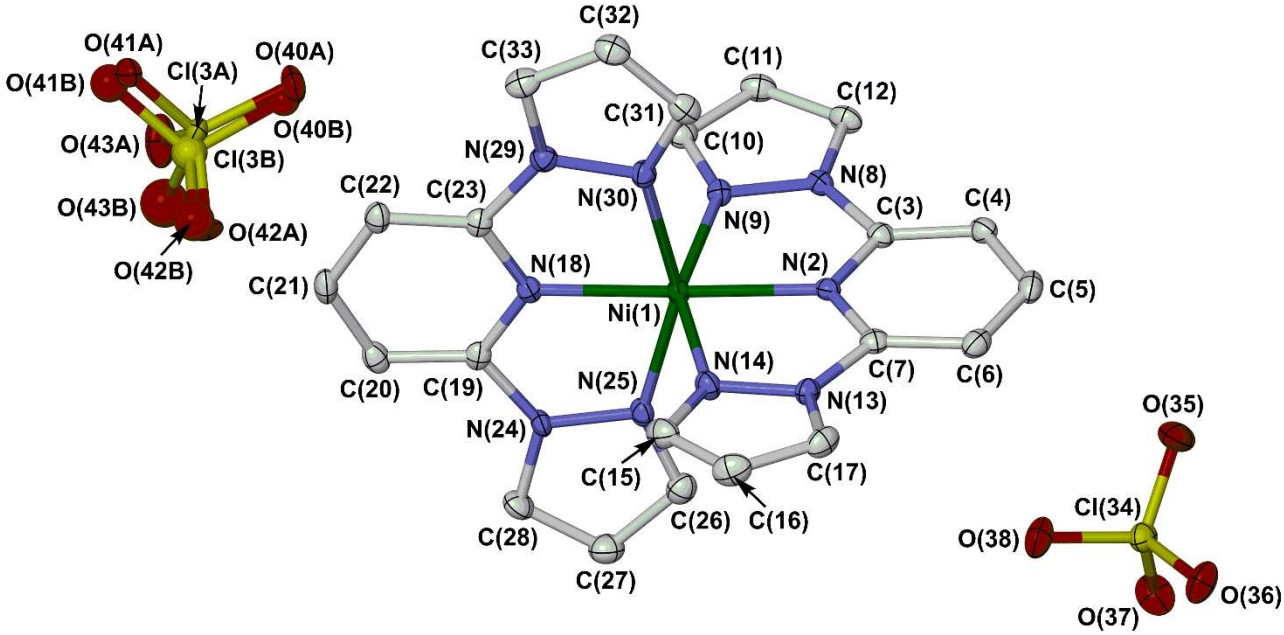

Figure S2 The asymmetric unit of $[Ni(bpp)_2][ClO_4]_2$, with the full atom numbering scheme. Displacement ellipsoids are at the 50 % probability level, and H atoms are omitted for clarity.

Colour code: C, white; Cl, yellow; N, blue; Ni, green; O, red.

Table S3 Selected bond lengths and angles (Å , °) for $[Ni(bpp)_2][ClO_4]_2$. See Figure S2 for the atom numbering scheme.

Ni(1)–N(2)	2.009(3)	Ni(1)–N(18)	2.004(3)
Ni(1)–N(9)	2.119(3)	Ni(1)–N(25)	2.123(3)
Ni(1)–N(14)	2.089(3)	Ni(1)–N(30)	2.101(3)
N(2)–Ni(1)–N(9)	76.81(11)	N(9)–Ni(1)–N(30)	92.59(11)
N(2)–Ni(1)–N(14)	76.97(11)	N(14)–Ni(1)–N(18)	102.18(11)
N(2)–Ni(1)–N(18) (ϕ)	177.10(12)	N(14)–Ni(1)–N(25)	92.94(11)
N(2)–Ni(1)–N(25)	106.09(11)	N(14)–Ni(1)–N(30)	90.68(11)
N(2)–Ni(1)–N(30)	100.00(11)	N(18)–Ni(1)–N(25)	76.68(11)
N(9)–Ni(1)–N(14)	153.75(11)	N(18)–Ni(1)–N(30)	77.20(11)
N(9)–Ni(1)–N(18)	103.95(11)	N(25)–Ni(1)–N(30)	153.81(11)
N(9)–Ni(1)–N(25)	95.49(11)		
Θ	382	θ	89.36(2)

These values are identical within experimental error to the BF_4^- salt of the same complex, which is isomorphous with this crystal.[17]

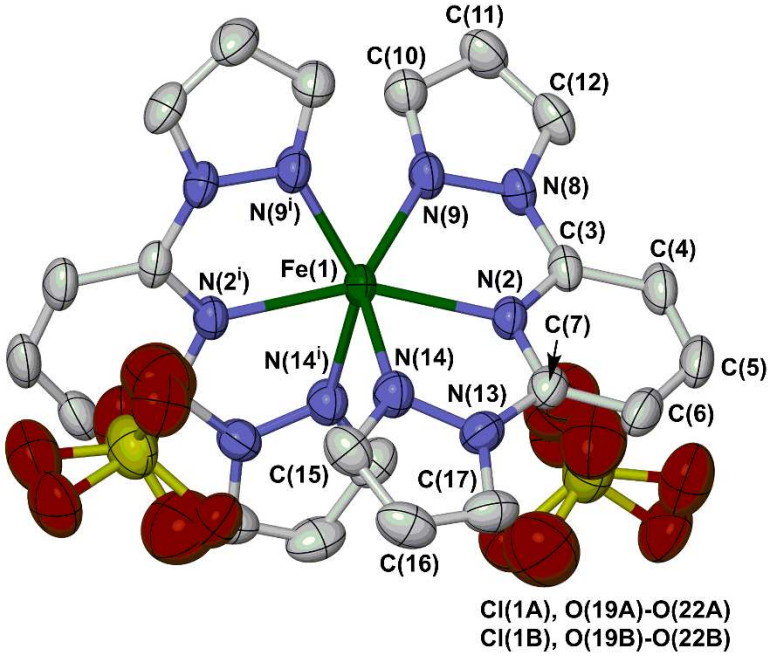

Figure S3 The formula unit in the crystals of $[Fe(bpp)_2][ClO_4]_2$ at 300 K, with the full atom numbering schemes. Displacement ellipsoids are at the 50 % probability level, and H atoms are omitted for clarity. Symmetry code: (i) $-x$, y, $\frac{1}{2}-z$.

Colour code: C, white; Cl, yellow; Fe, green; N, blue; O, red.

Table S4 Selected bond lengths and angles (Å , °) for $[Fe(bpp)_2][ClO_4]_2$ at 300 K. See Figure S3 for the atom numbering scheme, and page S13 for definitions of ϕ and θ. Symmetry code: (i) $-x$, y, $\frac{1}{2}-z$.

Fe(1)–N(2)	2.1662(19)	Fe(1)–N(14)	2.215(2)
Fe(1)–N(9)	2.183(2)		
N(2)–Fe(1)–N(9)	72.27(8)	N(9)–Fe(1)–N(9^i)	86.17(11)
N(2)–Fe(1)–N(14)	71.90(8)	N(9)–Fe(1)–N(14)	141.66(8)
N(2)–Fe(1)–N(2^i) (ϕ)	155.38(11)	N(9)–Fe(1)–N(14^i)	105.61(8)
N(2)–Fe(1)–N(9^i)	128.03(8)	N(14)–Fe(1)–N(14^i)	87.70(12)
N(2)–Fe(1)–N(14^i)	90.18(8)		
θ	66.42(2)		

These parameters are identical within experimental error to the previously published structures of the same compounds at 150 K.[18] The crystals were remeasured at 300 K in this study to afford more accurate simulations of the room temperature powder diffraction data.

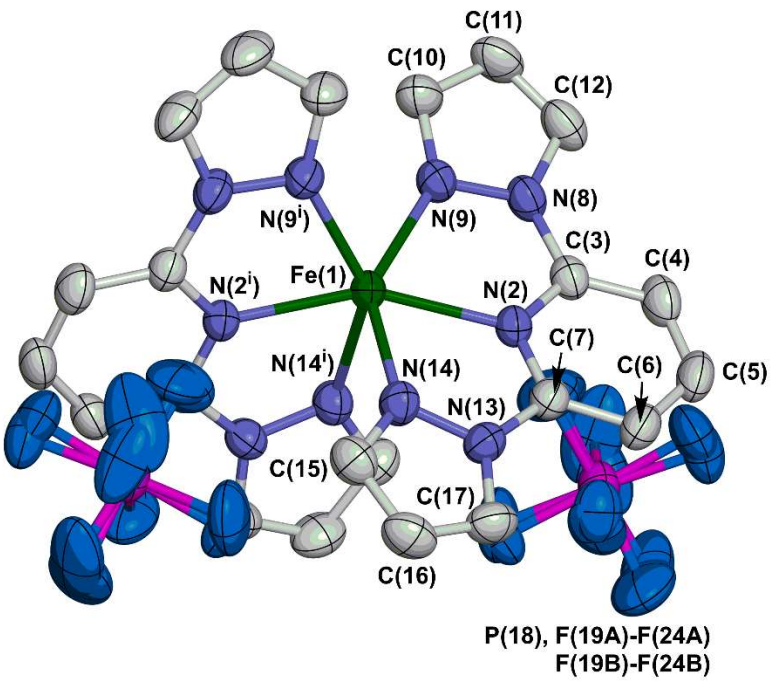

Figure S4 The formula units in the crystals of $[Fe(bpp)_2][PF_6]_2$ at 300 K, with the full atom numbering schemes. Displacement ellipsoids are at the 50 % probability level, and H atoms are omitted for clarity. Symmetry code: (i) $-x$, y, $\frac{1}{2}-z$.

Colour code: C, white; F, cyan; Fe, green; N, blue; P, purple.

Table S5 Selected bond lengths and angles (Å , °) for $[Fe(bpp)_2][PF_6]_2$ at 300 K. See Figure S4 for the atom numbering scheme, and page S13 for definitions of ϕ and θ. Symmetry code: (i) $-x$, y, $\frac{1}{2}-z$.

Fe(1)–N(2)	2.1695(14)	Fe(1)–N(14)	2.2184(16)
Fe(1)–N(9)	2.1961(16)		
N(2)–Fe(1)–N(9)	71.99(6)	N(9)–Fe(1)–N(9^i)	86.73(9)
N(2)–Fe(1)–N(14)	71.66(6)	N(9)–Fe(1)–N(14)	141.39(6)
N(2)–Fe(1)–N(2^i) (ϕ)	154.66(8)	N(9)–Fe(1)–N(14^i)	106.40(6)
N(2)–Fe(1)–N(9^i)	128.90(6)	N(14)–Fe(1)–N(14^i)	85.95(9)
N(2)–Fe(1)–N(14^i)	89.64(6)		
θ	64.42(2)[a]		

[a]This is 1.8° larger than for the same compound at 120 K [62.64(1)°].[12]

Aside from θ which is highlighted in the Table, these parameters are identical within experimental error to the previously published structures of the same compound at 120 K.[12] The crystals were remeasured at 300 K in this study to afford more accurate simulations of the room temperature powder diffraction data.

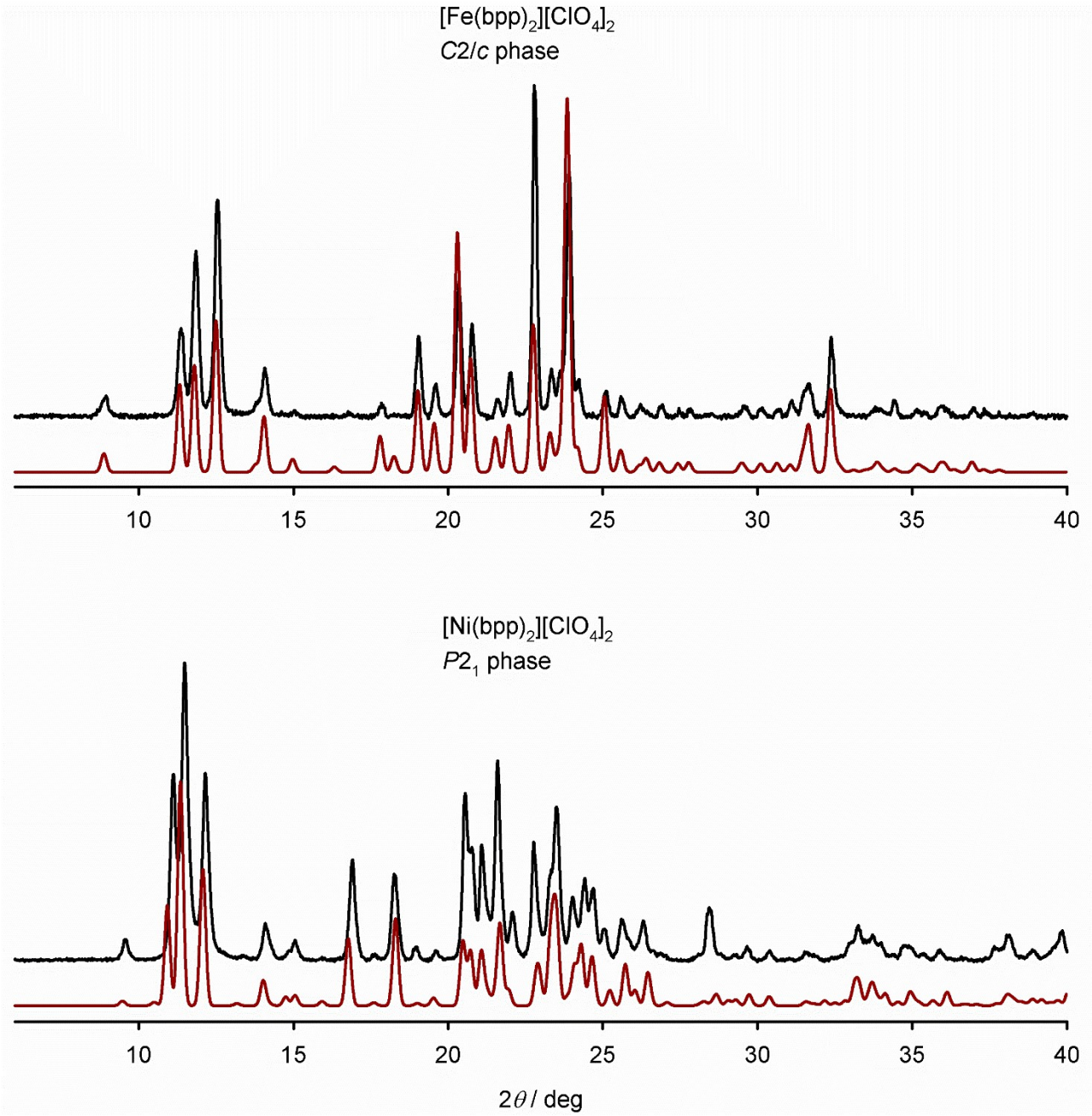

Figure S5 Room temperature X-ray powder diffraction data for the pure precursor compounds used to make the solid solutions (black), and their crystallographic simulations (red).

Data for the nickel complex are simulated reasonably well by its 100 K crystal structure, but simulations of the iron complex powder pattern using the published low temperature crystal structure[18] were less satisfactory. Hence, that crystal was remeasured at 300 K for this study. The simulations in this Figure and in Figure 3 (main article) are based on that room temperature measurement.

The difference could reflect the anisotropic thermal expansion shown by $[Fe(bpp)_2][ClO_4]_2$. The *c* unit cell dimension in that crystal expands by 0.4156(4) % between 150 and 300 K, which is *ca* half the expansion shown by *a* [0.7697(4) %] and *b* [0.8589(2) %]. In contrast, complexes adopting the $P2_1$ phase undergo almost isotropic thermal expansion over the same temperature range.[6]

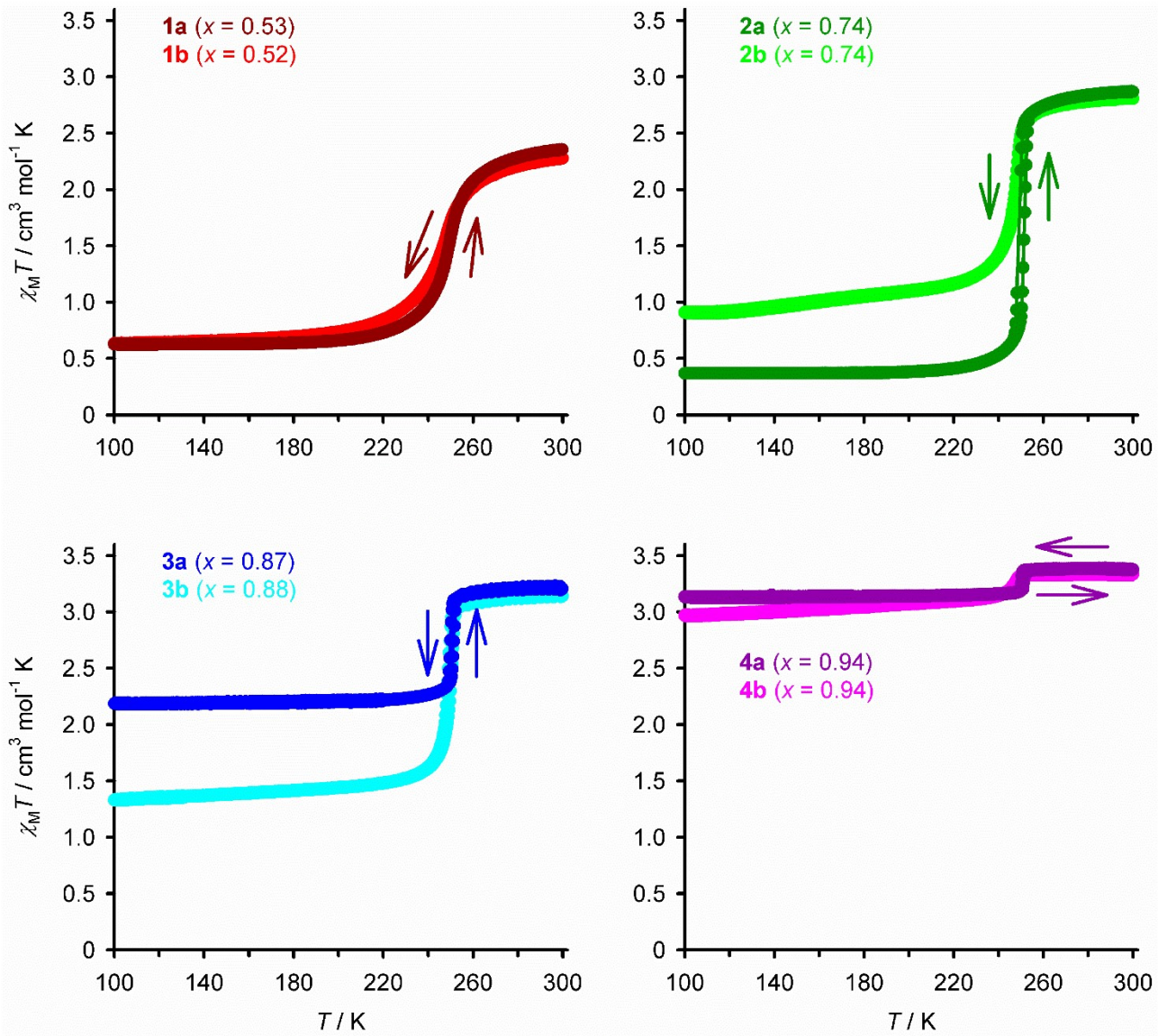

Figure S6 Variable temperature magnetic susceptibility data from **1a**-**4a** and **1b**-**4b**. Datapoints from each sample are connected by a spline curve for clarity. All the data were measured with a 300→100→300 K temperature cycle, at a scan rate of 2 K min^{-1}.

The colour coding for **1a**-**4a** is the same as in Figure 4 (main article).

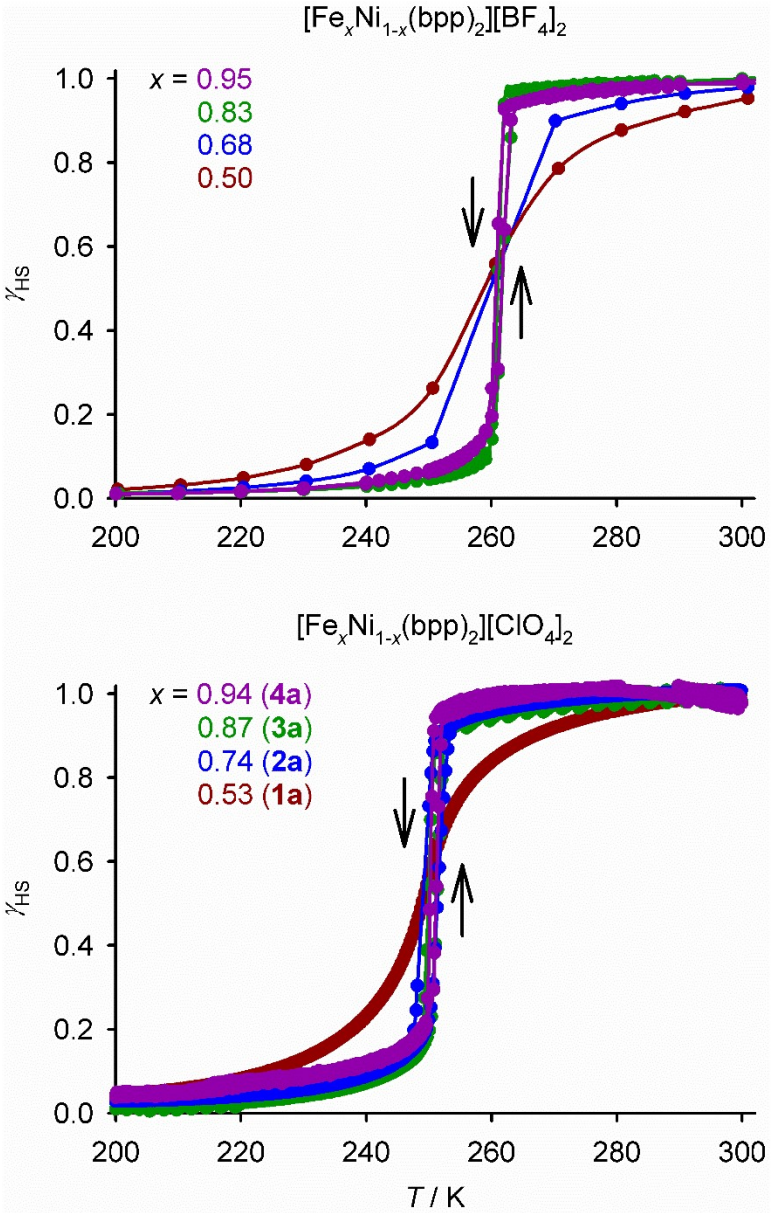

Figure S7 Comparison of the thermal SCO undergone by different compositions of polycrystalline $[Fe_xNi_{1-x}(bpp)_2][BF_4]_2$ and $[Fe_xNi_{1-x}(bpp)_2][ClO_4]_2$, from their magnetic susceptibility data. Data from each compound are linked by a spline curve for clarity, and samples of the two salts with similar compositions have the same colour coding. Data for the $[Fe_xNi_{1-x}(bpp)_2][BF_4]_2$ series are taken from ref. 1.

The precursor compounds $[Fe(bpp)_2][BF_4]_2$[12] and $[Ni(bpp)_2][BF_4]_2$[17] are isomorphous, but $[Fe(bpp)_2][ClO_4]_2$ and $[Ni(bpp)_2][ClO_4]_2$ are not. Hence, there is interest in comparing the solid solutions from these two salts.

All data in the Figure were measured at a 2 K min^{-1} scan rate. Compounds **1a**-**4a** and $[Fe_xNi_{1-x}(bpp)_2][BF_4]_2$ (x = 0.83 and 0.95) were measured in both cooling and warming modes, but the BF_4^- salt samples with higher nickel content (x = 0.50 and 0.68) were measured in warming mode only.[1]

- SCO in **1a**, **3a** and **4a** resembles the corresponding materials from the $[Fe_xNi_{1-x}(bpp)_2][BF_4]_2$ series, apart from their different $T_{½}$ values.
- The published data from $[Fe_{0.68}Ni_{0.32}(bpp)_2][BF_4]_2$ are too sparse to fully define the cooperativity of its SCO. However, the available data imply SCO in that sample may be less cooperative than in **2a**.

The plot for **4a** is a little noisier, because it shows only the 6 % of the sample which is SCO-active (Table 1, main article).

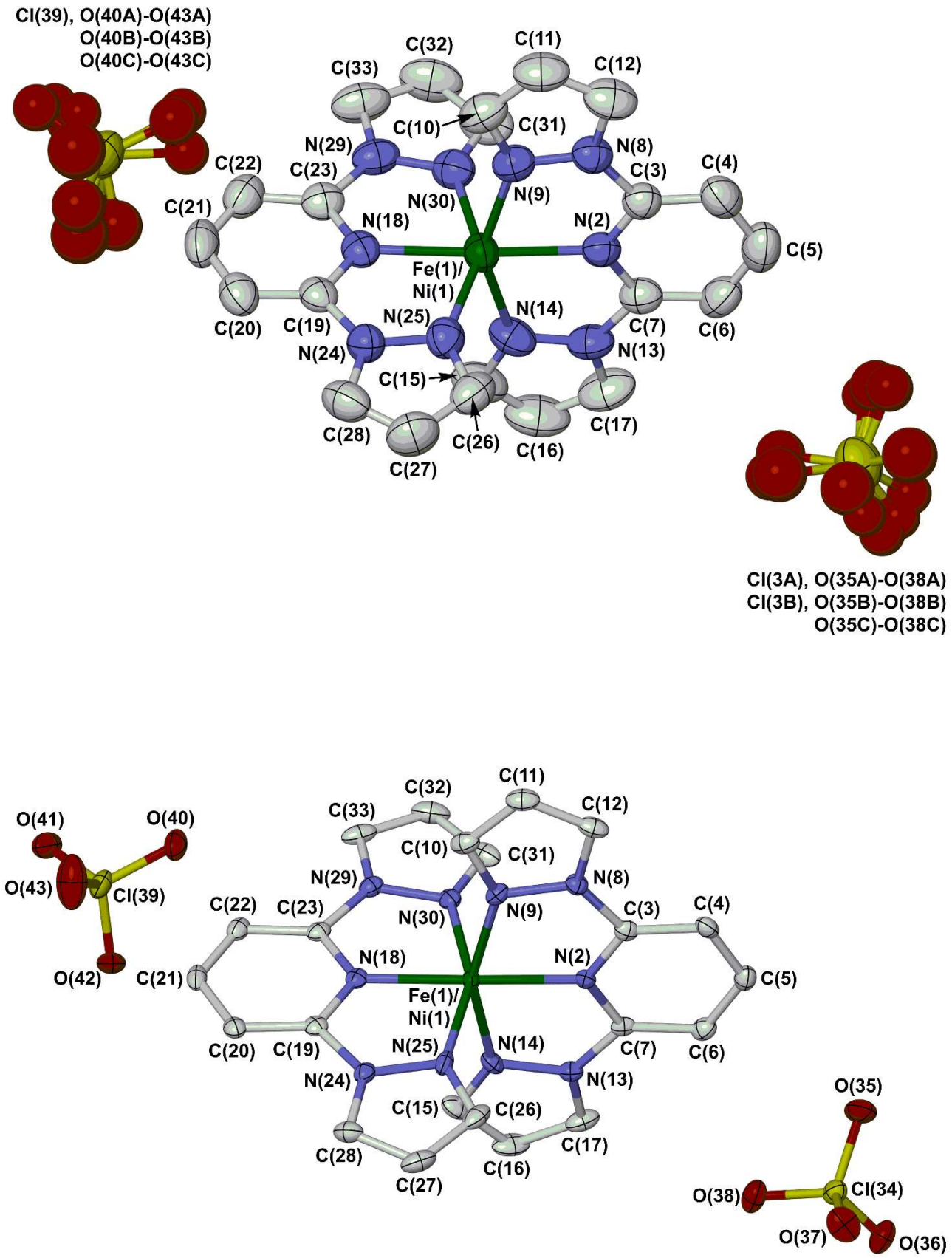

Figure S8 The asymmetric unit of **1a** at 300 K (top) and 100 K (bottom), with the full atom numbering scheme. Displacement ellipsoids are at the 50 % probability level, and H atoms are omitted for clarity.

Colour code: C, white; Cl, yellow; Fe/Ni, green; N, blue; O, red.

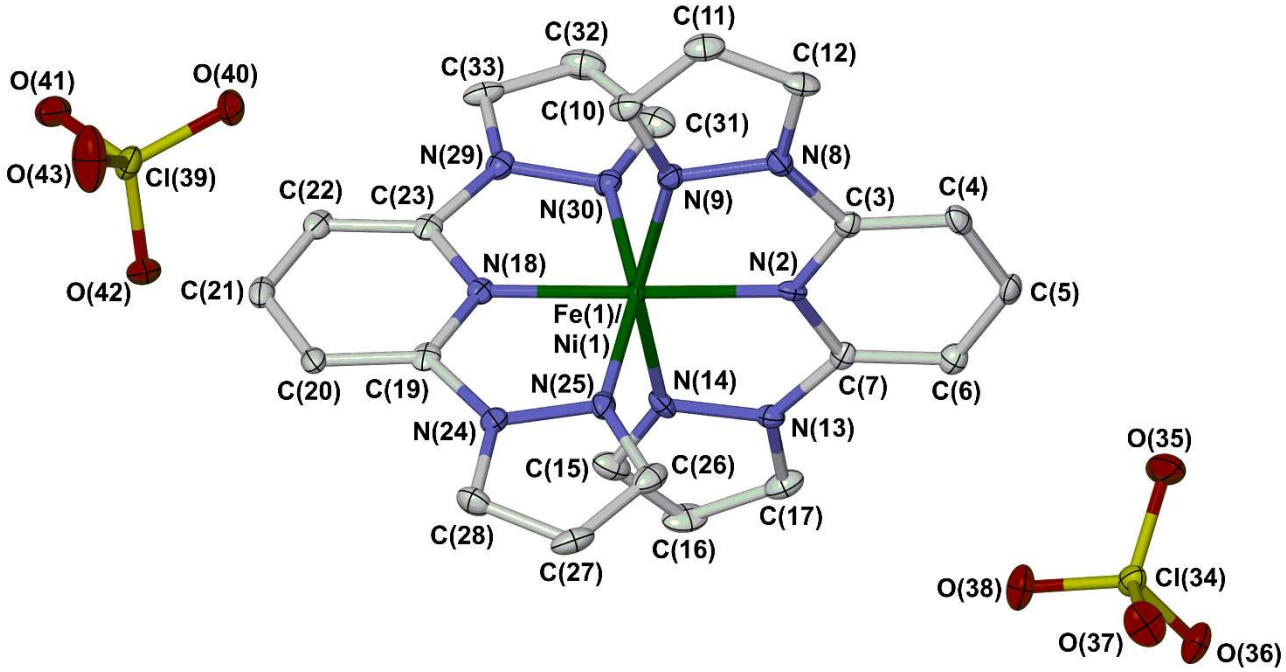

Figure S9 The asymmetric unit of **2a** at 100 K, with the full atom numbering schemes. Details as for Figure S8.

Table S6 Selected crystallographic bond lengths (Å) and angles (°) for the $[Fe_xNi_{1-x}(bpp)_2][ClO_4]_2$ single crystals at 100 K . The atom numbering is shown in Figures S8 and S9, with M(1) corresponding to the $Fe(1)_x/Ni(1)_{1-x}$ composite atom. Italicised parameters in curly brackets are expected values calculated from low-spin $[Fe(bpp)_2][BF_4]_2$[12] and $[Ni(bpp)_2][ClO_4]_2$ (Table S2), in the appropriate weighted averages.

	1a (x = 0.50)		**2a** (x = 0.76)
T	300 K	100 K	100 K
M(1)–N(2)	2.058(4) *{2.067(4)}*	1.952(3) *{1.955(3)}*	1.940(4) *{1.926(3)}*
M(1)–N(9)	2.150(5) *{2.156(4)}*	2.050(4) *{2.053(3)}*	2.022(5) *{2.018(3)}*
M(1)–N(14)	2.127(5) *{2.132(4)}*	2.024(4) *{2.029(3)}*	1.996(5) *{1.997(3)}*
M(1)–N(18)	2.063(4) *{2.066(4)}*	1.952(3) *{1.953(3)}*	1.936(4) *{1.927(3)}*
M(1)–N(25)	2.155(5) *{2.154(4)}*	2.050(4) *{2.056(4)}*	2.019(5) *{2.020(4)}*
M(1)–N(30)	2.132(5) *{2.143(4)}*	2.034(3) *{2.036(4)}*	2.007(5) *{2.002(4)}*
M(1)–N{pyridyl}$_{average}$	2.061(6) *{2.066(5)}*	1.952(4) *{1.954(5)}*	1.938(6) *{1.927(5)}*
M(1)–N{pyrazolyl}$_{average}$	2.141(10) *{2.146(8)}*	2.040(8) *{2.043(7)}*	2.011(10) *{2.009(7)}*
N(2)–M(1)–N(9)	75.29(19) *{75.14(14)}*	78.28(13) *{78.36(13)}*	78.82(17) *{79.16(13)}*
N(2)–M(1)–N(14)	74.9(2) *{75.31(14)}*	78.72(13) *{78.57(13)}*	79.64(17) *{79.39(13)}*
N(2)–M(1)–N(18) (ϕ)[a]	175.9(2) *{175.13(16)}*	177.49(15) *{177.55(15)}*	177.6(2) *{177.78(15)}*
N(2)–M(1)–N(25)	108.78(19) *{109.62(14)}*	104.13(13) *{104.02(14)}*	103.46(18) *{102.94(14)}*
N(2)–M(1)–N(30)	100.5(2) *{100.11(15)}*	99.01(13) *{98.97(13)}*	98.39(18) *{98.43(13)}*
N(9)–M(1)–N(14)	150.2(2) *{150.42(14)}*	156.98(13) *{156.91(13)}*	158.45(16) *{158.55(13)}*
N(9)–M(1)–N(18)	104.47(18) *{104.10(14)}*	102.59(13) *{102.36(13)}*	102.07(18) *{101.53(13)}*
N(9)–M(1)–N(25)	96.15(18) *{96.98(14)}*	94.32(13) *{94.31(13)}*	93.95(19) *{93.70(13)}*
N(9)–M(1)–N(30)	93.03(19) *{92.74(14)}*	92.32(13) *{92.37(13)}*	92.30(19) *{92.25(13)}*
N(14)–M(1)–N(18)	105.1(2) *{105.20(14)}*	100.35(13) *{100.67(13)}*	99.43(17) *{99.88(13)}*
N(14)–M(1)–N(25)	94.76(19) *{94.45(14)}*	92.13(13) *{92.18(13)}*	91.79(19) *{91.78(13)}*
N(14)–M(1)–N(30)	90.9(2) *{90.90(15)}*	90.38(13) *{90.42(13)}*	90.05(19) *{90.28(13)}*
N(18)–M(1)–N(25)	75.28(19) *{75.06(14)}*	78.20(13) *{78.31(13)}*	78.76(18) *{79.15(13)}*
N(18)–M(1)–N(30)	75.5(2) *{75.26(15)}*	78.63(14) *{78.68(13)}*	79.36(18) *{79.45(13)}*
N(25)–M(1)–N(30)	150.66(19) *{150.20(14)}*	156.77(13) *{156.92(13)}*	158.04(17) *{158.54(13)}*
α	75.2(4) {*75.2(3)*}	78.5(3) {*78.5(3)*}	79.1(3) {*79.3(3)*}
V_{Oh}	11.76(2) {*11.86(1)*}	10.384(11) {*10.470(7)*}	10.073(14) {*10.028(7)*}
θ[a]	89.46(4) *{89.68(3)}*	89.35(3) *{89.37(3)}*	89.31(4) *{89.37(3)}*
Θ[a]	435.6(17) *{438}*	332.9(11) *{330}*	311.6(15) *{308}*

[a]Defined on page S13.

α is the average internal chelate bite angle of the bpp ligands in the molecule. V_{Oh} is the volume of the MN_6 coordination octahedron in the complex.[8] Θ is a bond angle parameter describing the position of the coordination geometry along the octahedral−trigonal prismatic distortion pathway (page S13).[8] All these parameters are sensitive to both the metal composition of the crystal, and the spin state of its iron fraction.

θ and ϕ describe the angular Jahn-Teller distortion exhibited by many high-spin $[Fe(bpp)_2]^{2+}$ derivatives, which are also described on page S13.[12-14]

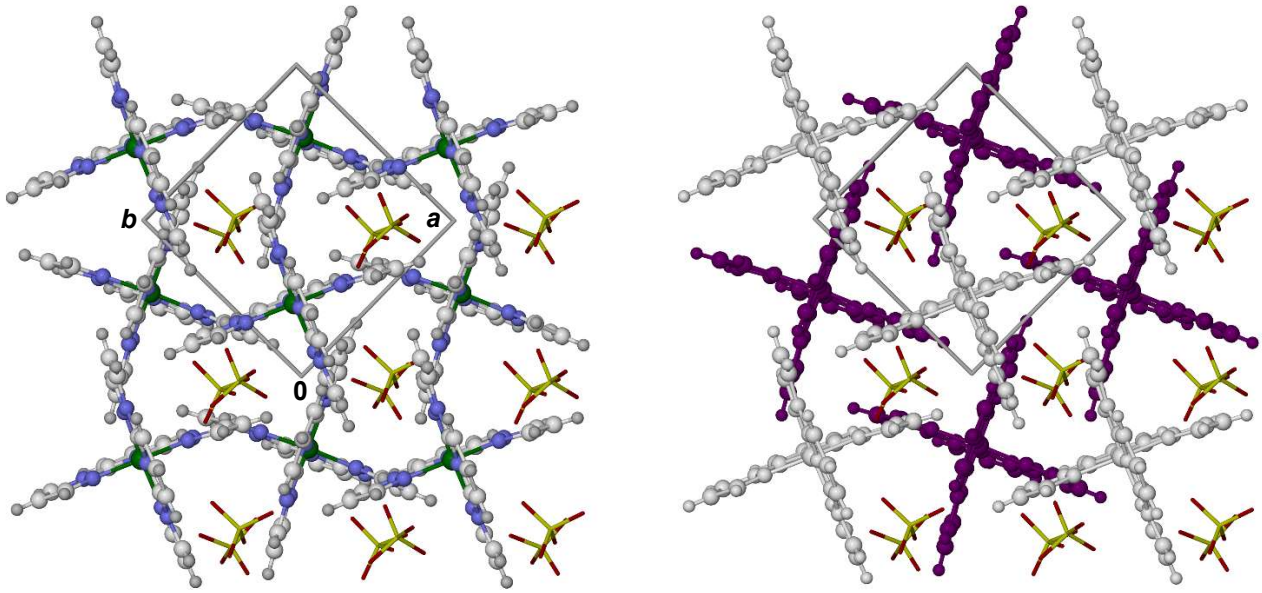

Figure S10 Packing diagrams of **2a** at 100 K viewed perpendicular to (001), which is the plane of the terpyridine embrace cation layers.[19,20] The ClO_4^- ions are de-emphasised for clarity. Left: colour coded by element as below. Right: the same view, with alternate cation layers colour coded white and purple.

Element colour code: C, white; H, pale grey; Cl, yellow; Fe/Ni, green; N, blue; O, red.

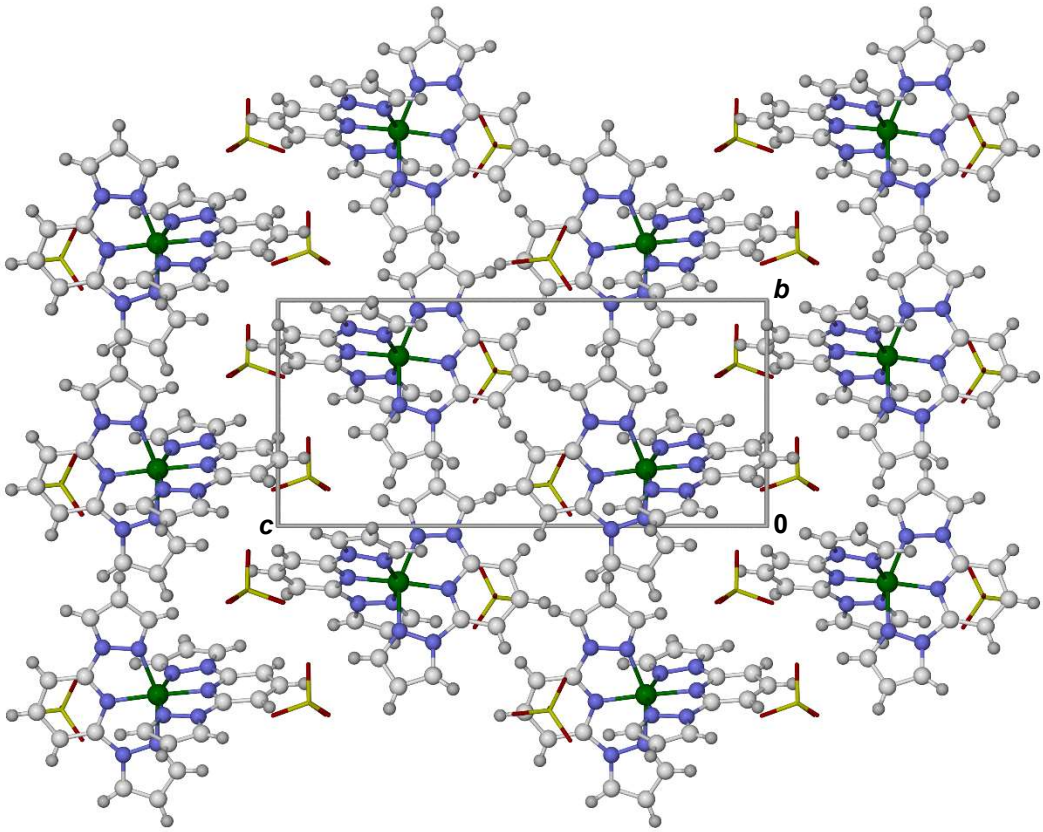

Figure S11 Packing diagram of **2a** at 100 K viewed perpendicular (100), within the plane of the terpyridine embrace cation layers. Details as for Figure S10.

Table S7 Variable temperature single crystal unit cells for **1a** (monoclinic, space group $P2_1$). Data at 300 K and 100 K are from full structure refinements at those temperatures, and thus have lower errors.

T / K	a / Å	b / Å	c / Å	β / °	V / Å^3
350	8.5942(18)	8.6594(16)	19.298(5)	95.97(2)	1428.4(6)
340	8.5866(14)	8.6510(12)	19.291(4)	96.126(17)	1424.8(4)
330	8.5812(18)	8.6494(15)	19.269(5)	96.17(2)	1421.9(5)
320	8.5789(14)	8.6423(12)	19.242(4)	96.229(6)	1418.2(4)
310	8.5704(13)	8.6391(11)	19.226(4)	96.342(15)	1414.8(4)
300	8.5567(7)	8.6233(6)	19.2053(15)	96.371(7)	1408.35(19)
290	8.5626(12)	8.6312(11)	19.184(3)	96.472(14)	1408.8(4)
280	8.5589(11)	8.6248(10)	19.160(3)	96.611(13)	1404.9(3)
270	8.5582(13)	8.6229(11)	19.122(4)	96.691(15)	1401.5(4)
260	8.5549(12)	8.624(10)	19.091(3)	96.845(13)	1398.5(4)
250	8.5617(11)	8.6315(9)	18.992(3)	97.302(12)	1392.1(3)
240	8.5599(13)	8.6318(10)	18.908(3)	97.707(13)	1384.4(4)
230	8.5471(11)	8.6193(10)	18.843(3)	97.827(12)	1375.3(3)
220	8.5413(9)	8.6126(8)	18.823(2)	97.929(9)	1371.5(3)
210	8.5389(9)	8.6088(8)	18.805(3)	97.978(9)	1369.0(3)
200	8.5313(9)	8.6036(8)	18.785(3)	98.007(10)	1365.4(3)
190	8.5299(8)	8.5992(7)	18.785(2)	98.050(8)	1364.3(2)
180	8.5248(9)	8.5935(8)	18.773(2)	98.054(9)	1361.7(3)
170	8.5243(7)	8.5920(7)	18.771(2)	98.108(7)	1361.0(2)
160	8.5216(9)	8.5853(8)	18.764(2)	98.127(9)	1359.0(3)
150	8.5173(10)	8.5831(9)	18.762(3)	98.158(9)	1357.7(3)
140	8.5095(8)	8.5737(7)	18.746(2)	98.158(8)	1353.9(2)
130	8.5097(8)	8.5741(7)	18.746(2)	98.189(8)	1353.8(2)
120	8.5071(7)	8.5668(7)	18.743(2)	98.222(7)	1351.9(2)
110	8.5042(7)	8.5627(7)	18.737(2)	98.223(7)	1350.4(2)
100	8.4917(4)	8.5533(4)	18.7301(8)	98.182(4)	1346.57(11)

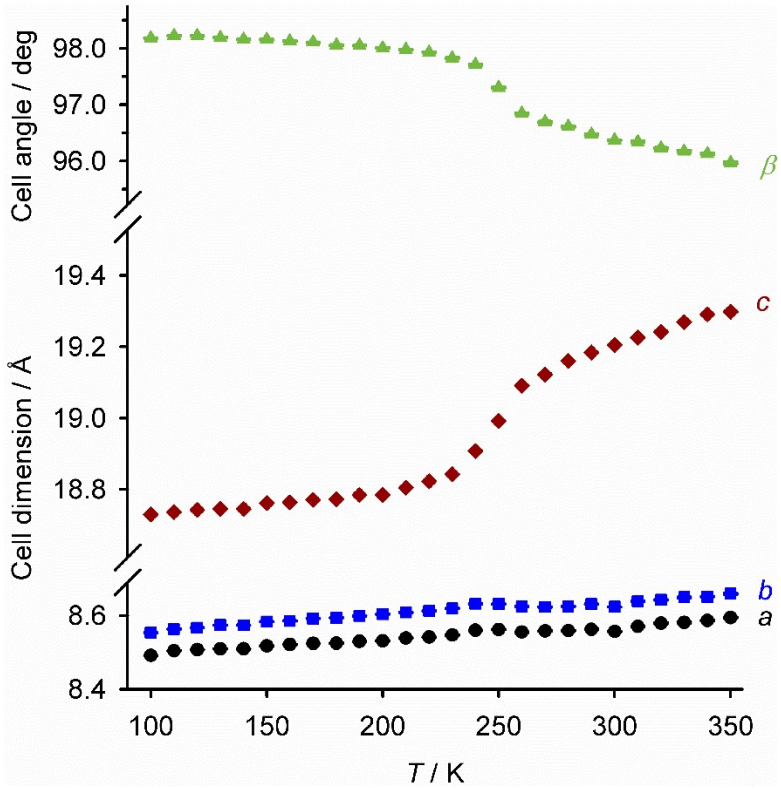

Figure S12 Variable temperature unit cell parameters for **1a** (Table S7).

Table S8 Variable temperature single crystal unit cells for **2a** (monoclinic, space group $P2_1$). Data at 100 K are from the full structure refinement at that temperature, and thus have lower errors.

T / K	a / Å	b / Å	c / Å	β / °	V / Å^3
350	8.585(4)	8.643(8)	19.422(9)	95.47(4)	1434.4(16)
340	8.580(3)	8.630(5)	19.396(8)	95.69(3)	1429.1(11)
330	8.5810(18)	8.631(2)	19.359(4)	95.844(18)	1426.2(5)
320	8.5697(16)	8.6124(19)	19.349(4)	95.831(17)	1420.7(5)
310	8.569(2)	8.611(2)	19.329(5)	95.92(2)	1418.6(7)
300	8.5415(13)	8.6051(14)	19.273(3)	95.935(13)	1409.0(4)
290	8.5551(15)	8.6059(16)	19.274(4)	96.051(16)	1411.1(4)
280	8.5491(15)	8.6041(16)	19.254(3)	96.102(16)	1408.3(4)
270	8.5503(14)	8.5991(15)	19.230(3)	96.197(16)	1405.6(4)
260	8.5465(16)	8.6001(17)	19.197(4)	96.289(17)	1402.5(5)
250	8.5440(13)	8.6253(13)	18.887(3)	97.656(14)	1379.4(4)
240	8.5532(9)	8.6213(10)	18.8314(19)	98.004(10)	1375.1(3)
230	8.5372(11)	8.6020(11)	18.800(2)	98.034(12)	1367.1(3)
220	8.5524(11)	8.6030(11)	18.800(2)	98.189(12)	1369.2(3)
210	8.5322(9)	8.6103(9)	18.7913(19)	98.103(10)	1366.7(3)
200	8.5305(9)	8.5939(9)	18.7702(19)	98.188(10)	1362.0(2)
190	8.5233(11)	8.5875(11)	18.762(2)	98.209(12)	1359.2(3)
180	8.5246(9)	8.5856(9)	18.7532(19)	98.249(10)	1358.3(2)
170	8.5154(8)	8.5865(8)	18.7501(18)	98.224(9)	1356.9(2)
160	8.5134(9)	8.5813(9)	18.736(2)	98.256(10)	1354.6(2)
150	8.5129(8)	8.5677(8)	18.7201(18)	98.317(9)	1351.0(2)
140	8.5056(8)	8.5722(8)	18.7230(17)	98.315(9)	1350.8(2)
130	8.5065(8)	8.5590(8)	18.7052(18)	98.367(9)	1347.4(2)
120	8.5005(8)	8.5521(8)	18.6939(17)	98.393(9)	1344.4(2)
110	8.4994(8)	8.5483(7)	18.6915(17)	98.413(9)	1343.4(2)
100	8.4873(5)	8.5486(5)	18.6946(10)	98.424(5)	1341.74(13)

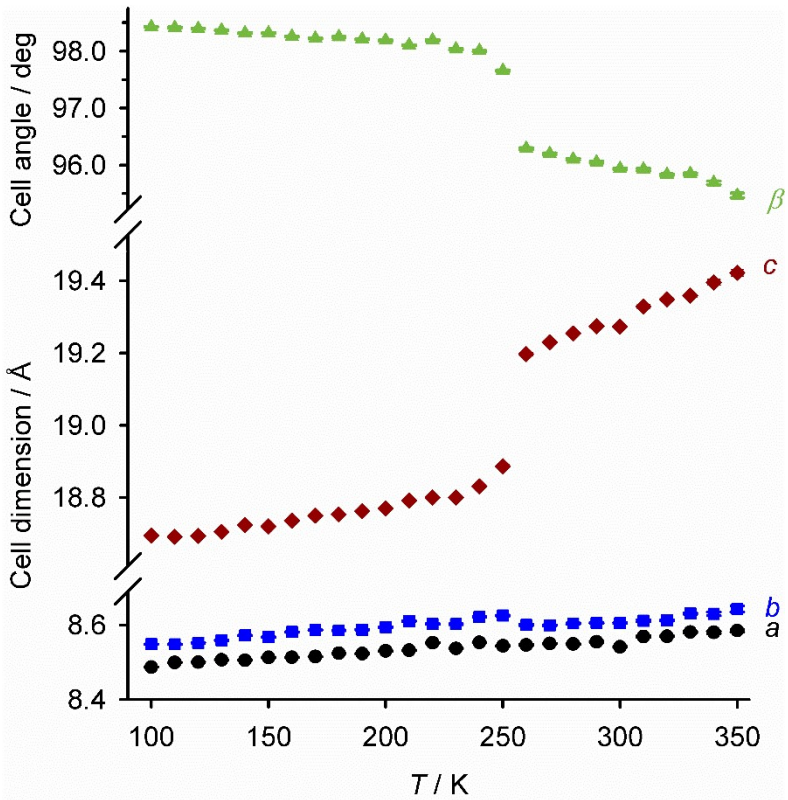

Figure S13 Variable temperature unit cell parameters for **2a** (Table S8).

Table S9 Absolute and % isothermal changes to the unit cell parameters during high→low-spin SCO, Δx_{SCO} ($x = a, b, c, \beta, V$), in **1a**, **1b** and materials from the $[Fe_xNi_{1-x}(bpp)_2][BF_4]_2$ series (ref. 6). Data for each compound are calculated at $T_{½}$ (Table 1, main article), by linear extrapolation of the low-spin and high-spin parameters to that temperature.

	x		Δa_{SCO} / Å	Δb_{SCO} / Å	Δc_{SCO} / Å	$\Delta\beta_{SCO}$ / deg	Δab_{SCO} / Å^2 [a]	ΔV_{SCO} / Å^3
1a	0.50	Δx_{SCO}	+0.0113(16)	+0.0149(13)	–0.264(4)	+1.030(18)	+0.22(2)	–19.0(5)
		%	+0.13	+0.17	–1.38	+1.06	+0.31	–1.36
2a	0.76	Δx_{SCO}	+0.015(2)	+0.030(2)	–0.351(5)	+1.67(2)	+0.38(3)	–21.9(6)
		%	+0.17	+0.35	–1.83	+1.73	+0.52	–1.57
$[Fe_{0.46}Ni_{0.54}(bpp)_2][BF_4]_2$	0.48	Δx_{SCO}	–0.0041(8)	+0.0213(10)	–0.264(2)	+0.800(10)	+0.146(16)	–18.8(3)
		%	–0.05	+0.25	–1.40	+0.83	+0.20	–1.38
$[Fe(bpp)_2][BF_4]_2$	1.00	Δx_{SCO}	+0.0231(6)	+0.074(2)	–0.5570(9)	+2.027(5)	+0.82(2)	–30.4(3)
		%	+0.27	+0.87	–2.93	+2.11	+1.14	–2.23

[a] Δab_{SCO} denotes the change in the area of the 2D cation layers in the unit cell during SCO, where ab is the product of the a and b unit cell dimensions (Figure S11). The change in the distance between the cation layers is given by Δc_{SCO}.

These parameters for **1a** and the $[Fe_{0.48}Ni_{0.52}(bpp)_2][BF_4]_2$ crystal are all broadly similar, leading to their identical ΔV_{SCO} values within experimental error.

Assuming a linear relationship with composition,[21] and if the $P2_1$ phase of $[Fe(bpp)_2][ClO_4]_2$ behaves similarly to the BF_4^- salt, then the values for **2a** should all be approximately midway between **1a** and $[Fe(bpp)_2][BF_4]_2$. On that basis, only $\Delta\beta_{SCO}$ is close to its expected value. The unit cell dimensions a, b and c all undergo smaller changes during SCO than expected in **2a**, contributing to its anomalously small ΔV_{SCO} (Figure S14).

A more detailed discussion of the structural changes during SCO in the $P2_1$ phase can be found in ref. 6.

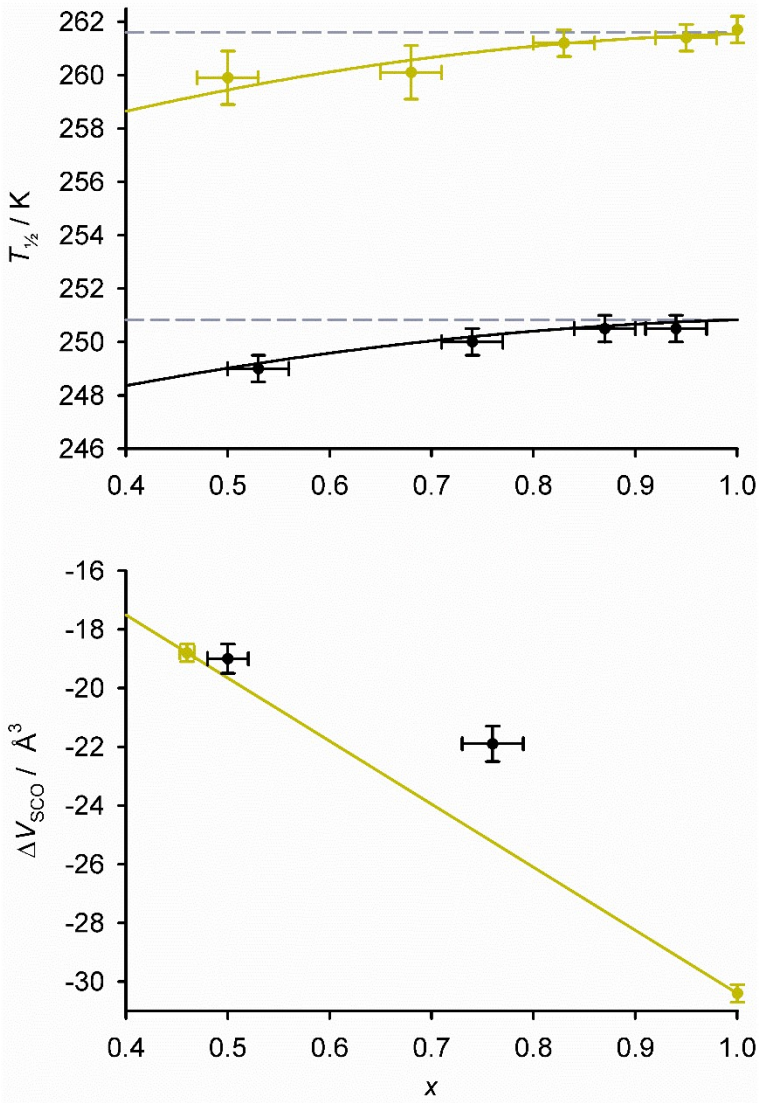

Figure S14 Variation of $T_{½}$ (top) and ΔV_{SCO} (bottom) with composition (x; Table 1, main article) for **1a**-**4a** (black), and for compounds from the $[Fe_xNi_{1-x}(bpp)_2][BF_4]_2$ series (yellow).[1,6] Datapoints on the $T_{½}$ graph are connected by regression curves for clarity, and the actual or predicted $T_{½}$ values for the $P2_1$ phases of both salts of the pure iron complex are shown with grey lines.

The dependence of $T_{½}$ on composition is small, and is similar for both salts. $T_{½}$ for the putative $P2_1$ phase of $[Fe(bpp)_2][ClO_4]_2$ is predicted to be 10 K below that of $[Fe(bpp)_2][BF_4]_2$.

A linear relationship between ΔV_{SCO} and x has been proposed in other SCO materials.[21] While ΔV_{SCO} for **1a** and for a crystal of formula $[Fe_{0.48}Ni_{0.52}(bpp)_2][BF_4]_2$[6] are very similar, on that basis ΔV_{SCO} for **2a** is smaller than expected based on the available data. The individual unit cell parameters a, b and c all undergo smaller changes during SCO in **2a** than predicted, based on previous work (Table S9).

That result could mean the relationship between ΔV_{SCO} and x is non-linear in these compounds. Alternatively the structural chemistry of **2a** might differ from the other samples if, for example, lattice effects make the iron coordination sphere in high-spin **2a** more compact than in the other materials.[6] That possibility can't be ruled out because a high-spin crystal structure of **2a** was not achieved (although the molecular structure of low-spin **2a** is as-expected, Table S6).

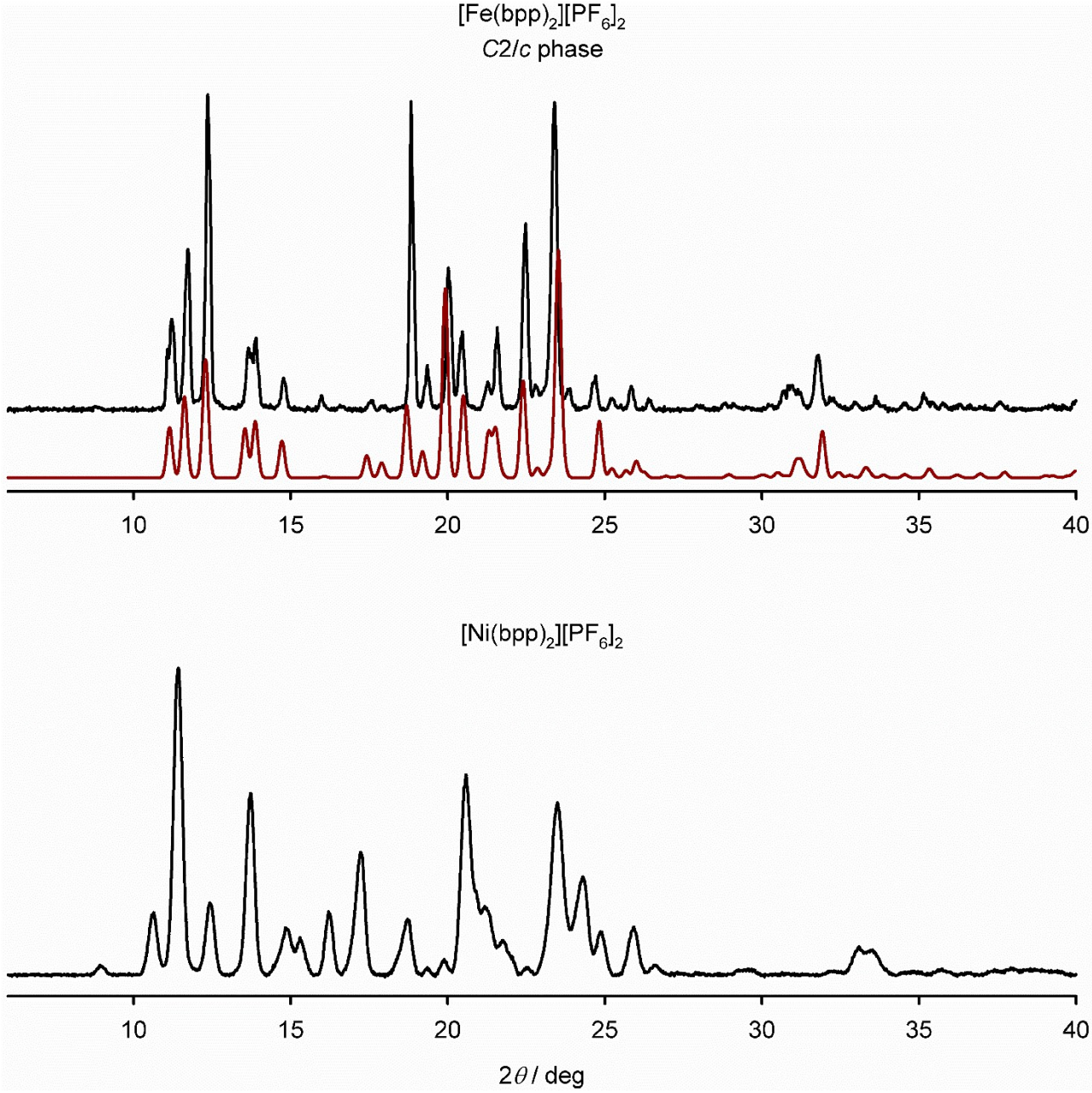

Figure S15 Room temperature X-ray powder diffraction data for the PF_6^- salts of the complexes in this work (black), and the crystallographic simulation of the iron complex (red).

The iron complex simulation is based on the room temperature single crystal refinement reported in this work. As for the corresponding perchlorate salt, simulations using the previously published low temperature crystal structure[3] were less satisfactory (*cf* Figure S16).

$[Fe(bpp)_2][PF_6]_2$ is isomorphous with $[Fe(bpp)_2][ClO_4]_2$, in the *C*2/*c* crystal phase.[12] However, $[Ni(bpp)_2][PF_6]_2$ and $[Ni(bpp)_2][ClO_4]_2$ (Figure S5) are not isomorphous, on the basis of these data. Since no crystal structure of $[Ni(bpp)_2][PF_6]_2$ was achieved – its single crystals are hard to obtain, and intractably sensitive to solvent loss – the structure of this material is unknown.

Because of that structural ambiguity, the solid solutions $[Fe_xNi_{1-x}(bpp)_2][PF_6]_2$ were not investigated in this study.

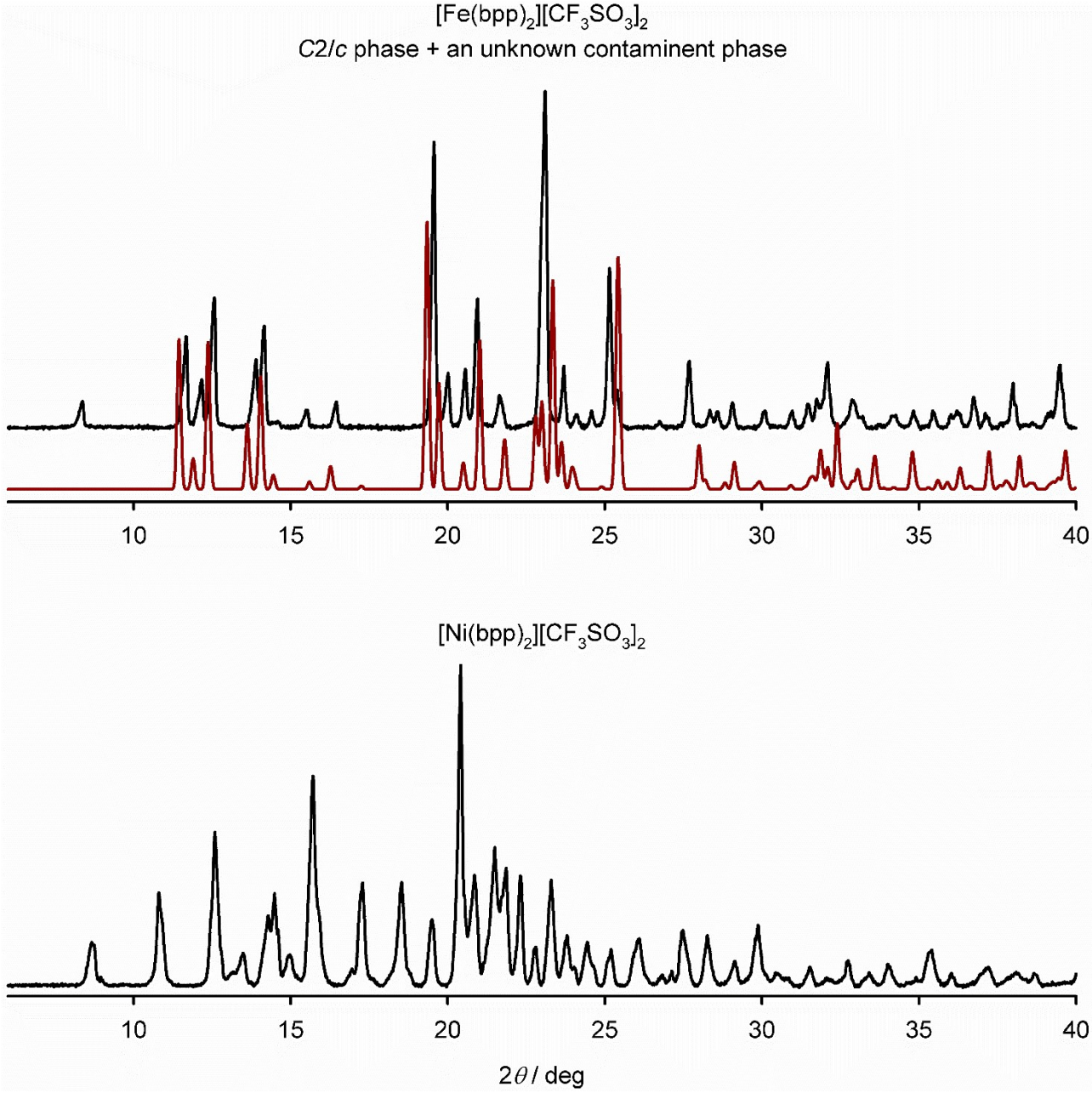

Figure S16 Room temperature X-ray powder diffraction data for the $CF_3SO_3^-$ salts of the complexes in this work (black), and the crystallographic simulation of the iron complex (red).

The iron complex crystallises from common organic solvents as a mixture of yellow solid (high-spin), and a brown (low-spin) material which can be oily in some samples. The yellow component is the major component of the samples, which also adopts the *C*2/*c* crystal phase.[14]

A room temperature crystal structure of $[Fe(bpp)_2][CF_3SO_3]_2$ was not achieved for this study, so the simulation in the Figure is based on the published structure of that salt at 120 K.[14] The measured and simulated peak 2θ values in the Figure show some differences, reflecting the different temperatures of the two measurements. However, the *C*2/*c* phase is clearly the main component of the sample, with a second polycrystalline contaminent. The same two phases, in different ratios, are obtained upon rapid precipitation or slow recrystallisation of the compound.

The powder pattern of $[Ni(bpp)_2][CF_3SO_3]_2$ is very different from $[Ni(bpp)_2][ClO_4]_2$ (Figure S5) and $[Ni(bpp)_2][PF_6]_2$ (Figure S15). Since no crystal structure of $[Ni(bpp)_2][CF_3SO_3]_2$ was achieved, and because both the iron and nickel triflate salts are difficult to crystallise, $[Fe_xNi_{1-x}(bpp)_2][CF_3SO_3]_2$ solid solutions were also not pursued further.

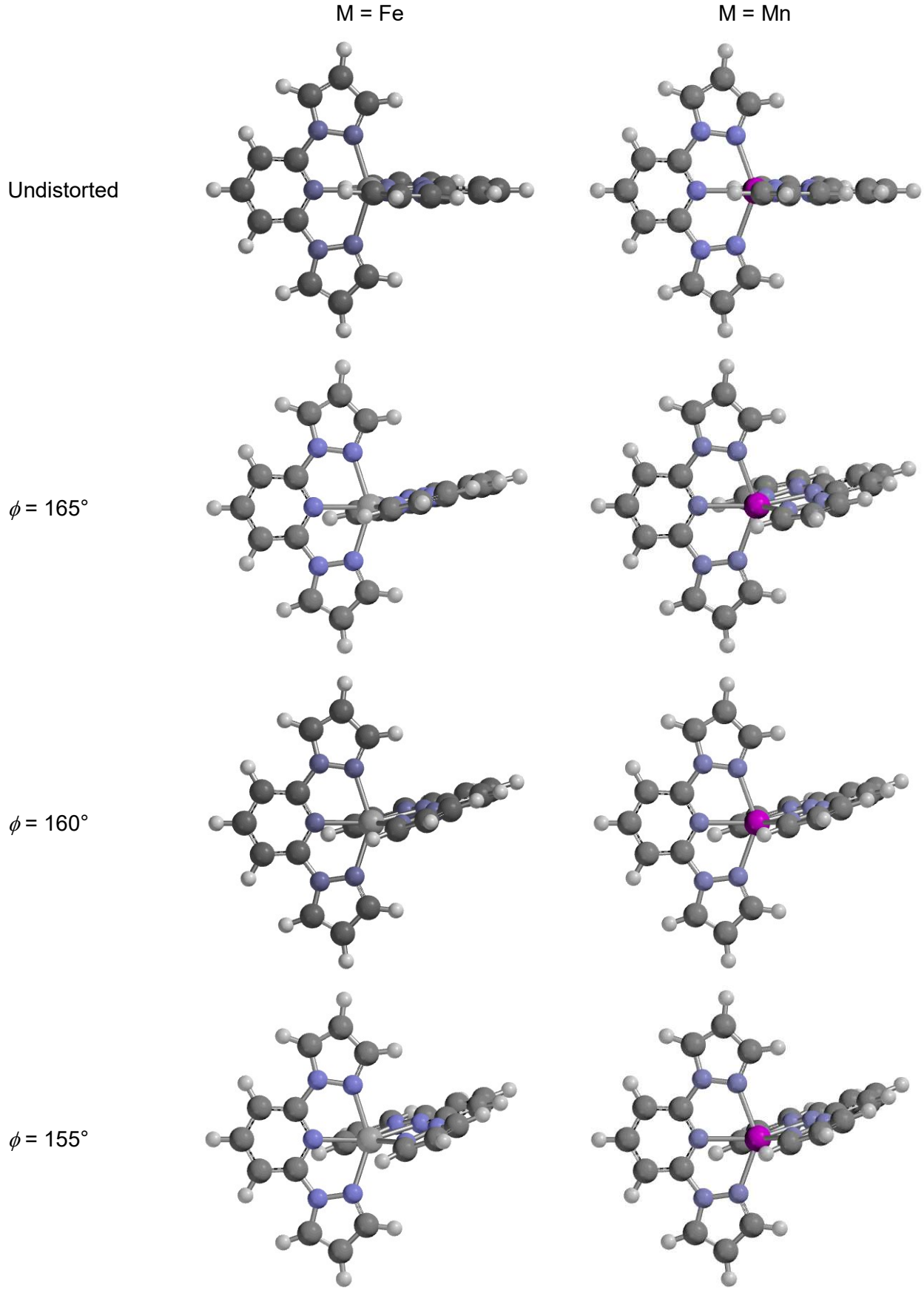

Figure S17 Views of the energy minimised $[M(bpp)_2]^{2+}$ molecules computed in the DFT study. The calculations of the iron complex are reproduced from ref. 14.

Colour code: C, dark grey; H, white; Fe, pale grey; Mn, purple; N, pale blue.

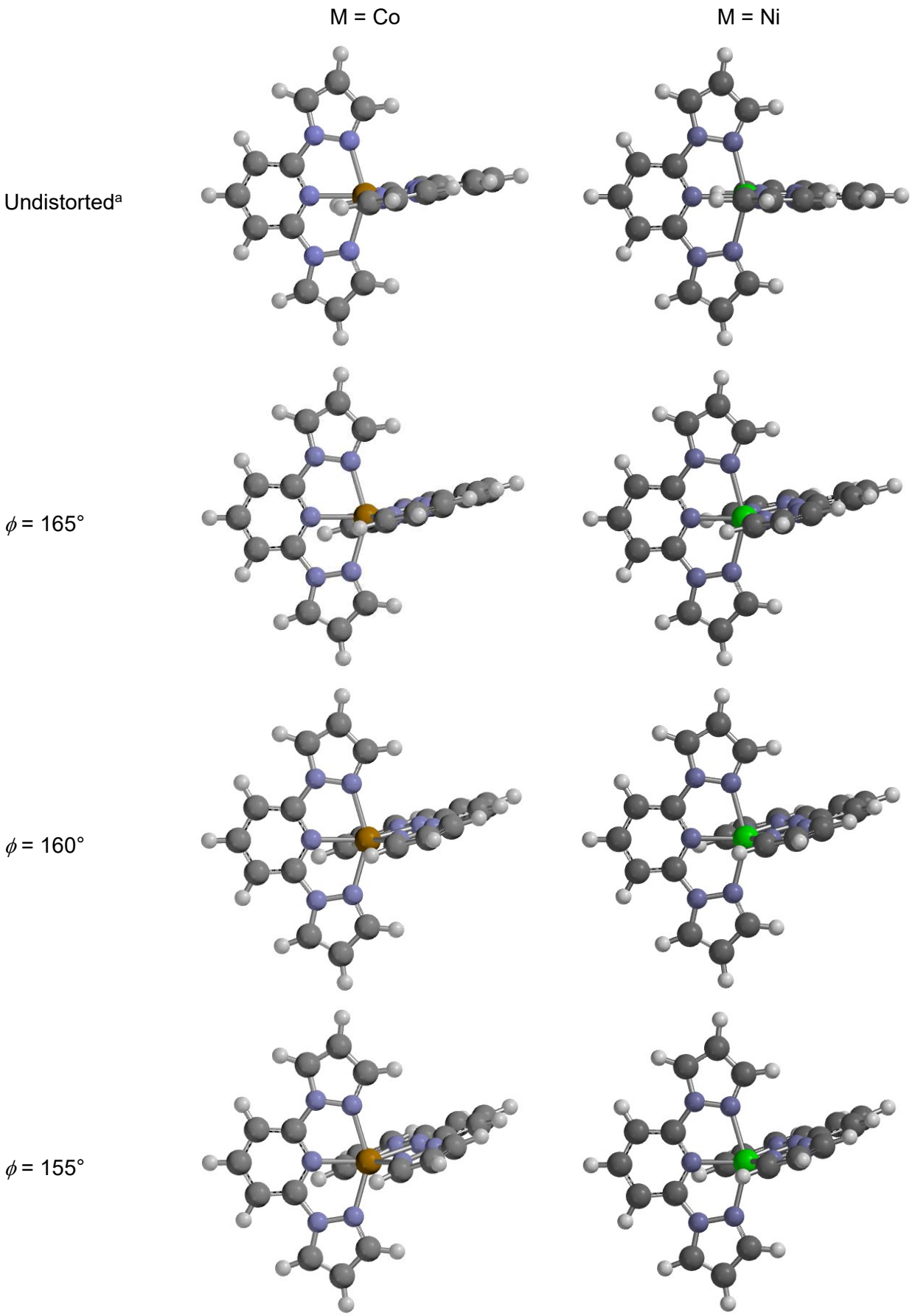

Figure S17 (continued).

Colour code: C, dark grey; H, white; Co, orange; N, pale blue; Ni, green. [a]The "undistorted" minimisation of $[Co(bpp)_2]^{2+}$ has ϕ = 171.4°. See the discussion on page S42 for more details.

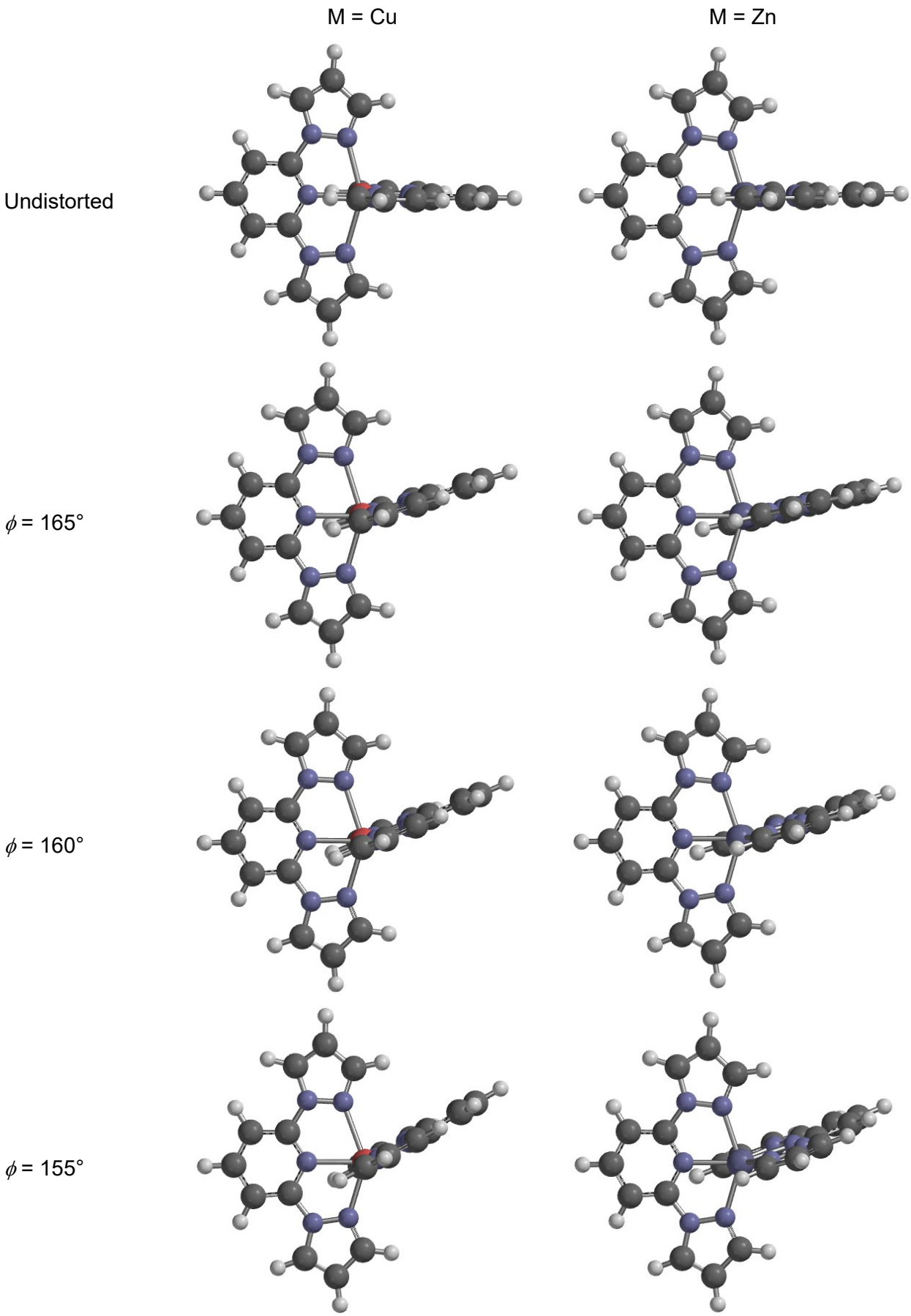

Figure S17 (continued).

Colour code: C, dark grey; H, white; Cu, pink; N, pale blue; Zn, dark blue.

M = Ru

Undistorted

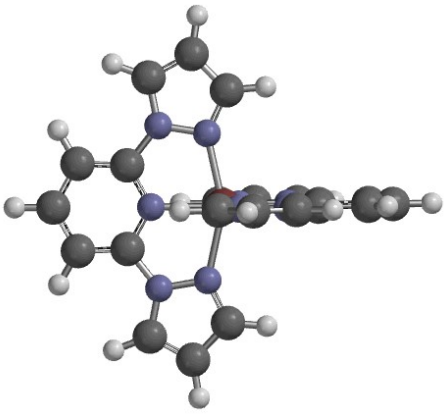

ϕ = 165°

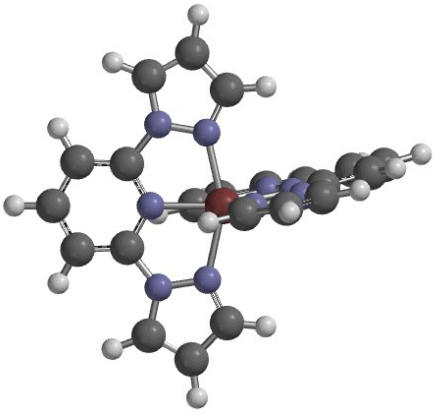

ϕ = 160°

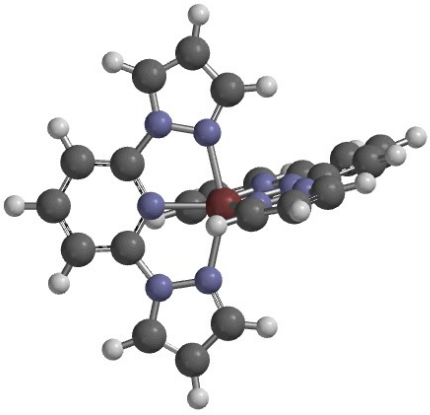

ϕ = 155°

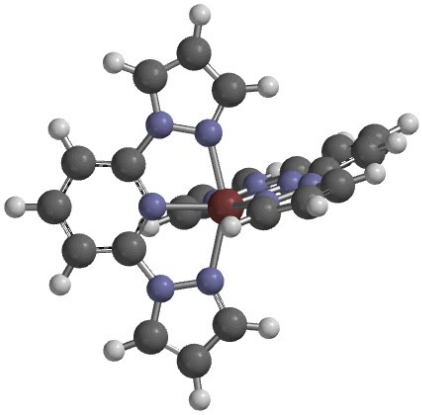

Figure S17 (continued).

Colour code: C, dark grey; H, white; N, pale blue; Ru, red.

Table S10 Computed energies for the minimised geometric distortions of high-spin $[Fe(bpp)_2]^{2+}$ and other $[M(bpp)_2]^{2+}$ complexes. These data are plotted in Figure 2 of the main article. ϕ is the *trans*-N{pyridyl}−Fe−N{pyridyl} bond angle (page S13).[12,13]

	S	ϕ / deg	E / Ha	ΔE{dist}/ kcal mol^{-1} [a]
M = Fe[b]	2	180	−2659.879095	0
		165[c]	−2659.879099	0
		160[c]	−2659.878865	+0.14
		155[c]	−2659.878283	+0.51
M = Mn	5/2[d]	180	−2547.182719	0
		165[c]	−2547.182533	+0.12
		160[c]	−2547.182218	+0.31
		155[c]	−2547.181612	+0.69
M = Co	3/2[d]	171.4[e]	−2778.945336	0
		165[c]	−2778.945028	+0.19
		160[c]	−2778.944104	+0.77
		155[c]	−2778.942577	+1.73
M = Ni	1	179.3	−2904.505787	0
		165[c]	−2904.503324	+1.55
		160[c]	−2904.501194	+2.88
		155[c]	−2904.498362	+4.66
M = Cu	1/2	180	−3036.642087	0
		165[c]	−3036.640850	+0.78
		160[c]	−3036.640122	+1.23
		155[c]	−3036.639626	+1.54
M = Zn	0	179.8	−3175.568354	0
		165[c]	−3175.567778	+0.36
		160[c]	−3175.567072	+0.80
		155[c]	−3175.566248	+1.32
M = Ru	0	179.8	−1491.073030	0
		165[c]	−1491.066177	+4.30
		160[c]	−1491.060492	+7.87
		155[c]	−1491.053195	+12.45

[a] ΔE(dist) is the energy relative to the corresponding undistorted molecule with $\phi \approx 180°$. [b] Taken from ref. 14. [c] Fixed during the minimisation. [d] Salts of $[Mn(bpp)_2]^{2+}$ and $[Co(bpp)_2]^{2+}$ are high-spin. [e] This molecule did not minimise successfully to an undistorted structure with $\phi \approx 180°$.

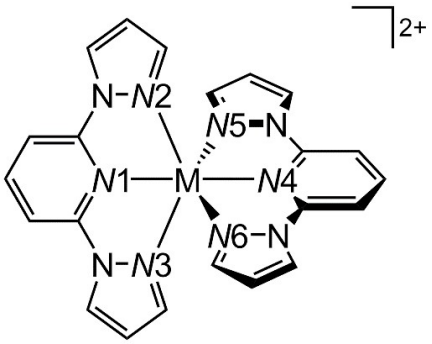

Scheme S3 Atom numbering scheme used for the DFT-minimised molecules in Tables S11-S17 (M^{2+} = Fe^{2+}, Mn^{2+}, Co^{2+}, Ni^{2+}, Cu^{2+}, Zn^{2+} or Ru^{2+}).

Table S11 Computed metric parameters for the energy-minimised geometries of $[Fe(bpp)_2]^{2+}$ (Å, °; Figure S17). The atom numbering is shown in Scheme S3, and crystallographic data for the undistorted complex are included in square brackets for comparison. ϕ and θ are defined on page S13. These data are reproduced from ref. 14.

ϕ	Undistorted[a]	165[b]	160[b]	155[b]
Fe–*N*1	2.163 [2.1390(14)]	2.167	2.171	2.175
Fe–*N*2	2.198 [2.2063(17)]	2.208	2.207	2.213
Fe–*N*3	2.198 [2.1865(19)]	2.189	2.187	2.182
Fe–*N*4	2.163 [2.1402(15)]	2.167	2.171	2.175
Fe–*N*5	2.198 [2.203(2)]	2.208	2.207	2.213
Fe–*N*6	2.198 [2.1964(19)]	2.189	2.186	2.182
Fe–N{pyridyl}$_{average}$	2.163 [2.140(2)]	2.167	2.171	2.175
Fe–N{pyrazolyl}$_{average}$	2.198 [2.198(4)]	2.199	2.197	2.198
*N*1–Fe–*N*2	72.9 [73.68(6)]	72.5	72.3	71.9
*N*1–Fe–*N*3	72.9 [73.23(6)]	73.0	72.9	72.9
*N*1–Fe–*N*4 (ϕ)	180.0 [172.98(7)]	165.0	160.0	155.0
*N*1–Fe–*N*5	107.1 [113.16(7)]	96.7	93.5	90.3
*N*1–Fe–*N*6	107.1 [100.15(7)]	118.2	122.4	126.6
*N*2–Fe–*N*3	145.8 [146.88(7)]	145.1	144.1	143.2
*N*2–Fe–*N*4	107.1 [104.33(6)]	96.7	93.5	90.3
*N*2–Fe–*N*5	96.8 [98.35(7)]	90.1	90.8	90.3
*N*2–Fe–*N*6	93.1 [93.03(7)]	99.3	99.8	100.5
*N*3–Fe–*N*4	107.1 [108.32(6)]	118.2	122.4	126.5
*N*3–Fe–*N*5	93.1 [95.93(7)]	99.3	99.8	100.5
*N*3–Fe–*N*6	96.8 [91.23(7)]	91.9	91.5	91.6
*N*4–Fe–*N*5	72.9 [73.68(7)]	72.5	72.3	71.9
*N*4–Fe–*N*6	72.9 [73.10(7)]	73.0	72.9	72.9
*N*5–Fe–*N*6	145.8 [146.60(7)]	145.1	144.1	143.2
α	72.9 [73.42(13)]	72.8	72.6	72.4
θ	87.0 [89.94(2)]	84.1	82.2	78.9

[a]Crystallographic data from $[Fe(bpp)_2]_2[BF_4]_2$, ref. 12. [b]Fixed value.

Table S12 Computed metric parameters for the energy-minimised geometries of $[Mn(bpp)_2]^{2+}$ (Å, °; Figure S17). The atom numbering is shown in Scheme S3, and ϕ and θ are defined on page S13.

ϕ	Undistorted	165	160	155
Mn–*N*1	2.268	2.266	2.266	2.268
Mn–*N*2	2.256	2.263	2.269	2.273
Mn–*N*3	2.256	2.246	2.240	2.236
Mn–*N*4	2.268	2.266	2.266	2.268
Mn–*N*5	2.256	2.263	2.269	2.273
Mn–*N*6	2.256	2.246	2.240	2.236
Mn–N{pyridyl}$_{average}$	2.268	2.266	2.266	2.268
Mn–N{pyrazolyl}$_{average}$	2.256	2.255	2.255	2.255
*N*1–Mn–*N*2	70.2	70.0	69.9	69.7
*N*1–Mn–*N*3	70.2	70.4	70.6	70.6
*N*1–Mn–*N*4 (ϕ)	180.0	165[b]	160[b]	155[b]
*N*1–Mn–*N*5	109.8	99.5	96.2	92.9
*N*1–Mn–*N*6	109.8	120.4	124.0	127.6
*N*2–Mn–*N*3	140.4	140.1	139.8	139.3
*N*2–Mn–*N*4	109.8	99.5	96.2	92.9
*N*2–Mn–*N*5	96.6	94.5	93.9	93.4
*N*2–Mn–*N*6	96.6	97.2	97.2	97.2
*N*3–Mn–*N*4	109.8	120.4	124.0	127.6
*N*3–Mn–*N*5	96.6	97.2	97.2	97.2
*N*3–Mn–*N*6	96.6	97.8	98.8	99.8
*N*4–Mn–*N*5	70.2	70.0	69.9	69.7
*N*4–Mn–*N*6	70.2	70.4	70.6	70.6
*N*5–Mn–*N*6	140.4	140.1	139.8	139.3
α	70.2	70.2	70.3	70.2
θ	90.0	85.8	84.3	81.4

[a]Fixed value.

Table S13 Computed metric parameters for the energy-minimised geometries of $[Co(bpp)_2]^{2+}$ (Å, °; Figure S17). The atom numbering is shown in Scheme S3, and crystallographic data for the undistorted complex are included in square brackets for comparison. ϕ and θ are defined on page S13.

ϕ	Undistorted[a]	165	160	155
Co–*N*1	2.109 [2.0802(13)]	2.109	2.114	2.119
Co–*N*2	2.169 [2.1683(16)]	2.181	2.192	2.204
Co–*N*3	2.162 [2.1438(16)]	2.154	2.145	2.136
Co–*N*4	2.108 [2.0822(14)]	2.109	2.114	2.119
Co–*N*5	2.168 [2.1644(18)]	2.181	2.192	2.204
Co–*N*6	2.164 [2.1520(18)]	2.154	2.145	2.136
Co–N{pyridyl}$_{average}$	2.109 [2.0812(19)]	2.109	2.114	2.119
Co–N{pyrazolyl}$_{average}$	2.166 [2.157(3)]	2.168	2.169	2.170
*N*1–Co–*N*2	74.3 [75.30(6)]	74.0	73.6	73.1
*N*1–Co–*N*3	74.2 [75.17(6)]	74.4	74.5	74.7
*N*1–Co–*N*4 (ϕ)	171.4 [173.70(7)][b]	165[c]	160[c]	155[c]
*N*1–Co–*N*5	99.5 [110.71(7)]	95.9	93.0	90.1
*N*1–Co–*N*6	112.5 [99.38(7)]	116.8	120.3	123.9
*N*2–Co–*N*3	147.4 [150.47(6)]	147.2	146.6	146.0
*N*2–Co–*N*4	100.4 [101.77(6)]	95.9	93.0	90.1
*N*2–Co–*N*5	98.9 [97.89(6)]	97.0	96.7	96.3
*N*2–Co–*N*6	93.4 [94.00(6)]	94.8	94.4	94.5
*N*3–Co–*N*4	111.9 [107.56(6)]	116.8	120.3	123.9
*N*3–Co–*N*5	94.2 [92.93(6)]	94.8	94.4	94.5
*N*3–Co–*N*6	90.8 [90.28(7)]	91.7	93.3	94.4
*N*4–Co–*N*5	74.4 [75.06(6)]	74.0	73.6	73.1
*N*4–Co–*N*6	74.1 [75.11(7)]	74.4	74.5	74.7
*N*5–Co–*N*6	147.7 [149.56(6)]	147.2	146.6	146.0
α	74.3 [75.16(13)]	74.2	74.1	73.9
θ	88.6 [89.86(2)]	85.3	84.4	81.9

[a]Crystallographic data from $[Co(bpp)_2]_2[BF_4]_2$, ref. 22. [b]This molecule would not minimise to a geometry with $\phi \approx 180°$. [c]Fixed value.

Table S14 Computed metric parameters for the energy-minimised geometries of $[Ni(bpp)_2]^{2+}$ (Å, °; Figure S17). The atom numbering is shown in Scheme S3, and crystallographic data for the undistorted complex are included in square brackets for comparison. ϕ and θ are defined on page S13.

ϕ	Undistorted[a]	165	160	155
Ni–*N*1	2.042 [2.0122(13)]	2.050	2.055	2.062
Ni–*N*2	2.131 [2.0944(16)]	2.155	2.167	2.181
Ni–*N*3	2.130 [2.1187(16)]	2.112	2.105	2.095
Ni–*N*4	2.043 [2.0143(14)]	2.050	2.055	2.062
Ni–*N*5	2.130 [2.1229(16)]	2.155	2.167	2.181
Ni–*N*6	2.132 [2.1006(16)]	2.112	2.105	2.095
Ni–N{pyridyl}$_{average}$	2.043 [2.0133(19)]	2.050	2.055	2.062
Ni–N{pyrazolyl}$_{average}$	2.131 [2.109(3)]	2.134	2.136	2.138
*N*1–Ni–*N*2	76.2 [77.08(6)]	75.2	74.8	74.2
*N*1–Ni–*N*3	76.2 [76.78(6)]	76.8	76.9	77.1
*N*1–Ni–*N*4 (ϕ)	179.3 [176.95(7)]	165[b]	160[b]	155[b]
*N*1–Ni–*N*5	104.5 [106.19(6)]	94.2	91.0	88.0
*N*1–Ni–*N*6	103.1 [99.90(6)]	113.8	117.2	120.5
*N*2–Ni–*N*3	152.4 [153.84(6)]	151.9	151.5	151.0
*N*2–Ni–*N*4	103.6 [102.84(6)]	94.2	91.0	88.0
*N*2–Ni–*N*5	93.5 [92.85(6)]	91.0	90.2	89.6
*N*2–Ni–*N*6	92.9 [90.65(6)]	93.1	93.1	93.0
*N*3–Ni–*N*4	104.1 [103.21(6)]	113.8	117.2	120.5
*N*3–Ni–*N*5	93.0 [95.34(6)]	93.1	93.1	93.0
*N*3–Ni–*N*6	93.7 [92.81(6)]	96.1	97.2	98.4
*N*4–Ni–*N*5	76.2 [76.86(6)]	75.2	74.8	74.2
*N*4–Ni–*N*6	76.2 [77.05(6)]	76.8	76.9	77.1
*N*5–Ni–*N*6	152.4 [153.81(6)]	151.9	151.5	151.0
α	76.2 [76.94(12)]	76.0	75.9	75.7
θ	89.3 [89.44(2)]	88.2	86.2	84.0

[a]Crystallographic data from $[Ni(bpp)_2]_2[BF_4]_2$, ref. 17. [b]Fixed value.

Table S15 Computed metric parameters for the energy-minimised geometries of $[Cu(bpp)_2]^{2+}$ (Å, °; Figure S17). The atom numbering is shown in Scheme S3, and crystallographic data for the undistorted complex are included in square brackets for comparison. ϕ and θ are defined on page S13.

ϕ	Undistorted[a]	165	160	155
Cu–*N*1	1.991 [1.9763(14)]	1.997	2.000	2.007
Cu–*N*2	2.112 [2.1080(17)]	2.070	2.061	2.049
Cu–*N*3	2.112 [2.1210(17)]	2.072	2.061	2.047
Cu–*N*4	2.055 [2.0175(15)]	2.114	2.140	2.196
Cu–*N*5	2.279 [2.2527(18)]	2.356	2.379	2.409
Cu–*N*6	2.278 [2.2259(18)]	2.241	2.216	2.182
Cu–N{pyridyl}$_{average}$	2.023 [1.9969(15)]	2.056	2.070	2.102
Cu–N{pyrazolyl}$_{average}$	2.195 [2.177(4)]	2.185	2.179	2.172
*N*1–Cu–*N*2	77.3 [77.64(6)]	77.5	77.5	77.4
*N*1–Cu–*N*3	77.3 [77.55(6)]	77.5	77.5	77.5
*N*1–Cu–*N*4 (ϕ)	180.0 [176.06(8)]	165[b]	160[b]	155[b]
*N*1–Cu–*N*5	105.1 [108.17(7]	92.6	88.5	85.3
*N*1–Cu–*N*6	105.2 [99.88(7)]	120.5	125.7	131.4
*N*2–Cu–*N*3	154.5 [155.14(6)]	155.0	154.8	154.7
*N*2–Cu–*N*4	102.7 [102.53(6)]	102.1	102.3	101.7
*N*2–Cu–*N*5	93.3 [92.51(6)]	91.6	91.3	90.0
*N*2–Cu–*N*6	93.3 [89.72(6)]	95.7	96.0	97.1
*N*3–Cu–*N*4	102.8 [102.11(6)]	102.6	102.3	102.5
*N*3–Cu–*N*5	93.3 [96.61(6)]	91.6	91.3	91.6
*N*3–Cu–*N*6	93.3 [93.03(6)]	95.1	96.0	96.7
*N*4–Cu–*N*5	74.8 [75.77(6)]	72.4	71.5	69.7
*N*4–Cu–*N*6	74.9 [76.19(6)]	74.4	74.3	73.6
*N*5–Cu–*N*6	149.7 [151.68(6)]	146.9	145.7	143.3
α	76.1 [75.16(13)]	75.5	75.2	74.6
θ	90.0 [89.5][c]	89.6	90.0	89.3

[a]Crystallographic data from $[Cu(bpp)_2]_2[BF_4]_2$ at 50 K, ref. 23. The complex exhibits fluxional disorder of its Jahn-Teller distortion at higher temperatures in the crystal. [b]Fixed value. [c]No error for this literature value could be calculated, because the crystal structure was not measured in our laboratory.

Table S16 Computed metric parameters for the energy-minimised geometries of $[Zn(bpp)_2]^{2+}$ (Å, °; Figure S17). The atom numbering is shown in Scheme S3, and crystallographic data for the undistorted complex are included in square brackets for comparison. ϕ and θ are defined on page S13.

ϕ	Undistorted[a]	165	160	155
Zn–*N*1	2.147 [2.104(3)]	2.151	2.156	2.159
Zn–*N*2	2.185 [2.160(3)]	2.212	2.224	2.239
Zn–*N*3	2.190 [2.185(3)]	2.163	2.151	2.142
Zn–*N*4	2.146 [2.097(3)]	2.151	2.156	2.159
Zn–*N*5	2.189 [2.184(4)]	2.212	2.224	2.239
Zn–*N*6	2.186 [2.176(4)]	2.163	2.151	2.142
Zn–N{pyridyl}$_{average}$	2.147 [2.101(4)]	2.151	2.156	2.159
Zn–N{pyrazolyl}$_{average}$	2.188 [2.176(7)]	2.188	2.190	2.191
*N*1–Zn–*N*2	73.5 [74.57(12)]	72.6	72.2	71.8
*N*1–Zn–*N*3	73.3 [74.15(12)]	73.8	74.0	74.2
*N*1–Zn–*N*4 (ϕ)	179.8 [172.99(15)]	165[b]	160[b]	155[b]
*N*1–Zn–*N*5	106.7 [111.98(14)]	96.8	93.8	90.7
*N*1–Zn–*N*6	106.5 [99.41(14)]	117.0	120.3	123.6
*N*2–Zn–*N*3	146.8 [148.69(12)]	146.1	145.8	145.4
*N*2–Zn–*N*4	106.3 [107.25(12)]	96.8	93.8	90.7
*N*2–Zn–*N*5	94.8 [94.90(13)]	93.3	92.5	92.0
*N*2–Zn–*N*6	94.8 [90.91(13)]	95.0	94.8	94.5
*N*3–Zn–*N*4	106.9 [103.64(12)]	117.0	120.3	123.6
*N*3–Zn–*N*5	94.6 [92.80(12)]	95.0	94.8	94.5
*N*3–Zn–*N*6	94.6 [97.95(13)]	96.2	97.7	99.0
*N*4–Zn–*N*5	73.4 [74.79(13)]	72.6	72.2	71.8
*N*4–Zn–*N*6	73.4 [73.93(14)]	73.8	74.0	74.2
*N*5–Zn–*N*6	146.8 [148.51(12)]	146.1	145.8	145.4
α	73.4 [74.4(3)]	73.2	73.1	73.0
θ	89.9 [89.81(4)]	87.2	85.6	83.4

[a]Crystallographic data from $[Zn(bpp)_2]_2[BF_4]_2$, ref. 24. [b]Fixed value.

Table S17 Computed metric parameters for the energy-minimised geometries of $[Ru(bpp)_2]^{2+}$ (Å, °; Figure S17). The atom numbering is shown in Scheme S3, and crystallographic data for the undistorted complex are included in square brackets for comparison. ϕ and θ are defined on page S13.

ϕ	Undistorted[a]	165	160	155
Ru–*N*1	2.007 [2.023(3)]	2.012	2.016	2.023
Ru–*N*2	2.089 [2.081(3)]	2.084	2.087	2.097
Ru–*N*3	2.093 [2.103(3)]	2.102	2.103	2.097
Ru–*N*4	2.006 [2.022(3)]	2.012	2.016	2.023
Ru–*N*5	2.092 [2.095(3)]	2.084	2.087	2.097
Ru–*N*6	2.089 [2.079(3)]	2.102	2.103	2.097
Ru–N{pyridyl}$_{average}$	2.007 [2.023(4)]	2.012	2.016	2.023
Ru–N{pyrazolyl}$_{average}$	2.091 [2.090(6)]	2.093	2.095	2.097
*N*1–Ru–*N*2	77.9 [78.35(11)]	77.4	77.1	76.5
*N*1–Ru–*N*3	77.8 [78.41(11)]	78.1	78.2	78.4
*N*1–Ru–*N*4 (ϕ)	179.8 [178.26(19)]	165[b]	160[b]	155[b]
*N*1–Ru–*N*5	102.2 [103.82(14)]	92.0	88.8	85.8
*N*1–Ru–*N*6	102.1 [99.83(13)]	112.4	115.8	118.9
*N*2–Ru–*N*3	155.8 [156.73(10)]	155.4	155.1	154.8
*N*2–Ru–*N*4	101.9 [101.06(11)]	92.0	88.8	85.8
*N*2–Ru–*N*5	92.5 [92.16(12)]	90.4	90.0	90.0
*N*2–Ru–*N*6	92.5 [90.29(12)]	92.0	91.7	91.0
*N*3–Ru–*N*4	102.4 [102.13(11)]	112.4	115.8	118.9
*N*3–Ru–*N*5	92.6 [94.46(11)]	92.0	91.7	91.0
*N*3–Ru–*N*6	92.5 [92.54(11)]	95.8	97.1	98.6
*N*4–Ru–*N*5	77.9 [77.82(13)]	77.4	77.0	76.5
*N*4–Ru–*N*6	77.9 [78.51(13)]	78.1	78.2	78.4
*N*5–Ru–*N*6	155.8 [156.23(10)]	155.4	155.1	154.8
α	77.9 [78.3(2)]	77.8	77.6	77.5
θ	89.9 [89.52(3)]	87.1	84.9	83.0

[a]Crystallographic data from $[Ru(bpp)_2]_2[BF_4]_2$, ref. 25. [b]Fixed value.

Discussion of the DFT minimisations

We have recently published a wider survey of the angular distortion landscape in high-spin $[Fe(bpp)_2]^{2+}$, and its derivatives bearing pyridyl ligand substituents.[14] The ω-B97X-D/6-311G** DFT protocol employed in that that study was also used in this work, to enable comparison between the results. $[Mn(bpp)_2]^{2+}$ and $[Co(bpp)_2]^{2+}$ were computed in their high-spin forms, which is the spin state adopted experimentally by those complexes.[22,26]

The computed distortion energies ΔE(dist), for the different $[M(bpp)_2]^{2+}$ complexes runs as follows (Figure 2, main article):

$$M = Fe^{2+} \approx Mn^{2+} < Zn^{2+} \approx Co^{2+} \lesssim Cu^{2+} << Ni^{2+} << Ru^{2+}$$

Experimentally, the angular distortion is common in high-spin iron(II) complexes with tridentate N-donor ligands, including bpp derivatives.[13,14,27] It is also found crystallographically in analogous manganese(II),[26,28] zinc(II)[29-31] and cobalt(II)[31,32] complexes. Copper(II) complexes of this type show a different, Jahn-Teller elongated distortion which is typical for that metal ion.[23,33] Nickel(II)[17,30,34,35] and ruthenium(II)[25,35,36] complexes adopt undistorted geometries close to the ideal D_{2d} molecular symmetry.

All the $[M(bpp)_2]^{2+}$ molecules minimised freely to undistorted geometries with $179.3 \leq \phi \leq 180°$ except for $M^{2+} = Co^{2+}$, which consistently minimised to $\phi = 170 \pm 1°$. Minimisations of that molecule with ϕ fixed at 180° were *ca* 5 kcal mol^{-1} higher in energy, and gave unrealistic distributions of Co−N bond lengths. Hence a minimised energy with $\phi = 171.4°$, which agrees reasonably with the crystallographic structure [173.70(7)°],[22] was taken as the reference for the ΔE{dist} calculations of that complex.

Agreement between the computed and experimental molecular geometries for the undistorted molecules is generally good. The computed M−N{pyridyl} bonds deviate from their crystallographic values by 0.8-2.2 %, while the M−N{pyrazolyl} bonds show smaller deviations of 0.1-1.0 %. The best agreement was found for $M^{2+} = Ru^{2+}$, while the $M^{2+} = Zn^{2+}$ calculation differed most from experiment. This comparison excludes $[Mn(bpp)_2]^{2+}$, since no crystal structure of that undistorted molecule is available.

Most of the molecules behave consistently when ϕ is reduced. The distorted molecules minimise with perfect C_2 molecular symmetry; the M−N bond lengths evolve towards a [2+2+2] distribution; and the two ligands become canted with respect to each other (*ie* $\theta < 90°$, page S13; Scheme S4). This corresponds to distortion pathway A in our previous computational study.[14] The degree of ligand canting as the distortion progresses for different metals runs as:

$$M = Fe^{2+} > Mn^{2+} \approx Co^{2+} > Zn^{2+} \approx Ru^{2+} \approx Ni^{2+}$$

The exception is $[Cu(bpp)_2]^{2+}$, which shows no significant ligand canting as ϕ decreases. Rather, the Jahn-Teller-elongated copper ion evolves towards five-coordination, with one elongated Cu−N bond lengthening further to 2.409 Å at $\phi = 155°$ (Scheme S4). This is distortion pathway C in our earlier report.[14]

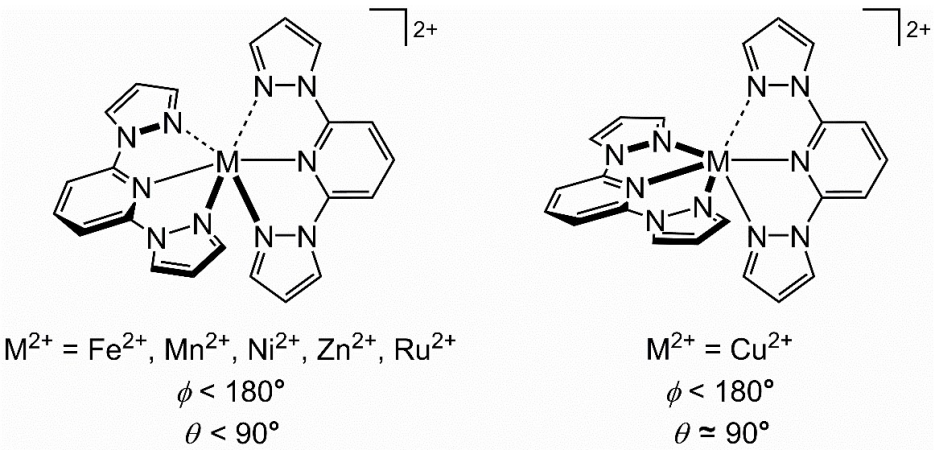

Scheme S4 The minimum angular distortion pathways computed for different $[M(bpp)_2]^{2+}$ complexes. Thick, thin and dashed bonds correspond to short, medium and long M−N distances in the most distorted geometries for each metal ion.

Table S18 Atomic coordinates for DFT-minimised $[M(bpp)_2]^{2+}$ (M = Mn, Co, Ni, Cu, Zn, Ru) with different angular distortions. The corresponding calculations for $[Fe(bpp)_2]^{2+}$ are presented in ref. 14.

$[Mn(bpp)_2]^{2+}$, undistorted − ϕ = 180° (minimised)

Mn	0.000000	0.000000	0.000000
N	-0.000001	0.000001	-2.267558
C	-0.811702	-0.811680	-2.937874
C	-0.854556	-0.854535	-4.321429
C	0.000001	-0.000002	-5.005712
H	0.000002	-0.000003	-6.088828
C	0.854558	0.854532	-4.321429
H	1.518601	1.518553	-4.855828
C	0.811701	0.811680	-2.937874
N	-1.616392	-1.616352	-2.110731
N	-1.501325	-1.501296	-0.764073
C	-2.365205	-2.365150	-0.258145
H	-2.464828	-2.464777	0.811898
C	-3.053288	-3.053202	-1.273306
H	-3.810793	-3.810680	-1.163119
C	-2.549715	-2.549641	-2.441822
H	-2.785588	-2.785501	-3.466444
N	1.616391	1.616354	-2.110732
N	1.501324	1.501297	-0.764074
C	2.365204	2.365152	-0.258146
H	2.464828	2.464778	0.811897
C	3.053286	3.053204	-1.273307
H	3.810791	3.810682	-1.163121
C	2.549713	2.549643	-2.441824
H	2.785585	2.785504	-3.466445
N	0.000001	0.000001	2.267558
C	-0.811701	0.811680	2.937874
C	-0.854558	0.854532	4.321429
H	-1.518601	1.518553	4.855828
C	-0.000001	-0.000002	5.005712
H	-0.000002	-0.000003	6.088828
C	0.854556	-0.854535	4.321429
C	0.811702	-0.811680	2.937874
N	-1.616391	1.616354	2.110732
N	-1.501324	1.501297	0.764074
C	-2.365204	2.365152	0.258146
H	-2.464828	2.464778	-0.811897
C	-3.053286	3.053204	1.273307
H	-3.810790	3.810683	1.163121
C	-2.549713	2.549643	2.441824
H	-2.785585	2.785504	3.466445
N	1.616392	-1.616352	2.110731
N	1.501325	-1.501296	0.764073
C	2.365205	-2.365150	0.258145
H	2.464828	-2.464777	-0.811898
C	3.053288	-3.053202	1.273306
H	3.810793	-3.810680	1.163119
C	2.549715	-2.549641	2.441822
H	2.785588	-2.785501	3.466443
H	1.518598	-1.518557	4.855828
H	-1.518598	-1.518557	-4.855828

$[Mn(bpp)_2]^{2+}$, $\phi = 165°$ (fixed)

Mn	0.000000	0.000002	-0.282899
N	2.215593	0.373085	0.012896
C	3.104511	-0.308006	-0.702171
C	4.471537	-0.172822	-0.524165
C	4.894673	0.724607	0.447775
C	3.978813	1.450223	1.198439
C	2.636383	1.232788	0.934518
N	2.524540	-1.169552	-1.651382
N	1.172260	-1.221067	-1.758808
C	0.924570	-2.088259	-2.726757
H	-0.094435	-2.307843	-3.006772
C	2.115184	-2.609900	-3.261106
H	2.224988	-3.329829	-4.054476
C	3.114853	-1.999243	-2.553491
H	4.185629	-2.094870	-2.627690
N	1.593560	1.897380	1.604681
N	0.311104	1.632523	1.253674
C	-0.436076	2.398362	2.029826
H	-1.511377	2.370000	1.940568
C	0.355133	3.174555	2.895019
H	0.026658	3.887680	3.632079
C	1.644979	2.829877	2.594264
H	2.578223	3.176889	3.006295
N	-2.215593	-0.373084	0.012896
C	-3.104512	0.308005	-0.702172
C	-4.471537	0.172821	-0.524165
C	-4.894671	-0.724605	0.447778
C	-3.978811	-1.450221	1.198442
C	-2.636382	-1.232786	0.934519
N	-2.524542	1.169547	-1.651387
N	-1.172261	1.221071	-1.758807
C	-0.924572	2.088270	-2.726750
H	0.094433	2.307865	-3.006757
C	-2.115188	2.609902	-3.261105
H	-2.224992	3.329833	-4.054473
C	-3.114857	1.999227	-2.553506
H	-4.185633	2.094839	-2.627717
N	-1.593558	-1.897379	1.604680
N	-0.311103	-1.632520	1.253674
C	0.436078	-2.398359	2.029826
H	1.511380	-2.369995	1.940570
C	-0.355130	-3.174555	2.895017
H	-0.026655	-3.887681	3.632076
C	-1.644977	-2.829881	2.594260
H	-2.578221	-3.176897	3.006287
H	5.954880	0.863680	0.619985
H	-5.954878	-0.863677	0.619990
H	5.186529	-0.731714	-1.110753
H	4.311357	2.152849	1.949011
H	-5.186531	0.731711	-1.110753
H	-4.311355	-2.152846	1.949015

$[Mn(bpp)_2]^{2+}$, $\phi = 160°$ (fixed)

Mn	0.000000	-0.000003	-0.369559
N	2.185814	0.450195	0.023950

C	3.125183	-0.187209	-0.666279
C	4.478679	-0.001665	-0.437544
C	4.831379	0.900610	0.557986
C	3.861910	1.584051	1.279948
C	2.539196	1.318549	0.964882
N	2.612439	-1.056968	-1.647098
N	1.268431	-1.132875	-1.827402
C	1.089744	-1.992459	-2.817277
H	0.091515	-2.226890	-3.154436
C	2.317294	-2.483973	-3.293265
H	2.482995	-3.191175	-4.088377
C	3.265770	-1.867531	-2.522852
H	4.340508	-1.945155	-2.538150
N	1.448017	1.941173	1.596437
N	0.191744	1.646707	1.179858
C	-0.612240	2.385740	1.924595
H	-1.680716	2.331178	1.781467
C	0.114962	3.171891	2.835907
H	-0.267484	3.868941	3.562262
C	1.426409	2.860866	2.598880
H	2.328635	3.224859	3.062199
N	-2.185814	-0.450197	0.023950
C	-3.125183	0.187202	-0.666284
C	-4.478678	0.001656	-0.437553
C	-4.831381	-0.900613	0.557981
C	-3.861912	-1.584044	1.279952
C	-2.539197	-1.318542	0.964890
N	-2.612436	1.056961	-1.647103
N	-1.268428	1.132876	-1.827397
C	-1.089740	1.992470	-2.817263
H	-0.091509	2.226912	-3.154411
C	-2.317288	2.483983	-3.293254
H	-2.482988	3.191194	-4.088359
C	-3.265766	1.867522	-2.522860
H	-4.340505	1.945137	-2.538168
N	-1.448018	-1.941159	1.596453
N	-0.191745	-1.646719	1.179853
C	0.612235	-2.385774	1.924571
H	1.680710	-2.331244	1.781417
C	-0.114968	-3.171904	2.835899
H	0.267475	-3.868966	3.562245
C	-1.426410	-2.860823	2.598921
H	-2.328635	-3.224777	3.062275
H	5.878518	1.079704	0.768827
H	-5.878520	-1.079710	0.768818
H	-5.236103	0.522605	-1.005509
H	-4.139568	-2.294086	2.045739
H	4.139566	2.294095	2.045732
H	5.236104	-0.522618	-1.005494

$[Mn(bpp)_2]^{2+}$, $\phi = 155°$ (fixed)

Mn	-0.000001	0.000001	-0.455511
N	2.150115	0.528132	0.035329
C	3.138099	-0.065564	-0.624700
C	4.473382	0.149582	-0.326626
C	4.752417	1.037758	0.704466

C	3.731298	1.682360	1.390131
C	2.433121	1.388764	1.005996
N	2.695961	-0.920292	-1.652908
N	1.364475	-1.030827	-1.895654
C	1.257153	-1.866862	-2.915743
H	0.282391	-2.124930	-3.300961
C	2.519570	-2.300620	-3.354909
H	2.742584	-2.975065	-4.164374
C	3.413315	-1.673897	-2.529180
H	4.490131	-1.710448	-2.504115
N	1.294956	1.973880	1.588995
N	0.071634	1.652554	1.102934
C	-0.789413	2.357475	1.816030
H	-1.847414	2.273878	1.618932
C	-0.132257	3.154538	2.770253
H	-0.570133	3.833170	3.482608
C	1.198015	2.885799	2.594252
H	2.065765	3.271688	3.103551
N	-2.150116	-0.528134	0.035327
C	-3.138100	0.065561	-0.624703
C	-4.473382	-0.149587	-0.326629
C	-4.752417	-1.037766	0.704462
C	-3.731297	-1.682366	1.390127
C	-2.433120	-1.388767	1.005993
N	-2.695962	0.920292	-1.652908
N	-1.364477	1.030828	-1.895654
C	-1.257156	1.866863	-2.915743
H	-0.282394	2.124930	-3.300963
C	-2.519573	2.300622	-3.354907
H	-2.742587	2.975068	-4.164371
C	-3.413317	1.673899	-2.529177
H	-4.490133	1.710452	-2.504110
N	-1.294955	-1.973880	1.588994
N	-0.071634	-1.652552	1.102935
C	0.789415	-2.357469	1.816032
H	1.847416	-2.273869	1.618935
C	0.132260	-3.154532	2.770256
H	0.570138	-3.833161	3.482613
C	-1.198013	-2.885797	2.594252
H	-2.065762	-3.271688	3.103551
H	5.782952	1.238248	0.970706
H	-5.782952	-1.238258	0.970700
H	-5.270989	0.338439	-0.868184
H	-3.952570	-2.384714	2.180921
H	5.270988	-0.338445	-0.868180
H	3.952572	2.384708	2.180926

$[Co(bpp)_2]^{2+}$, undistorted − ϕ = 171.4° (minimised)

Co	0.036066	-0.007322	-0.108863
N	0.080836	2.100558	-0.054422
C	1.147362	2.753830	-0.503518
C	1.244242	4.134851	-0.457371
C	0.161731	4.824272	0.075580
H	0.193939	5.905746	0.128079
C	-0.967930	4.152952	0.529242
H	-1.813954	4.695425	0.926369

C	-0.955852	2.771830	0.435811
N	2.135137	1.903619	-1.024545
N	1.885979	0.568967	-1.067524
C	2.948578	0.024471	-1.628975
H	2.993750	-1.043628	-1.776391
C	3.905466	1.002659	-1.962135
H	4.864714	0.856070	-2.429104
C	3.352859	2.188729	-1.564097
H	3.729097	3.196857	-1.625957
N	-2.019888	1.939865	0.826934
N	-1.918922	0.603593	0.605897
C	-3.058579	0.085096	1.027659
H	-3.224716	-0.979088	0.958426
C	-3.917358	1.080565	1.527017
H	-4.906372	0.957492	1.934928
C	-3.222783	2.251016	1.380745
H	-3.493912	3.264871	1.626114
N	-0.105811	-2.095842	0.137196
C	-0.624200	-2.845642	-0.829908
C	-0.775962	-4.216761	-0.703552
H	-1.197809	-4.823200	-1.492226
C	-0.350629	-4.789830	0.488719
H	-0.448606	-5.859385	0.628920
C	0.209053	-4.018108	1.500528
C	0.311865	-2.657645	1.266921
N	-0.984080	-2.106937	-1.967600
N	-0.729727	-0.772768	-1.982595
C	-1.132721	-0.345381	-3.163796
H	-1.036346	0.697860	-3.421854
C	-1.653826	-1.401329	-3.936674
H	-2.053925	-1.353565	-4.935372
C	-1.541739	-2.509427	-3.143413
H	-1.811309	-3.536611	-3.326618
N	0.867262	-1.736309	2.172842
N	0.971762	-0.434649	1.799599
C	1.554278	0.181724	2.812696
H	1.750427	1.241541	2.757762
C	1.838220	-0.714386	3.858675
H	2.308157	-0.501116	4.803862
C	1.388501	-1.928538	3.414411
H	1.403007	-2.897808	3.885299
H	0.551265	-4.471528	2.419757
H	2.113402	4.662344	-0.823481

$[Co(bpp)_2]^{2+}$, $\phi = 165°$ (fixed)

Co	0.000006	-0.000009	-0.229957
N	2.075355	0.257834	0.045364
C	2.926292	-0.468958	-0.670755
C	4.296542	-0.402708	-0.481928
C	4.756022	0.472401	0.494753
C	3.875536	1.249015	1.239160
C	2.526407	1.102971	0.965791
N	2.292623	-1.284932	-1.622029
N	0.939222	-1.227128	-1.730454
C	0.624678	-2.036800	-2.723872
H	-0.407920	-2.163069	-3.010590

C	1.773909	-2.633080	-3.277315
H	1.825995	-3.331251	-4.095679
C	2.818400	-2.128630	-2.552863
H	3.879001	-2.301174	-2.632901
N	1.502635	1.822186	1.606945
N	0.218516	1.618420	1.216158
C	-0.512032	2.437403	1.951699
H	-1.584131	2.463618	1.827536
C	0.291031	3.187636	2.829699
H	-0.024651	3.931439	3.542176
C	1.570558	2.770136	2.579973
H	2.507449	3.076935	3.015208
N	-2.075347	-0.257820	0.045372
C	-2.926284	0.468983	-0.670737
C	-4.296535	0.402730	-0.481909
C	-4.756024	-0.472383	0.494765
C	-3.875538	-1.248999	1.239168
C	-2.526409	-1.102952	0.965798
N	-2.292609	1.284954	-1.622008
N	-0.939211	1.227125	-1.730449
C	-0.624661	2.036777	-2.723881
H	0.407934	2.162989	-3.010638
C	-1.773891	2.633066	-3.277320
H	-1.825979	3.331236	-4.095683
C	-2.818378	2.128645	-2.552847
H	-3.878977	2.301185	-2.632884
N	-1.502647	-1.822183	1.606946
N	-0.218532	-1.618444	1.216143
C	0.512013	-2.437435	1.951677
H	1.584109	-2.463662	1.827488
C	-0.291054	-3.187657	2.829679
H	0.024619	-3.931451	3.542165
C	-1.570575	-2.770127	2.579974
H	-2.507470	-3.076901	3.015212
H	5.821167	0.555239	0.674068
H	-5.821170	-0.555222	0.674074
H	4.985770	-0.995665	-1.065688
H	4.240698	1.934190	1.990515
H	-4.985770	0.995690	-1.065656
H	-4.240693	-1.934164	1.990537

$[Co(bpp)_2]^{2+}$, $\phi = 160°$ (fixed)

Co	0.000000	-0.000043	-0.311793
N	2.048168	0.371681	0.055261
C	2.964350	-0.297338	-0.636646
C	4.321366	-0.157449	-0.399354
C	4.696348	0.738373	0.594964
C	3.747876	1.464084	1.306528
C	2.419542	1.241172	0.987827
N	2.410717	-1.137034	-1.617114
N	1.061633	-1.142177	-1.785034
C	0.828813	-1.968740	-2.787358
H	-0.183876	-2.146228	-3.115521
C	2.027404	-2.511662	-3.287757
H	2.148104	-3.210167	-4.098701
C	3.014830	-1.957066	-2.520995

H	4.084952	-2.081904	-2.553479
N	1.335982	1.902424	1.590637
N	0.082439	1.636306	1.144427
C	-0.718877	2.415609	1.848562
H	-1.784375	2.387947	1.677388
C	0.006572	3.200829	2.762233
H	-0.375062	3.925338	3.461774
C	1.314886	2.848688	2.567500
H	2.215897	3.198880	3.044310
N	-2.048160	-0.371750	0.055243
C	-2.964347	0.297267	-0.636665
C	-4.321364	0.157346	-0.399390
C	-4.696342	-0.738495	0.594911
C	-3.747865	-1.464185	1.306490
C	-2.419531	-1.241243	0.987812
N	-2.410727	1.137007	-1.617098
N	-1.061645	1.142213	-1.784993
C	-0.828827	1.968852	-2.787250
H	0.183863	2.146396	-3.115378
C	-2.027427	2.511764	-3.287639
H	-2.148135	3.210319	-4.098539
C	-3.014851	1.957082	-2.520936
H	-4.084975	2.081894	-2.553428
N	-1.335968	-1.902451	1.590668
N	-0.082412	-1.636307	1.144501
C	0.718896	-2.415540	1.848723
H	1.784400	-2.387849	1.677599
C	-0.006566	-3.200743	2.762398
H	0.375062	-3.925199	3.461997
C	-1.314883	-2.848670	2.567576
H	-2.215900	-3.198868	3.044366
H	5.747926	0.882540	0.811586
H	-5.747920	-0.882686	0.811517
H	-5.063600	0.706290	-0.961242
H	-4.045897	-2.173487	2.065339
H	4.045910	2.173382	2.065379
H	5.063599	-0.706399	-0.961204

$[Co(bpp)_2]^{2+}$, $\phi = 155°$ (fixed)

Co	0.000031	-0.000129	-0.397032
N	2.021440	0.437984	0.061446
C	2.982349	-0.195247	-0.602639
C	4.324168	-0.027694	-0.305078
C	4.633807	0.860385	0.718565
C	3.638295	1.552242	1.398910
C	2.330521	1.302640	1.020257
N	2.491384	-1.029597	-1.621263
N	1.151139	-1.064031	-1.848643
C	0.983237	-1.872527	-2.878788
H	-0.009705	-2.066991	-3.254493
C	2.215544	-2.373939	-3.337845
H	2.388954	-3.050052	-4.158191
C	3.154320	-1.813025	-2.516219
H	4.227779	-1.910154	-2.505337
N	1.206028	1.929225	1.582911
N	-0.018054	1.641335	1.074169

C	-0.869571	2.391232	1.750586
H	-1.925055	2.342324	1.529008
C	-0.206780	3.179074	2.708510
H	-0.637215	3.884742	3.398990
C	1.117285	2.859699	2.571248
H	1.986281	3.222612	3.095657
N	-2.021471	-0.437795	0.061568
C	-2.982272	0.195650	-0.602450
C	-4.324102	0.028520	-0.304699
C	-4.633862	-0.859403	0.719049
C	-3.638465	-1.551546	1.399273
C	-2.330668	-1.302353	1.020420
N	-2.491151	1.029738	-1.621220
N	-1.150930	1.063591	-1.848827
C	-0.982868	1.871827	-2.879159
H	0.010089	2.065814	-3.255067
C	-2.215050	2.373622	-3.338121
H	-2.388329	3.049635	-4.158576
C	-3.153916	1.813236	-2.516230
H	-4.227336	1.910780	-2.505198
N	-1.206261	-1.929299	1.582842
N	0.017762	-1.642040	1.073598
C	0.869190	-2.392255	1.749770
H	1.924608	-2.343867	1.527774
C	0.206396	-3.179679	2.708038
H	0.636768	-3.885469	3.398431
C	-1.117574	-2.859720	2.571234
H	-1.986540	-3.222173	3.096011
H	5.671341	1.026470	0.982279
H	-5.671410	-1.025165	0.982914
H	-5.102870	0.549629	-0.843207
H	-3.886412	-2.257023	2.179430
H	5.103015	-0.548624	-0.843641
H	3.886138	2.257789	2.179035

$[Ni(bpp)_2]^{2+}$, undistorted − ϕ = 179.3° (minimised)

Ni	0.015715	-0.000646	0.002339
N	0.048709	2.039188	-0.110925
C	1.112651	2.653547	-0.617391
C	1.184081	4.032170	-0.725793
C	0.085801	4.756378	-0.276074
H	0.100645	5.837416	-0.341899
C	-1.031197	4.122180	0.255930
H	-1.881343	4.692300	0.603006
C	-0.997861	2.739040	0.314342
N	2.122755	1.764117	-1.017210
N	1.915621	0.430599	-0.858846
C	3.007336	-0.157427	-1.306694
H	3.088024	-1.233406	-1.288295
C	3.943531	0.789825	-1.765293
H	4.918819	0.606601	-2.183403
C	3.346401	2.003501	-1.565547
H	3.695590	3.002975	-1.766279
N	-2.034455	1.932432	0.810491
N	-1.869831	0.583905	0.806598
C	-2.983008	0.085697	1.307748

H	-3.098692	-0.982309	1.410549
C	-3.890777	1.108301	1.646397
H	-4.873976	1.004266	2.073196
C	-3.252853	2.271569	1.315784
H	-3.569897	3.298171	1.397960
N	-0.043644	-2.038928	0.118627
C	-0.546429	-2.741239	-0.891225
C	-0.630110	-4.123053	-0.856950
H	-1.038777	-4.694980	-1.677964
C	-0.165102	-4.753281	0.291728
H	-0.214930	-5.833028	0.361299
C	0.360034	-4.026566	1.354199
C	0.399505	-2.649713	1.212610
N	-0.971819	-1.938545	-1.961760
N	-0.840754	-0.590341	-1.857535
C	-1.312697	-0.096303	-2.985162
H	-1.316913	0.970536	-3.148046
C	-1.759004	-1.121243	-3.842284
H	-2.189718	-1.020520	-4.824120
C	-1.526091	-2.281603	-3.157621
H	-1.711268	-3.308625	-3.426021
N	0.896165	-1.758322	2.176859
N	0.853753	-0.426075	1.913690
C	1.382679	0.164380	2.967130
H	1.461435	1.240102	3.000818
C	1.778803	-0.780174	3.934141
H	2.238429	-0.594797	4.890186
C	1.453196	-1.994653	3.397129
H	1.576664	-2.992740	3.784181
H	0.716897	-4.523357	2.245290
H	2.047907	4.532678	-1.139891

$[Ni(bpp)_2]^{2+}$, $\phi = 165°$ (fixed)

Ni	0.000003	0.000011	-0.260695
N	2.010483	0.297137	0.006870
C	2.865998	-0.420846	-0.713180
C	4.237100	-0.308036	-0.556748
C	4.689017	0.602005	0.392244
C	3.801455	1.358613	1.148567
C	2.451144	1.164465	0.911063
N	2.233661	-1.285823	-1.621813
N	0.874628	-1.305513	-1.672361
C	0.562857	-2.188043	-2.601583
H	-0.472443	-2.386761	-2.831774
C	1.718700	-2.756009	-3.171149
H	1.774658	-3.498932	-3.948833
C	2.763754	-2.158327	-2.523195
H	3.827768	-2.285165	-2.638028
N	1.415013	1.835381	1.577341
N	0.134270	1.531683	1.249081
C	-0.621357	2.299841	2.008856
H	-1.696654	2.243723	1.933686
C	0.162942	3.117640	2.845742
H	-0.175582	3.842313	3.566961
C	1.456791	2.793755	2.544250
H	2.387290	3.170490	2.936254

N	-2.010479	-0.297132	0.006862
C	-2.866000	0.420840	-0.713192
C	-4.237102	0.308016	-0.556762
C	-4.689012	-0.602029	0.392229
C	-3.801444	-1.358629	1.148552
C	-2.451135	-1.164467	0.911053
N	-2.233674	1.285820	-1.621828
N	-0.874643	1.305538	-1.672372
C	-0.562876	2.188075	-2.601591
H	0.472424	2.386814	-2.831772
C	-1.718727	2.756015	-3.171165
H	-1.774695	3.498939	-3.948848
C	-2.763778	2.158303	-2.523224
H	-3.827794	2.285117	-2.638068
N	-1.415000	-1.835377	1.577331
N	-0.134258	-1.531664	1.249076
C	0.621373	-2.299818	2.008852
H	1.696669	-2.243689	1.933688
C	-0.162922	-3.117629	2.845732
H	0.175606	-3.842301	3.566950
C	-1.456773	-2.793757	2.544234
H	-2.387270	-3.170504	2.936231
H	5.754411	0.723868	0.545199
H	-5.754405	-0.723902	0.545182
H	4.932743	-0.893032	-1.141402
H	4.159532	2.064383	1.884466
H	-4.932750	0.893004	-1.141417
H	-4.159516	-2.064403	1.884449

$[Ni(bpp)_2]^{2+}$, $\phi = 160°$ (fixed)

Ni	-0.000004	-0.000028	-0.345418
N	1.988202	0.375639	0.011348
C	2.896756	-0.304722	-0.679816
C	4.255269	-0.156723	-0.458093
C	4.636615	0.749433	0.525357
C	3.693375	1.467793	1.250603
C	2.361660	1.240364	0.946880
N	2.332426	-1.172956	-1.630302
N	0.977683	-1.240456	-1.737270
C	0.735888	-2.109925	-2.699347
H	-0.281408	-2.340155	-2.975718
C	1.933713	-2.621696	-3.233806
H	2.047802	-3.342646	-4.025744
C	2.929363	-2.003431	-2.529519
H	4.001141	-2.087955	-2.604415
N	1.278073	1.872738	1.572796
N	0.023378	1.534868	1.184788
C	-0.787048	2.275513	1.915223
H	-1.856011	2.189623	1.792055
C	-0.065203	3.108684	2.792216
H	-0.456102	3.818158	3.502022
C	1.249443	2.824147	2.546755
H	2.150631	3.224608	2.981339
N	-1.988208	-0.375640	0.011371
C	-2.896749	0.304746	-0.679781
C	-4.255263	0.156786	-0.458047

C	-4.636624	-0.749363	0.525404
C	-3.693396	-1.467750	1.250639
C	-2.361679	-1.240356	0.946904
N	-2.332397	1.172966	-1.630266
N	-0.977646	1.240424	-1.737230
C	-0.735839	2.109880	-2.699319
H	0.281461	2.340086	-2.975695
C	-1.933652	2.621680	-3.233782
H	-2.047723	3.342628	-4.025725
C	-2.929316	2.003451	-2.529488
H	-4.001091	2.088001	-2.604381
N	-1.278102	-1.872757	1.572810
N	-0.023402	-1.534933	1.184779
C	0.787010	-2.275590	1.915214
H	1.855973	-2.189737	1.792028
C	0.065153	-3.108720	2.792234
H	0.456040	-3.818195	3.502048
C	-1.249487	-2.824143	2.546790
H	-2.150680	-3.224567	2.981394
H	5.689880	0.898652	0.729940
H	-5.689891	-0.898556	0.729995
H	-4.993784	0.712171	-1.018538
H	-3.995575	-2.170861	2.013697
H	3.995543	2.170908	2.013662
H	4.993800	-0.712086	-1.018592

$[Ni(bpp)_2]^{2+}$, $\phi = 155°$ (fixed)

Ni	-0.000031	-0.000025	-0.428931
N	1.963596	0.445366	0.017424
C	2.917467	-0.203945	-0.641816
C	4.260746	-0.034038	-0.353058
C	4.576081	0.861940	0.663008
C	3.585039	1.548889	1.354027
C	2.273922	1.301488	0.982745
N	2.416415	-1.067821	-1.632479
N	1.069838	-1.170598	-1.798460
C	0.892884	-2.017280	-2.794616
H	-0.105357	-2.267883	-3.118638
C	2.125643	-2.479524	-3.292176
H	2.292831	-3.173407	-4.098843
C	3.072914	-1.855024	-2.529018
H	4.148784	-1.906948	-2.562140
N	1.149145	1.901796	1.565164
N	-0.076819	1.535510	1.118324
C	-0.938072	2.252415	1.813417
H	-1.998092	2.141185	1.641109
C	-0.278679	3.098460	2.726283
H	-0.718731	3.795325	3.419717
C	1.052806	2.847870	2.540180
H	1.923071	3.268893	3.016615
N	-1.963618	-0.445374	0.017471
C	-2.917473	0.203959	-0.641762
C	-4.260750	0.034084	-0.353025
C	-4.576100	-0.861891	0.663041
C	-3.585073	-1.548855	1.354076
C	-2.273957	-1.301481	0.982794

N	-2.416365	1.067842	-1.632399
N	-1.069761	1.170540	-1.798345
C	-0.892820	2.017200	-2.794526
H	0.105418	2.267762	-3.118563
C	-2.125555	2.479481	-3.292119
H	-2.292713	3.173338	-4.098816
C	-3.072830	1.855119	-2.528901
H	-4.148686	1.907117	-2.561988
N	-1.149190	-1.901804	1.565208
N	0.076769	-1.535550	1.118349
C	0.938018	-2.252467	1.813431
H	1.998036	-2.141257	1.641111
C	0.278623	-3.098489	2.726314
H	0.718671	-3.795357	3.419748
C	-1.052857	-2.847866	2.540232
H	-1.923123	-3.268863	3.016682
H	5.615205	1.027631	0.920699
H	-5.615229	-1.027567	0.920724
H	-5.036400	0.564972	-0.886717
H	-3.836083	-2.243533	2.143119
H	5.036409	-0.564913	-0.886742
H	3.836034	2.243576	2.143067

$[Cu(bpp)_2]^{2+}$, undistorted − ϕ = 180° (minimised)

Cu	-0.000498	-0.000035	0.089536
N	0.000462	-0.000505	2.080440
C	0.000625	1.156286	2.741333
C	0.000642	1.210553	4.123843
C	0.000600	-0.001181	4.804556
H	0.000527	-0.001459	5.887753
C	0.000636	-1.212572	4.123238
H	0.000599	-2.152177	4.657128
C	0.000620	-1.157620	2.740749
N	0.000566	2.272077	1.896598
N	0.000288	2.059812	0.555997
C	0.000524	3.254772	0.000270
H	0.000509	3.352103	-1.074359
C	0.000838	4.266976	0.980273
H	0.001083	5.333003	0.826680
C	0.000664	3.605487	2.176835
H	0.000723	3.977301	3.188498
N	0.000562	-2.272999	1.895467
N	0.000290	-2.060099	0.554945
C	0.000529	-3.254802	-0.001346
H	0.000519	-3.351651	-1.076024
C	0.000843	-4.267481	0.978217
H	0.001093	-5.333437	0.824113
C	0.000658	-3.606542	2.175094
H	0.000711	-3.978825	3.186588
N	-0.000669	0.000385	-1.965917
C	-1.155271	0.000383	-2.643392
C	-1.205185	0.000390	-4.027870
H	-2.144041	0.000375	-4.561561
C	-0.001165	0.000398	-4.714415
H	-0.001354	0.000391	-5.797505
C	1.203087	0.000394	-4.028319

C	1.153676	0.000385	-2.643830
N	-2.312905	0.000364	-1.854297
N	-2.199772	0.000226	-0.505509
C	-3.433860	0.000237	-0.045920
H	-3.614395	0.000149	1.018221
C	-4.374585	0.000400	-1.097434
H	-5.449192	0.000465	-1.025246
C	-3.624797	0.000463	-2.238051
H	-3.924821	0.000589	-3.272452
N	2.311574	0.000366	-1.855169
N	2.198941	0.000229	-0.506433
C	3.433071	0.000240	-0.047230
H	3.613773	0.000152	1.016808
C	4.373383	0.000402	-1.098803
H	5.447986	0.000465	-1.026990
C	3.623337	0.000463	-2.239186
H	3.923074	0.000589	-3.273635
H	2.141758	0.000381	-4.562190
H	0.000607	2.149921	4.658016

$[Cu(bpp)_2]^{2+}$, $\phi = 165°$ (fixed)

Cu	0.101926	0.204864	0.211218
N	2.074286	-0.030213	0.413435
C	2.896509	0.678293	-0.353539
C	4.267993	0.502571	-0.306451
C	4.748911	-0.454668	0.581177
C	3.891381	-1.206390	1.378105
C	2.537704	-0.950944	1.251759
N	2.215627	1.581155	-1.180607
N	0.858074	1.604292	-1.116347
C	0.468267	2.530700	-1.969090
H	-0.582375	2.739198	-2.098880
C	1.575548	3.126296	-2.603707
H	1.567723	3.909725	-3.342664
C	2.671082	2.498373	-2.077630
H	3.723075	2.636159	-2.268394
N	1.514037	-1.601821	1.952728
N	0.230657	-1.246091	1.681415
C	-0.526425	-1.989790	2.463811
H	-1.600251	-1.889109	2.432368
C	0.260836	-2.844075	3.259594
H	-0.077121	-3.559319	3.990392
C	1.554278	-2.569548	2.909096
H	2.484494	-2.981092	3.265985
N	-1.922039	0.056605	-0.380595
C	-2.836000	0.818715	0.227810
C	-4.186093	0.757832	-0.073598
C	-4.582257	-0.145200	-1.048541
C	-3.650582	-0.950349	-1.683477
C	-2.321487	-0.813514	-1.312698
N	-2.327552	1.694033	1.202195
N	-1.000535	1.697880	1.467365
C	-0.827364	2.600240	2.412900
H	0.160753	2.792752	2.801894
C	-2.049925	3.198793	2.778629
H	-2.217243	3.963375	3.518486

C	-2.985941	2.598139	1.985373
H	-4.050927	2.747236	1.923895
N	-1.305405	-1.582995	-1.896808
N	-0.028741	-1.427255	-1.482485
C	0.680807	-2.273633	-2.199910
H	1.748676	-2.341246	-2.055471
C	-0.131685	-2.999007	-3.096907
H	0.169071	-3.754116	-3.803526
C	-1.395247	-2.531995	-2.876820
H	-2.330019	-2.799997	-3.339778
H	5.816974	-0.621740	0.650424
H	-5.629352	-0.223705	-1.313953
H	4.941566	1.077309	-0.926209
H	4.273361	-1.952620	2.060292
H	-4.910292	1.383761	0.426628
H	-3.958758	-1.657862	-2.438889

$[Cu(bpp)_2]^{2+}$, $\phi = 160°$ (fixed)

Cu	0.073739	0.000000	0.393353
N	2.073865	0.000000	0.427268
C	2.723699	1.157117	0.387082
C	4.104452	1.214779	0.317381
C	4.782467	0.000000	0.287486
C	4.104452	-1.214779	0.317380
C	2.723699	-1.157116	0.387081
N	1.855791	2.257043	0.413754
N	0.519427	2.010816	0.457596
C	-0.068287	3.190637	0.491103
H	-1.144383	3.258052	0.530101
C	0.885239	4.226061	0.470823
H	0.704503	5.287557	0.491680
C	2.098772	3.595709	0.422518
H	3.100463	3.993347	0.398035
N	1.855791	-2.257043	0.413752
N	0.519427	-2.010816	0.457594
C	-0.068287	-3.190638	0.491100
H	-1.144383	-3.258052	0.530099
C	0.885240	-4.226061	0.470818
H	0.704503	-5.287557	0.491674
C	2.098772	-3.595709	0.422513
H	3.100464	-3.993346	0.398029
N	-1.924899	0.000000	-0.372711
C	-2.942020	0.000000	0.491349
C	-4.268373	-0.000001	0.094138
C	-4.523446	-0.000001	-1.269354
C	-3.480887	-0.000001	-2.181726
C	-2.186828	-0.000001	-1.681425
N	-2.564243	0.000001	1.846120
N	-1.250451	0.000001	2.169777
C	-1.205928	0.000002	3.488349
H	-0.254028	0.000002	3.996956
C	-2.500840	0.000003	4.042326
H	-2.775218	0.000004	5.083776
C	-3.343099	0.000003	2.965936
H	-4.419298	0.000003	2.919546
N	-1.064017	-0.000001	-2.522629

N	0.174863	-0.000001	-1.983856
C	1.003853	-0.000002	-3.007389
H	2.070513	-0.000002	-2.837925
C	0.310204	-0.000002	-4.235960
H	0.721154	-0.000002	-5.231493
C	-1.010023	-0.000002	-3.888609
H	-1.894227	-0.000001	-4.503471
H	5.864431	0.000000	0.235289
H	-5.546839	-0.000001	-1.623815
H	-5.078999	-0.000001	0.807958
H	-3.679513	-0.000002	-3.243240
H	4.639367	-2.153532	0.286930
H	4.639367	2.153532	0.286933

$[Cu(bpp)_2]^{2+}$, $\phi = 155°$ (fixed)

Cu	-0.080019	-0.366991	-0.337251
N	1.885929	0.572653	-0.061240
C	2.896305	0.134129	-0.810132
C	4.182948	0.636468	-0.716159
C	4.400711	1.643060	0.214005
C	3.363008	2.111460	1.004214
C	2.111394	1.539204	0.826036
N	2.547434	-0.890842	-1.713365
N	1.274436	-1.348039	-1.738366
C	1.245539	-2.287983	-2.665709
H	0.325923	-2.811887	-2.876825
C	2.510594	-2.453512	-3.258704
H	2.790324	-3.140552	-4.039523
C	3.316829	-1.546908	-2.625942
H	4.362545	-1.325972	-2.761015
N	0.990980	1.942263	1.569513
N	-0.193574	1.325167	1.374241
C	-1.036168	1.914324	2.198600
H	-2.067856	1.595658	2.234274
C	-0.405777	2.931068	2.945653
H	-0.839956	3.577623	3.689562
C	0.890987	2.920652	2.517635
H	1.729275	3.529465	2.812062
N	-2.030818	-0.647398	0.040224
C	-2.923397	0.096409	-0.600161
C	-4.271156	0.041606	-0.291139
C	-4.643800	-0.825535	0.732033
C	-3.706786	-1.592452	1.418546
C	-2.386485	-1.460013	1.026041
N	-2.330386	0.913122	-1.573699
N	-0.976591	0.871295	-1.699031
C	-0.672231	1.713568	-2.667628
H	0.357457	1.856279	-2.956582
C	-1.832493	2.314314	-3.190277
H	-1.898001	3.035634	-3.987294
C	-2.868125	1.783132	-2.469517
H	-3.931168	1.951607	-2.531557
N	-1.286513	-2.119674	1.589623
N	-0.051364	-1.823024	1.104105
C	0.797549	-2.570938	1.782102
H	1.854672	-2.513474	1.574112

C	0.120150	-3.369805	2.721821
H	0.545919	-4.079346	3.411095
C	-1.203852	-3.057469	2.570894
H	-2.079603	-3.430818	3.076782
H	5.391794	2.065520	0.324857
H	-5.689235	-0.900159	1.005742
H	-5.005540	0.641259	-0.810275
H	-4.005425	-2.253871	2.219652
H	4.989586	0.267431	-1.332751
H	3.534034	2.892289	1.730718

$[Zn(bpp)_2]^{2+}$, undistorted − ϕ = 179.8° (minimised)

Zn	-0.001617	-0.000269	0.005941
N	0.118705	2.142566	0.049085
C	0.626017	2.757632	1.110370
C	0.731680	4.136178	1.189021
C	0.281116	4.864660	0.094798
H	0.345251	5.945890	0.113051
C	-0.250382	4.231956	-1.022505
H	-0.598145	4.803590	-1.871101
C	-0.308324	2.848825	-0.990609
N	1.036479	1.874679	2.124895
N	0.883077	0.541325	1.934515
C	1.347264	-0.032628	3.028627
H	1.334693	-1.107843	3.121634
C	1.810867	0.926179	3.948567
H	2.241044	0.756395	4.921231
C	1.596958	2.131971	3.338796
H	1.799331	3.135809	3.674612
N	-0.815203	2.055406	-2.035220
N	-0.817607	0.707553	-1.893678
C	-1.339530	0.230991	-3.008604
H	-1.450617	-0.834441	-3.140608
C	-1.684467	1.269622	-3.893255
H	-2.126365	1.185339	-4.871861
C	-1.335978	2.419583	-3.239137
H	-1.419616	3.451622	-3.538066
N	-0.122731	-2.142641	-0.046447
C	0.887015	-2.849692	-0.538837
C	0.857741	-4.232035	-0.614503
H	1.681586	-4.804250	-1.016599
C	-0.288948	-4.862839	-0.147347
H	-0.355014	-5.943350	-0.187638
C	-1.352966	-4.133451	0.369269
C	-1.213752	-2.755920	0.395945
N	1.967846	-2.058096	-0.966300
N	1.878139	-0.710356	-0.854838
C	3.017423	-0.235484	-1.322654
H	3.191877	0.829515	-1.340805
C	3.866075	-1.274963	-1.746477
H	4.853094	-1.192025	-2.169492
C	3.163875	-2.423788	-1.504133
H	3.424307	-3.455953	-1.672240
N	-2.192267	-1.872134	0.884807
N	-1.947580	-0.539400	0.850492
C	-3.019102	0.035205	1.363892

H	-3.068255	1.110161	1.446956
C	-3.978494	-0.922669	1.741118
H	-4.944758	-0.752331	2.185300
C	-3.417302	-2.128450	1.420873
H	-3.794035	-3.131810	1.534258
H	-2.242802	-4.629446	0.729815
H	1.144396	4.633611	2.055087

$[Zn(bpp)_2]^{2+}$, $\phi = 165°$ (fixed)

Zn	0.000002	-0.000009	-0.260778
N	2.079486	0.472146	0.019956
C	2.991992	-0.170270	-0.698069
C	4.350403	0.041183	-0.535129
C	4.729950	0.973307	0.423771
C	3.783671	1.657409	1.176741
C	2.452956	1.364887	0.927599
N	2.437915	-1.071545	-1.626284
N	1.088919	-1.186554	-1.705019
C	0.858509	-2.069381	-2.660470
H	-0.155390	-2.336400	-2.916301
C	2.061643	-2.540681	-3.216604
H	2.187013	-3.260920	-4.007453
C	3.047697	-1.881941	-2.533868
H	4.120231	-1.928673	-2.628807
N	1.373186	1.970704	1.592291
N	0.113286	1.604239	1.258238
C	-0.683498	2.336790	2.013772
H	-1.754276	2.227653	1.932996
C	0.054109	3.193203	2.852782
H	-0.322016	3.901826	3.571233
C	1.363598	2.932513	2.556017
H	2.272192	3.355649	2.951938
N	-2.079488	-0.472140	0.019962
C	-2.991988	0.170284	-0.698060
C	-4.350402	-0.041150	-0.535110
C	-4.729955	-0.973265	0.423795
C	-3.783681	-1.657378	1.176761
C	-2.452963	-1.364875	0.927609
N	-2.437905	1.071548	-1.626283
N	-1.088909	1.186538	-1.705027
C	-0.858490	2.069355	-2.660486
H	0.155411	2.336358	-2.916325
C	-2.061622	2.540669	-3.216615
H	-2.186985	3.260905	-4.007468
C	-3.047680	1.881946	-2.533870
H	-4.120214	1.928691	-2.628803
N	-1.373196	-1.970706	1.592294
N	-0.113295	-1.604260	1.258229
C	0.683486	-2.336826	2.013750
H	1.754266	-2.227705	1.932963
C	-0.054125	-3.193230	2.852766
H	0.321997	-3.901862	3.571210
C	-1.363613	-2.932520	2.556015
H	-2.272209	-3.355644	2.951943
H	5.782500	1.171972	0.584890
H	-5.782507	-1.171916	0.584921

H	5.090391	-0.484398	-1.121526
H	4.083973	2.384368	1.917695
H	-5.090387	0.484438	-1.121505
H	-4.083988	-2.384331	1.917719

$[Zn(bpp)_2]^{2+}$, $\phi = 160°$ (fixed)

Zn	0.000008	-0.000001	-0.354584
N	2.038169	0.595227	0.019813
C	3.011438	0.002490	-0.659840
C	4.349895	0.266270	-0.425374
C	4.640740	1.198243	0.564666
C	3.630265	1.829940	1.278720
C	2.327014	1.486472	0.958763
N	2.541607	-0.906393	-1.627891
N	1.204268	-1.083777	-1.769489
C	1.057628	-1.955693	-2.751389
H	0.069600	-2.264595	-3.056740
C	2.305105	-2.357110	-3.262073
H	2.499162	-3.052984	-4.060833
C	3.227861	-1.667567	-2.522910
H	4.304519	-1.660485	-2.572193
N	1.190051	2.033485	1.577155
N	-0.032405	1.606127	1.183365
C	-0.899208	2.293529	1.902660
H	-1.958279	2.130860	1.771578
C	-0.246128	3.181346	2.778378
H	-0.689774	3.866928	3.480467
C	1.087390	2.988313	2.542723
H	1.953950	3.455420	2.981248
N	-2.038162	-0.595231	0.019809
C	-3.011432	-0.002492	-0.659844
C	-4.349891	-0.266275	-0.425378
C	-4.640736	-1.198249	0.564662
C	-3.630260	-1.829944	1.278716
C	-2.327007	-1.486475	0.958761
N	-2.541608	0.906393	-1.627899
N	-1.204276	1.083786	-1.769510
C	-1.057638	1.955707	-2.751405
H	-0.069612	2.264613	-3.056759
C	-2.305120	2.357121	-3.262080
H	-2.499184	3.052997	-4.060837
C	-3.227868	1.667567	-2.522914
H	-4.304527	1.660480	-2.572192
N	-1.190045	-2.033488	1.577155
N	0.032413	-1.606129	1.183372
C	0.899214	-2.293530	1.902672
H	1.958285	-2.130859	1.771597
C	0.246130	-3.181345	2.778389
H	0.689772	-3.866925	3.480483
C	-1.087387	-2.988319	2.542721
H	-1.953947	-3.455429	2.981240
H	5.674562	1.437771	0.781577
H	-5.674558	-1.437780	0.781571
H	-5.139886	0.219380	-0.980135
H	-3.862183	-2.555604	2.045066
H	3.862188	2.555599	2.045071

H	5.139890	-0.219387	-0.980130

$[Zn(bpp)_2]^{2+}$, $\phi = 155°$ (fixed)

Zn	0.000000	-0.000026	-0.444762
N	1.990286	0.695118	0.022601
C	3.014453	0.152067	-0.622212
C	4.330408	0.456690	-0.320432
C	4.541545	1.378316	0.699235
C	3.477192	1.959444	1.376843
C	2.203225	1.576813	0.990004
N	2.623038	-0.751661	-1.629691
N	1.301438	-0.979419	-1.835177
C	1.234105	-1.832003	-2.843223
H	0.274063	-2.173302	-3.199239
C	2.518004	-2.169032	-3.306765
H	2.775794	-2.835131	-4.112882
C	3.377912	-1.460811	-2.511308
H	4.454386	-1.407235	-2.513429
N	1.020055	2.070806	1.564064
N	-0.165569	1.601411	1.110616
C	-1.089550	2.247764	1.796065
H	-2.134839	2.046781	1.615627
C	-0.511466	3.150127	2.709122
H	-1.012519	3.811039	3.396089
C	0.837762	3.009920	2.533351
H	1.665057	3.504957	3.015017
N	-1.990292	-0.695119	0.022620
C	-3.014452	-0.152049	-0.622188
C	-4.330410	-0.456652	-0.320406
C	-4.541557	-1.378280	0.699257
C	-3.477213	-1.959426	1.376862
C	-2.203241	-1.576811	0.990022
N	-2.623019	0.751678	-1.629660
N	-1.301408	0.979379	-1.835164
C	-1.234061	1.831956	-2.843216
H	-0.274012	2.173214	-3.199251
C	-2.517955	2.169036	-3.306740
H	-2.775728	2.835141	-4.112855
C	-3.377881	1.460864	-2.511259
H	-4.454358	1.407339	-2.513358
N	-1.020076	-2.070817	1.564082
N	0.165555	-1.601452	1.110613
C	1.089529	-2.247818	1.796060
H	2.134822	-2.046864	1.615608
C	0.511432	-3.150155	2.709138
H	1.012478	-3.811068	3.396110
C	-0.837795	-3.009917	2.533385
H	-1.665096	-3.504925	3.015073
H	5.554979	1.649626	0.968355
H	-5.554994	-1.649580	0.968375
H	-5.161930	-0.010394	-0.846832
H	-3.647256	-2.677331	2.166367
H	5.161935	0.010444	-0.846860
H	3.647227	2.677347	2.166351

$[Ru(bpp)_2]^{2+}$, undistorted − ϕ = 179.8° (minimised)

Ru	-0.000607	-0.000449	0.005668
N	0.111198	2.003032	0.046944
C	0.621349	2.609661	1.121238
C	0.720060	3.987678	1.193676
C	0.266828	4.714822	0.097599
H	0.328392	5.795792	0.117942
C	-0.263978	4.085717	-1.024089
H	-0.612356	4.660011	-1.871032
C	-0.322556	2.703734	-1.003689
N	1.021294	1.698214	2.109711
N	0.853690	0.355052	1.882713
C	1.312627	-0.252485	2.959842
H	1.288710	-1.329198	3.021315
C	1.784568	0.680760	3.903653
H	2.212457	0.477346	4.870763
C	1.585527	1.905871	3.332662
H	1.798518	2.897356	3.697951
N	-0.817983	1.881349	-2.026491
N	-0.803513	0.520641	-1.850653
C	-1.319206	0.008938	-2.951743
H	-1.415205	-1.060611	-3.054015
C	-1.677338	1.024185	-3.860327
H	-2.118585	0.906055	-4.835559
C	-1.346223	2.196807	-3.242448
H	-1.444910	3.218863	-3.570206
N	-0.114232	-2.002994	-0.042464
C	0.907655	-2.704772	-0.538699
C	0.870464	-4.085990	-0.605432
H	1.693705	-4.661041	-1.005550
C	-0.278441	-4.713275	-0.134125
H	-0.343672	-5.793610	-0.170328
C	-1.346171	-3.985072	0.380746
C	-1.216674	-2.607933	0.406383
N	1.964876	-1.884151	-0.959134
N	1.840090	-0.523363	-0.832919
C	2.965095	-0.013713	-1.296250
H	3.108711	1.055444	-1.302408
C	3.838488	-1.029866	-1.731089
H	4.821984	-0.913126	-2.154063
C	3.173820	-2.201364	-1.502405
H	3.464009	-3.223657	-1.682537
N	-2.171047	-1.695811	0.880789
N	-1.891840	-0.353333	0.826424
C	-2.947477	0.255551	1.331017
H	-2.967180	1.332105	1.396512
C	-3.928695	-0.676528	1.722116
H	-4.889410	-0.472123	2.163683
C	-3.404118	-1.902001	1.422998
H	-3.808413	-2.892732	1.552620
H	-2.235502	-4.481909	0.742378
H	1.131213	4.486122	2.060313

$[Ru(bpp)_2]^{2+}$, ϕ = 165° (fixed)

Ru	0.000001	-0.000012	-0.265818
N	1.973482	0.290182	-0.003214

C	2.836649	-0.457802	-0.696343
C	4.199792	-0.381511	-0.472129
C	4.633306	0.511370	0.503047
C	3.735714	1.284947	1.232206
C	2.392398	1.136572	0.939096
N	2.198752	-1.296076	-1.623847
N	0.824679	-1.323298	-1.674983
C	0.518514	-2.180907	-2.629082
H	-0.516307	-2.378552	-2.860053
C	1.679444	-2.723924	-3.214799
H	1.736056	-3.443180	-4.014328
C	2.723879	-2.142087	-2.554876
H	3.788184	-2.259235	-2.677866
N	1.329828	1.805442	1.561977
N	0.050411	1.477879	1.202120
C	-0.738797	2.245779	1.930631
H	-1.810275	2.171575	1.826485
C	0.015233	3.084574	2.773700
H	-0.354470	3.815024	3.473298
C	1.321959	2.779846	2.513606
H	2.235329	3.179842	2.922836
N	-1.973483	-0.290185	-0.003207
C	-2.836644	0.457810	-0.696332
C	-4.199786	0.381536	-0.472110
C	-4.633306	-0.511337	0.503072
C	-3.735720	-1.284924	1.232226
C	-2.392404	-1.136569	0.939105
N	-2.198741	1.296073	-1.623841
N	-0.824668	1.323278	-1.674982
C	-0.518494	2.180891	-2.629077
H	0.516329	2.378526	-2.860051
C	-1.679422	2.723926	-3.214785
H	-1.736028	3.443189	-4.014308
C	-2.723863	2.142087	-2.554871
H	-3.788168	2.259243	-2.677863
N	-1.329840	-1.805455	1.561979
N	-0.050420	-1.477904	1.202120
C	0.738781	-2.245806	1.930637
H	1.810259	-2.171612	1.826490
C	-0.015256	-3.084592	2.773710
H	0.354441	-3.815042	3.473311
C	-1.321978	-2.779851	2.513616
H	-2.235352	-3.179838	2.922847
H	5.693507	0.600344	0.704949
H	-5.693506	-0.600296	0.704981
H	4.905253	-0.985910	-1.024793
H	4.081203	1.968349	1.995131
H	-4.905243	0.985942	-1.024771
H	-4.081213	-1.968320	1.995154

$[Ru(bpp)_2]^{2+}$, $\phi = 160°$ (fixed)

Ru	-0.000001	0.000021	-0.355410
N	1.950600	0.371853	-0.005267
C	2.868605	-0.349000	-0.656330
C	4.214042	-0.252763	-0.347763
C	4.570674	0.631283	0.666100

C	3.615433	1.374478	1.352237
C	2.295569	1.207296	0.975072
N	2.305464	-1.188628	-1.630668
N	0.936344	-1.267361	-1.747409
C	0.708598	-2.115125	-2.731524
H	-0.306098	-2.347958	-3.013438
C	1.915884	-2.600264	-3.272954
H	2.037157	-3.299291	-4.083182
C	2.905286	-1.993603	-2.553415
H	3.977931	-2.066002	-2.630266
N	1.184409	1.840961	1.546157
N	-0.062320	1.474258	1.120819
C	-0.912452	2.214441	1.809161
H	-1.974594	2.107260	1.650831
C	-0.229883	3.073858	2.690881
H	-0.657330	3.791080	3.370991
C	1.097698	2.811125	2.497781
H	1.976312	3.239273	2.952057
N	-1.950597	-0.371854	-0.005280
C	-2.868615	0.348976	-0.656351
C	-4.214053	0.252697	-0.347803
C	-4.570672	-0.631362	0.666053
C	-3.615419	-1.374529	1.352201
C	-2.295556	-1.207307	0.975054
N	-2.305487	1.188621	-1.630683
N	-0.936366	1.267389	-1.747409
C	-0.708632	2.115173	-2.731512
H	0.306063	2.348039	-3.013412
C	-1.915928	2.600284	-3.272951
H	-2.037212	3.299319	-4.083170
C	-2.905323	1.993580	-2.553435
H	-3.977971	2.065946	-2.630301
N	-1.184386	-1.840945	1.546150
N	0.062335	-1.474212	1.120823
C	0.912481	-2.214375	1.809172
H	1.974621	-2.107170	1.650850
C	0.229926	-3.073813	2.690882
H	0.657384	-3.791028	3.370993
C	-1.097659	-2.811099	2.497783
H	-1.976265	-3.239261	2.952056
H	5.614633	0.735342	0.934371
H	-5.614632	-0.735453	0.934309
H	-4.962902	0.836233	-0.864696
H	-3.899812	-2.048293	2.148226
H	3.899836	2.048231	2.148267
H	4.962881	-0.836320	-0.864648

$[Ru(bpp)_2]^{2+}$, $\phi = 155°$ (fixed)

Ru	0.000000	0.000019	-0.441745
N	1.910533	0.500676	-0.003887
C	2.894258	-0.168270	-0.614087
C	4.215604	-0.016266	-0.231529
C	4.476653	0.868284	0.810636
C	3.452771	1.554854	1.454709
C	2.163830	1.333888	1.004379
N	2.424418	-1.022300	-1.626073

N	1.068064	-1.178161	-1.808967
C	0.935988	-2.021614	-2.813443
H	-0.049586	-2.308812	-3.144630
C	2.193382	-2.425968	-3.304956
H	2.392338	-3.102007	-4.119513
C	3.111951	-1.775370	-2.531820
H	4.189480	-1.782968	-2.561532
N	0.995629	1.903533	1.524660
N	-0.206213	1.468384	1.041188
C	-1.127754	2.160150	1.686838
H	-2.174311	1.995960	1.480225
C	-0.536620	3.055372	2.597546
H	-1.035001	3.748834	3.253619
C	0.811413	2.866555	2.468709
H	1.642704	3.343105	2.962576
N	-1.910527	-0.500662	-0.003890
C	-2.894262	0.168268	-0.614093
C	-4.215607	0.016235	-0.231548
C	-4.476646	-0.868328	0.810610
C	-3.452756	-1.554882	1.454686
C	-2.163818	-1.333888	1.004367
N	-2.424431	1.022307	-1.626075
N	-1.068079	1.178192	-1.808965
C	-0.936017	2.021639	-2.813448
H	0.049553	2.308855	-3.144633
C	-2.193415	2.425964	-3.304972
H	-2.392382	3.101988	-4.119538
C	-3.111973	1.775355	-2.531833
H	-4.189503	1.782929	-2.561553
N	-0.995612	-1.903522	1.524647
N	0.206224	-1.468353	1.041186
C	1.127771	-2.160107	1.686842
H	2.174327	-1.995904	1.480239
C	0.536644	-3.055341	2.597543
H	1.035032	-3.748795	3.253620
C	-0.811391	-2.866552	2.468688
H	-1.642681	-3.343121	2.962538
H	5.499023	1.016031	1.135971
H	-5.499016	-1.016098	1.135935
H	-5.017395	0.557465	-0.714184
H	-3.662130	-2.227803	2.274546
H	5.017384	-0.557512	-0.714162
H	3.662152	2.227764	2.274576

References

1. C. A. Tovee, C. A. Kilner, J. A. Thomas and M. A. Halcrow, *CrystEngComm*, 2009, **11**, 2069–2077.
2. G. M. Sheldrick, *Acta Cryst. Sect. A.: Found. Adv.*, 2015, **71**, 3–8.
3. G. M. Sheldrick, *Acta Cryst. Sect. C.: Struct. Chem.*, 2015, **71**, 3–8.
4. L. J. Barbour, *J. Appl. Cryst.,* 2020, **53**, 1141–1146.
5. O. V. Dolomanov, L. J. Bourhis, R. J. Gildea, J. A. K. Howard and H. Puschmann, *J. Appl. Cryst.*, 2009, **42**, 339–341.
6. P. Ghosh, C. M. Pask, H. B. Vasili, N. Yoshinari, T. Konno, O. Cespedes, C. Enachescu, P. Chakraborty and M. A. Halcrow, *J. Mater. Chem. C*, 2023, **11**, 12570–12582.
7. J. K. McCusker, A. L. Rheingold and D. N. Hendrickson, *Inorg. Chem.*, 1996, **35**, 2100–2112.
8. P. Guionneau, M. Marchivie, G. Bravic, J.-F. Létard and D. Chasseau, *Top. Curr. Chem.*, 2004, **234**, 97–128.
9. M. A. Halcrow, *Chem. Soc. Rev.,* 2011, **40**, 4119–4142.
10. M. Marchivie, P. Guionneau, J.-F. Létard and D. Chasseau, *Acta Cryst. Sect. B: Struct. Sci.*, *2*005, **61**, 25–28.
11. a) M. A. Halcrow, I. Capel Berdiell, C. M. Pask and R. Kulmaczewski, *Inorg. Chem.*, 2019, **58**, 9811–9821;
    b) E. Michaels, C. M. Pask, I. Capel Berdiell, H. B. Vasili, M. J. Howard, O. Cespedes and M. A. Halcrow, *Cryst. Growth Des.*, 2022, **22**, 6809–6817.
12. J. M. Holland, J. A. McAllister, C. A. Kilner, M. Thornton-Pett, A. J. Bridgeman and M. A. Halcrow, *J. Chem. Soc., Dalton Trans.*, 2002, 548–554.
13. L. J. Kershaw Cook, R. Mohammed, G. Sherborne, T. D. Roberts, S. Alvarez and M. A. Halcrow *Coord. Chem. Rev*., 2015, **289–290**, 2–12.
14. I. Capel Berdiell, E. Michaels, O. Q. Munro and M. A. Halcrow, *Inorg. Chem.*, 2024, **63**, 2732–2744.
15. S. Vela, J. J. Novoa and J. Ribas-Arino, *Phys. Chem. Chem. Phys.*, 2014, **16**, 27012–27024.
16. a) L. J. Kershaw Cook, F. L. Thorp-Greenwood, T. P. Comyn, O. Cespedes, G. Chastanet and M. A. Halcrow, *Inorg. Chem.*, 2015, **54**, 6319–6330;
    b) I. Capel Berdiell, R. Kulmaczewski, N. Shahid, O. Cespedes and M. A. Halcrow, *Chem. Commun.*, 2021, **57**, 6566–6569;
    c) N. Suryadevara, A. Mizuno, L. Spieker, S. Salamon, S. Sleziona, A. Maas, E. Pollmann, B. Heinrich, M. Schleberger, H. Wende, S. K. Kuppusamy and M. Ruben, *Chem. – Eur. J.*, 2022, **28**, e202103853;
    d) R. Kulmaczewski, L. J. Kershaw Cook, C. M. Pask, O. Cespedes and M. A. Halcrow, *Cryst. Growth Des.*, 2022, **22**, 1960–1971.
17. J. M. Holland, C. A. Kilner, M. Thornton-Pett and M. A. Halcrow, *Polyhedron*, 2001, **20**, 2829–2840.
18. J. Elhaïk, D. J. Evans, C. A. Kilner and M. A. Halcrow, *Dalton Trans.*, 2005, 1693–1700.
19. I. Dance and M. Scudder, *CrystEngComm*, 2009, **11**, 2233–2247.
20. R. Pritchard, C. A. Kilner and M. A. Halcrow, *Chem. Commun.*, 2007, 577–579.
21. J. Kusz, H. Spiering and P. Gütlich, *J. Appl. Cryst.*, 2004, **37**, 589–595.
22. M. A. Halcrow and G. Chastanet, *Polyhedron*, 2017, **136**, 5–12.
23. M. A. Leech, N. K. Solanki, M. A. Halcrow, J. A. K. Howard and S. Dahaoui, *Chem. Commun.*, 1999, 2245–2246.
24. N. K. Solanki, M. A. Leech, E. J. L. McInnes, F. E. Mabbs, J. A. K. Howard, C. A. Kilner, J. M. Rawson and M. A. Halcrow, *J. Chem. Soc. Dalton Trans.*, 2002, 1295–1301.
25. M. A. Halcrow, *Chem. Commun.*, 2010, **46**, 4761–4763.

26. K. N. Lazarou, I. Stamatopoulos, V. Psycharis, C. Duboc, C. P. Raptopoulou and Y. Sanakis, *Polyhedron*, 2018, **155**, 291–301.

27. See *eg*
a) E. C. Constable, G. Baum, E. Bill, R. Dyson, R. van Eldik, D. Fenske, S. Kaderli, D. Morris, A. Neubrand, M. Neuburger, D. R. Smith, K. Wieghardt, M. Zehnder and A. D. Zuberbühler, *Chem. – Eur. J.*, 1999, **5**, 498–508;
b) S. Y. Brauchli, E. C. Constable, K. Harris, D. Häussinger, C. E. Housecroft, P. J. Rösel and J. A. Zampese, *Dalton Trans.*, 2010, **39**, 10739–10748;
c) S. M. Fatur, S. G. Shepard, R. F. Higgins, M. P. Shores and N. H. Damrauer, *J. Am. Chem. Soc.*, 2017, **139**, 4493–4505 and 2018, **140**, 1181–1182 (correction);
d) A. Kimura and T. Ishida, *Inorganics*, 2017, **5**, 52;
e) K. E. Burrows, S. E. McGrath, R. Kulmaczewski, O. Cespedes, S. A. Barrett and M. A. Halcrow, *Chem. – Eur. J.*, 2017, **23**, 9067–9075;
f) N. Shahid, K. E. Burrows, C. M. Pask, O. Cespedes, M. J. Howard, P. C. McGowan and M. A. Halcrow, *Inorg. Chem.*, 2021, **60**, 14336–14348.

28. See *eg*
a) R. Rajan, R. Rajaram, B. U. Nair, T. Ramasami and S. K. Mandal, *J. Chem. Soc. Dalton Trans.*, 1996, 2019–2021;
b) C. W. Glynn and M. M. Turnbull, *Transition Met. Chem.*, 2002, **27**, 822–831;
c) G. Stupka, L. Gremaud, G. Bernardinelli and A. F. Williams, *Dalton Trans.*, 2004, 407–412;
d) B. S. Hammes, B. J. Damiano, P. H. Tobash, M. J. Hidalgo and G. P. A. Yap, *Inorg. Chem. Commun.*, 2005, **8**, 513–516;
e) H. Wu, X. Huang, J. Yuan, F. Kou, F. Jia, B. Liu and K. Wang, *Eur. J. Med. Chem.*, 2010, **45**, 5324–5330.

29. See *eg*
a) F. Dumitru, Y.-M. Legrand, A. Van der Lee and M. Barboiu, *Chem. Commun.*, 2009, 2667–2669;
b) K. E. Burrows, R. Kulmaczewski, O. Cespedes, S. A. Barrett and M. A. Halcrow, *Polyhedron*, 2018, **149**, 134–141;
c) C. M. Pask, S. Greatorex, R. Kulmaczewski, A. Baldansuren, E. J. L. McInnes, F. Bamiduro, M. Yamada, N. Yoshinari, T. Konno and M. A. Halcrow, *Chem. – Eur. J.*, 2020, **26**, 4833–4841.

30. K. Pringouri, M. U. Anwar, L. Mansour, N. Doupnik, Y. Beldjoudi, E. L. Gavey, M. Pilkington and J. M. Rawson, *Dalton Trans.*, 2018, **47**, 15725–15736.

31. L. Rigamonti, N. Bridonneau, G. Poneti, L. Tesi, L. Sorace, D. Pinkowicz, J. Jover, E. Ruiz, R. Sessoli and A. Cornia, *Chem. – Eur. J.*, 2018, **24**, 8857–8868.

32. See *eg*
a) L. J. Kershaw Cook, F. Tuna and M. A. Halcrow, *Dalton Trans.*, 2013, **42**, 2254–2265;
b) Z.-Y. Ding, Y.-S. Meng, Y. Xiao, Y.-Q. Zhang, Y.-Y. Zhu and S. Gao, *Inorg. Chem. Front.*, 2017, **4**, 1909–1916;
c) A. A. Pavlov, A. S. Belov, S. A. Savkina, A. V. Polezhaev, D. Yu. Aleshin, V. V. Novikov and Yu. V. Nelyubina, *Russ. J. Coord. Chem.,* 2018, **44**, 489–495;
d) V. García-López, F. J. Orts-Mula, M. Palacios-Corella, J. M. Clemente-Juan, M. Clemente-León and E. Coronado, *Polyhedron*, 2018, **150**, 54–60;
e) A. Oulmidi, S. Radi, A. Idir, A. Zyad, I. Kabach, M. Nhiri, K. Robeyns, A. Rotaru and Y. Garcia, *RSC Adv.*, 2021, **11**, 34742–34753.

33. See *eg*
a) J. V. Folgado, W. Henke, R. Allmann, H. Stratemeier, D. Beltrán-Porter, T. Rojo and D. Reinen, *Inorg. Chem.*, 1990, **29**, 2035–2042;
b) P. Gamez, R. H. Steensma, W. L. Driessen and J. Reedijk, *Inorg. Chim. Acta*, 2002, **333**, 51–56;
c) K. Mack, A. Wünsche von Leupoldt, C. Förster, M. Ezhevskaya, D. Hinderberger, K. W. Klinkhammer and K. Heinze, *Inorg. Chem.*, 2012, **51**, 7851–7858;
d) A. Meyer, G. Schnakenburg, R. Glaum and O. Schiemann, *Inorg. Chem.*, 2015, **54**, 8456–8464;
e) A. J. Peloquin, M. B. Houck, C. D. McMillen, S. T. Iacono and W. T. Pennington, *Eur. J. Inorg. Chem.*, 2020, 1720–1727.

34. See *eg*
a) K. H. Sugiarto, D. C. Craig, A. D. Rae and H. A. Goodwin, *Aust. J. Chem.*, 1993, **46**, 1269–1290;
b) A. T. Baker, D. C. Craig and A. D. Rae, *Aust. J. Chem.*, 1995, **48**, 1373–1378;
c) J. McMurtrie and I. Dance, *CrystEngComm*, 2005, **7**, 216–229;
d) N. Xing, L. T. Xu, X. Liu, Q. Wu, X. T. Ma and Y. H. Xing, *ChemPlusChem*, 2014, **79**, 1198–1207;
e) N. R. East, C. Dab, C. Förster, K. Heinze and C. Reber, *Inorg. Chem.*, 2023, **62**, 9025–9034.

35. J. P. Byrne, J. A. Kitchen, O. Kotova, V. Leigh, A. P. Bell, J. J. Boland, M. Albrecht and T. Gunnlaugsson, *Dalton Trans.*, 2014, **43**, 196–209.

36. See *eg*
a) M. L. Scudder, D. C. Craig and H. A. Goodwin, *CrystEngComm*, 2005, **7**, 642–649;
b) Y. Li, J. C. Huffman and A. H. Flood, *Chem. Commun.*, 2007, 2692–2694;
c) Q.-H. Wei, S. P. Argent, H. Adams and M. D. Ward, *New J. Chem.*, 2008, **32**, 73–82;
d) F. Schramm, R. Chandrasekar, T. A. Zevaco, M. Rudolph, H. Görls, W. Poppitz and M. Ruben, *Eur. J. Inorg. Chem.*, 2009, 53–61;
e) J. Moll, C. Wang, A. Päpcke, C. Förster, U. Resch-Genger, S. Lochbrunner and K. Heinze, *Chem. – Eur. J.*, 2020, **26**, 6820–6832.